67-12,556

CANTE, Charles John, 1941-
THE ABSORPTION INDUCED ELECTRODE POTENTIAL PHENOMENON.

The City University of New York, Ph.D., 1967
Chemistry, physical

University Microfilms, Inc., Ann Arbor, Michigan

The Absorption Induced Electrode Potential Phenomenon

by

Charles John Cante

A dissertation submitted to the Graduate Faculty in Chemistry in partial fulfillment of the requirements for the degree of Doctor of Philosophy, The City University of New York.

1967

This manuscript has been read and accepted for the University Committee in Chemistry in satisfaction of the dissertation requirement for the degree of Doctor of Philosophy.

May 3, 1967
date

Henri L. Rosano
Chairman of Examining Committee

May 3, 1967
date

Richard A. Wiley
Executive Officer

Sylvan M. Edmonds
Dr. Sylvan M. Edmonds

Joseph Glickstein
Dr. Joseph Glickstein

Henri L. Rosano
Dr. Henri L. Rosano

Supervisory Committee

The City University of New York

Preface

The work described in this dissertation was carried out in the Marlies Laboratory, Department of Chemistry at the City College of the City University of New York during the period September 1964--January 1967. Except where otherwise indicated, the work is original and has not previously been submitted for a degree in any other university.

I wish to express my deep gratitude to my mentor, Professor H.L. Rosano, for receiving me into his laboratory and for his constant encouragement, assistance and advice. I have learned much and benefited from his broad knowledge and experience.

I am also grateful to my associates, M.E. Feinstein and A.P. Christodoulou, for their constant support and stimulating discussions.

I wish as well to thank all those, in the City University and especially at the City College, whose friendly attitude and advice have contributed to make these years of research and learning an enriching experience. In particular, I acknowledge Professor N. Birnbaum for the unending guidance which he has given me as my teaching supervisor.

I would like to thank the E. I. du Pont de Nemours and Company for the Du Pont Postgraduate Teaching Assistant Award of which I was the recipient for the academic year 1966-67.

Finally, my sincere thanks are due to Professor Louis Melites of the Polytechnic Institute of Brooklyn for his review and helpful comments on a portion of the work herein described.

New York, March 1967

Contents

Tables

Chapter 1

Chapter 3

Chapter 4

Illustrations

Introduction

It had been observed by Rosano and Scheps[8-10] that the absorption of alcohol vapors into the electrolyte meniscus formed on the partially emerging electrode of the cell: Pt blade anode (partially emerging into the gas phase)/ fresh nitrochromic acid oxidizing electrolyte/ Pt or Carbon cathode (completely immersed in the electrolyte) resulted in a current which could be recorded. When both electrodes were completely immersed in the electrolyte, the cell failed to respond to the incoming alcohol vapors. It was also recognized by the authors that in order to have a sensitive cell, the emerging electrode had to be wettable by the electrolyte so that a meniscus (solid/liquid and liquid/gas interfaces) could form. The use of an exposed electrode with a three phase interface (gas/liquid/solid interface) apparently allows and electroactive component of the gas phase to be brought to reaction at an electrode without prior dissolution of the species in the bulk of the electrolyte.

The Absorption Induced Electrode Potential phenomenon of Rosano and Scheps[8-10] provides a basis for the study of the role of the "meniscus" electrode in electrochemicals cells. It also allows for the simultaneous study of absorption and electrochemical or chemical interaction which is fundamental to the understanding of gas/liquid/electrode reactions such as those encountered in fuel cells.

The investigation of the absorption induced electrode

potential phenomenon was undertaken in order to study the mechanism of the phenomenon. The phenomenon was also examined in order to determine the respective contributions of the meniscus and adjacent film to the total response of the cell.

In fact, the results presented in this work are important and applicable to fields where electrodes employing solid/liquid and liquid/gas interfaces, i.e. electrode/electrolyte/gas interfaces, play major roles, e.g. in the fields of gas detection[1,8-23] fuel cell technology [2-6, 24-31] and olfaction[7-10, 15-19, 32-34].

With these objectives in mind, the research has been organized into three study areas.

Study I. Absorption of an Ionizable Vapor in a Reversible Electrochemical Cell

The absorption of an ionizable vapor (one that ionizes in the cell's electrolyte, e.g. HCl) into the liquid meniscus formed on the exposed electrode of the absorption induced electrode potential cell: Ag/AgCl (exposed blade)/ aqueous HCl electrolyte/ AgCl/Ag (immersed wire) counter electrode is discussed in chapter 3. This system is reversible in the thermodynamic sense and its potential can be described using the thermodynamic equation for electrode potentials. This study has been divided into two parts. The first is the potentiometric measurement of the transient emf produced by the absorption of HCl vapor into the

electrolyte meniscus formed on the exposed electrode of the cell. The second part involves the measurement of the transient current produced by absorbed HCl vapor when an external emf has been applied to the electrodes of the cell described above.

In order to determine the relative contributions of the meniscus and film to the total cell response, it is necessary to probe these regions at various levels. Practically, a solid blade electrode cannot be raised above the plane of the electrolyte solution, for this purpose, because the blade will not support the meniscus. A unique feature of this study is the use of semi-silvered, sandblasted, glass slides as exposed electrodes. With these electrodes, it is possible to probe various levels in the electrolyte meniscus and film by positioning the bottom edge of the silvered portion of the semi-silvered electrode at any height in the meniscus or film. Since the lower portion of the semi-silvered electrode is sandblasted glass, it will support the meniscus.

Study II. Irreversible Organic Oxidation on the Surface of Partially Exposed Platinum Electrodes

In this study, an organic vapor (nonionizable vapor), 1-butanol, is oxidized at the exposed electrode of the AIEP cell comprised of a sandblasted, partially exposed, platinum anode, nitrochromic acid oxidizing electrolyte and an immersed platinum cathode. The oxidation of the alcohol, which in acid solutions yields first the corresponding aldehyde

and then the carboxylic acid, is an irreversible process from the thermodynamic standpoint. That is, in contrast to the Ag/AgCl system of study I where the system gave a definite potential varying with the relative concentrations of the oxidized and reduced species in accordance with the requirements of the Nernst equation (thermodynamic reversibility), the system used in study II will certainly adopt a potential, but the value will depend more on the acidity, nature of the electrolyte, and on the previous history of the electrode than on the concentrations of alcohol and aldehyde. The study of irreversible systems is therefore more complicated. However, one can readily see that an AIEP cell which responds to alcohol vapors will also respond to aldehyde vapors. Therefore, the developments arising from study II may permit the extension of the technique to the detection of organic compounds containing other functional groups, e.g. amines, olefins, etc; although this has not been done in the present work.

The distinction between chemical and thermodynamic reversibility must be kept in mind: the system alcohol/aldehyde is reversible in the chemical sense but it does not behave as a thermodynamically reversible system giving a definite electrode potential. Even though alcohol may be oxidized electrochemically at an anode to an aldehyde (and the latter may be reduced to the alcohol at a cathode), the process does not begin to take place at potentials determined only by the relative concentrations of the oxidized and reduced species.

Study III. Depolarization of a Partially Exposed Platinum Electrode by an Ionic Redox Couple

Two primary cases of ideal electrodes exist: (1) the ideally polarizable electrode and (2) the nonpolarizable electrode. In study III, an exposed platinum electrode is polarized in a solution containing iodide and iodate ions (with excess potassium nitrate as a supporting electrolyte). It has been found that the introduction of an ionizable acidic vapor (HCl or acetic acid) into the AIEP cell: exposed Pt blade/ $I^-, IO_3^-KNO_3$ (pH > 7) / immersed Pt wire, results in the depolarization of the exposed electrode by the reversible I^-/I_2 couple. The iodine was formed in the meniscus by the chemical interaction of the acidic vapor with the electrolyte. In chapter 5, it will be shown that the current which is produced is proportional to the amount of iodine present, and therefore is also proportional to the amount of acidic vapor initially injected into the cell since the two, acid and iodine, are stoichiometrically related.

Since the study of the absorption induced electrode potential phenomenon has been approached from both a surface chemical and electrochemical view point, it will be useful to discuss some of the concepts in each area which are pertinent to the understanding of the experiments and results herein described. With this in mind, the first and second chapters of this work are intended to summarize the relationship between a solid/liquid interface and the surface of a solid, and electrical phenomena at interfaces respectively.

CHAPTER 1

Relationship Between a Solid/Liquid Interface and the Surface of a Solid

Part I. Wettability

In considering the hydrodynamic aspects of the present work it would be best to examine a solid, perfectly wettable, blade which is vertically withdrawn from a quiescent liquid. If the blade is maintained so that it is partially immersed in the liquid phase and partially extending into the gas phase, a thin film of liquid remains on the exposed surface.

Because of the forces acting between the molecules of a liquid themselves, and between these molecules and those of the solid material, with which it is in contact, e.g. silver, glass, platinum, etc. the surface of a liquid on a vertical planar or tubular surface is always curved, i.e. a meniscus is formed. The nature of the curvature of the meniscus will depend on whether or not the liquid and the solid attract one another strongly. In the former case, the liquid "wets" the solid and the meniscus is concave upwards while in the latter case the solid is not wetted and the meniscus is concave downward (figure 1.1). In general, the topic of wetting can be divided into two major parts: (a) wetting as a contact angle phenomenon and (b) wetting as a capillarity phenomenon.

In the case of contact angle phenomenon, the term wetting usually means that the contact angle between a solid, liquid and gas is zero while in the case of nonwetting the contact is much greater than 90°. For intermediate values of the contact angle ($\theta = 90^\circ$ to 0°) the degree of wetting increases with decreasing contact angle and the degree of nonwetting increases with increasing contact angle ($\theta = 90^\circ$

to $\theta = 180^{o}$). According to the Young and Dupre equation (eq. 1.1)[36], the contact angle, θ , is given by

$$\cos\theta = (\gamma_{S/V} - \gamma_{S/L})/\gamma_{L/V} \qquad \text{eq. 1.1}$$

where $\gamma_{S/V}$, $\gamma_{S/L}$ and $\gamma_{L/V}$ denote the solid/gas, solid/liquid and liquid/gas interfacial tensions respectively.

Some types of wetting involve more than the contact angle in their basic mechanisms. In these cases, the phenomenon is essentially that of a capillary rise, where the driving force is that of the pressure difference across the curved surface of a meniscus. The fundamental relationship is given by the Laplace equation of capillarity [36]

$$\Delta P = (2\gamma_{L/V}/R)\cos\theta \qquad \text{eq. 1.2}$$

where R. is the radius of curvature of the surface. For the special case of $\theta = 0^{o}$ (where $\cos\theta = 1$) equation 1.2 reduces to:

$$\Delta P = (2\gamma_{L/V}/R) \qquad \text{eq. 1.3}$$

and a large value of $\gamma_{L/V}$ is desireable.

In reality, for a completely wettable surface, the meniscus is supported by a sheath of wetting which covers the surface of a solid. The thickness of the sheath of wetting is determined by the electrolyte and the surface of the solid. [39-45] It represents the minimum possible liquid thickness on the solid.

The foregoing discussion was based on the concept of the equilibrium contact angle. It is evident from the reported works on the hysteresis of contact angle that the phenomenon is complicated by several factors. One of the most serious experimental difficulties faced in surface

chemistry is the rapid contamination of fresh surfaces and the difficulty of producing "clean" surfaces with reproducible properties. This problem makes it extremely difficult to study phenomena such as the wettability of solids [46]. Various interpretations of the causes and effects of hysteresis and its incompatibility with the concept of an equilibrium contact angle have been published [35,36-38,47-55]. Of these explanations only surface roughness is of interest in the present work.

II. Surface Roughness and the Degree of Wettability of a Solid

In a study of the spreading of liquids on solid surfaces Bailey and Shuttleworth[55] showed that hysteresis of the contact angle is the result of the roughness of a solid surface. They considered as in figure 1.2, α and β to be the maximum and minimum slopes of a rough surface respectively. The apparent contact angle, θ app, would then depend on the point at which the liquid front is resting. In the case of an advancing liquid, the liquid front is assumed to stop as in figure 1.2a with $\theta_{app} = \theta_{act} + \alpha$. In the case of a receding liquid, $\theta_{app} = \theta_{act} - \beta$ (figure 1.2b). Shuttleworth and Bailey[55] and Cassie[61], recognizing that the average apparent contact angle is affected by surface roughness, attempted to relate θ_{app} to the ratio, R, of the true surface area to the apparent surface area of the solid they investigated. Essentially, they noted that:

$$\cos \theta_{app} = R \cos \theta_{act} \qquad \text{eq. 1.4}$$

This implied that for an increase in the apparent area of ΔA, the solid/liquid/gas interface actually increases by $R\,\Delta A$. While the above represents a step forward, the actual problem is more complex since surfaces usually consist of small regions with each region having different apparent areas.

Because the value of the contact angle greatly depends on the nature of the solid employed for electrodes, all electrodes used as the exposed electrodes in the experiments described in this work were sandblasted using a model C Airbrasive unit (S.S. White, Dental Manufacturing Co., N.Y.) in order to insure perfect wettability.

We began this chapter by considering a perfectly wettable solid which is vertically withdrawn from a quiescent liquid. We saw that a meniscus formed on the solid and that the meniscus was concave upward. That is, if the blade is long enough so that when its final position is such that the bottom edge of the solid is still in contact with the bulk liquid, a meniscus and a thin film of liquid remain on that portion of the solid which is above the plane of the electrolyte. It is natural to ask (a) how high is the meniscus, (b) what is its shape and (c) what factors affect both its height and shape. Therefore, let us now consider these points.

III. Height and Shape of the Meniscus on a Vertical Planar Surface

The Laplace equation of capillarity allows the calcula-

tion of the height of a meniscus if the surface tension and density of the liquid are known[62]:

$$h = (2\gamma/\rho g)^{1/2} \qquad \text{eq. 1.5}$$

where h is the height of the meniscus (cm), g is the acceleration of gravity (cm/sec^2), ρ is the density of the liquid (gm/cm^3) and γ is the surface tension of the liquid against the gas phase (dynes/cm). For a liquid with γ = 72 dynes/cm, e.g. water, h is 0.384 cm. Table 1.1 presents a few typical values of h calculated using equation 1.5 and experimental values of γ and ρ [63-65].

Table 1.1

Calculated Values of h from Experimental Data

Electrolyte	ρ, density (gm/cm^3)	γ, surface tension (dynes/cm)	h, height (cm)
HCl, 1M	1.0156	72.40	0.381
HCl, 1M with Igepal CO-630 Surfactant (10^{-6}M)	1.0156	30.84	0.249
HCl, 1M with Igepal CO-730 Surfactant (10^{-6}M)	1.0156	35.45	0.267
KCl, 1M	1.0467	74.30	0.380
Nitrochromic acid (70%HNO_3 saturated with 99% CrO_3)	1.3985	58.53	0.292

Mathematically, the shape of a meniscus on a vertical planar surface is represented by [66]:

$$X = X^o - \sqrt{2h^2 - y^2} + (h/\sqrt{2}) \ln \left[(h\sqrt{2} + \sqrt{2h^2 - y^2}) / y \right] \qquad \text{eq. 1.6}$$

with:

$$x^{o} = 0.377 \left(\gamma / \rho g \right)^{\frac{1}{2}} \qquad \text{eq. 1.7}$$

where h is given by equation 1.5, y is the vertical position in the meniscus, X_o is a constant of integration - and X is the horizontal distance from the vertically oriented surface. Figure 1.3 shows the relationship between a partially exposed surface, sheath of wetting and the meniscus on that exposed surface.

Figure 1.1

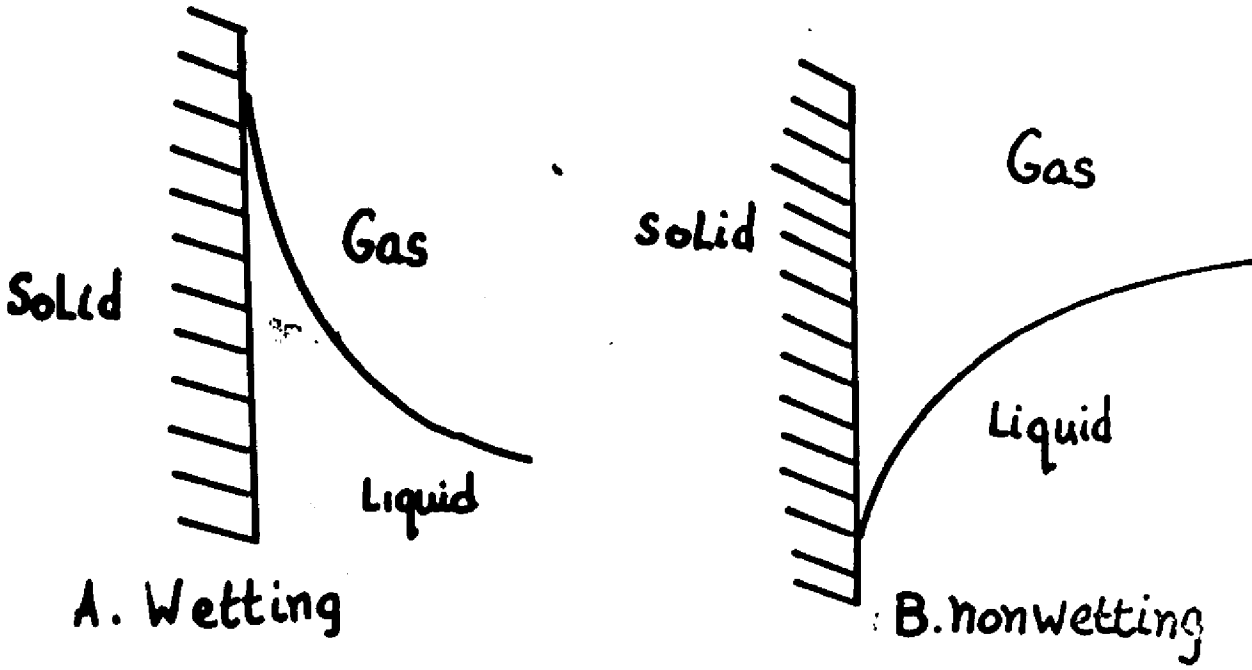

Figure 1.2

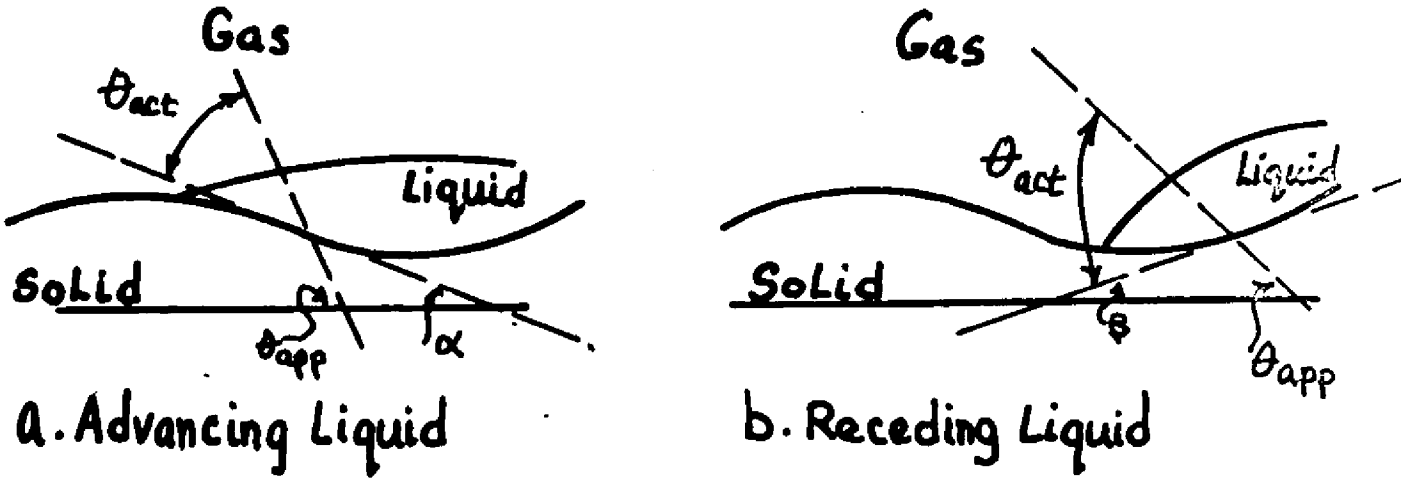

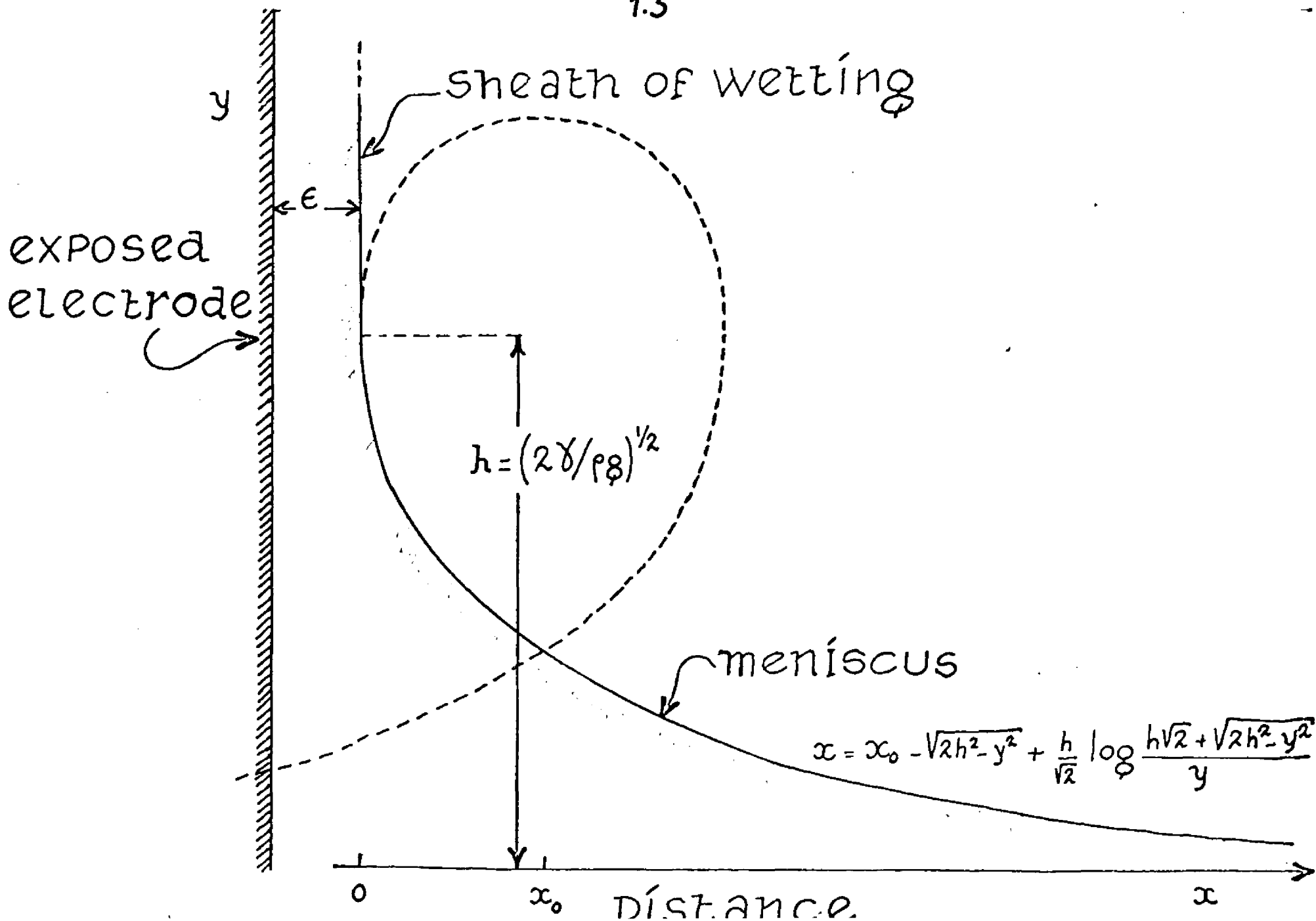
y
sheath of wetting
ϵ
exposed
electrode
$h = (2\gamma/\rho g)^{1/2}$
meniscus
$x = x_0 - \sqrt{2h^2 - y^2} + \frac{h}{\sqrt{2}} \log \frac{h\sqrt{2} + \sqrt{2h^2 - y^2}}{y}$
0
x_0
Distance
x

CHAPTER 2

Electrical Phenomena at Interfaces

In chapter 1 we noted that when a perfectly wettable solid surface was vertically withdrawn from a quiescent liquid, a meniscus was formed on that surface. The height of the meniscus which is a function of the surface tension and the density of the liquid could then be calculated using the Laplace equation of capillarity. In addition, a thin liquid film extended vertically from the upper boundary of the meniscus; its height was determined by experimental conditions.

Suppose that the solid surface mentioned above is now an electrode. After all, in the electrical aspects of the problem the objectives are to measure transient potentials (emf vs. time) and currents (i vs. time). Perhaps then, those parameters can be related to processes occuring at the exposed electrode/ electrolyte/gas interface. Certainly, though, both the emf and the current will depend on the electrical nature of the electrode/electrolyte interface at the very least. Let us first consider the effect of potential differences at interfaces on the emf of electrochemical cells.

I. The Effect of Potential Differences at Interfaces on the Emf of Electrochemical cells

The emf of a reversible cell is often thought of as a measure of the free energy pertaining to an overall chemical reaction [75]. In actuality, the overall cell reaction consists of several processes occurring in different sections of the cell. Hence, the observed emf must be the sum of the

individual potential differences which arise at the various phase boundaries in the cell. The Nernst potential, for example, fundamentally involves a potential which results from the transport of a species across an interface. Another example of a potential resulting from transport across an interface is the Liquid-junction potential. The emf of a concentration cell with transference is, in part, dependent upon a liquid-junction potential [69].

A. Liquid-junction Potentials and Concentration Cells with Transference

In the experiments described in chapter 3 utilizing the AIEP cell Ag/AgCl (exposed blade)/ HCl aqueous/ AgCl/Ag wire immersed), when HCl vapor is injected into the cell, the HCl concentration in the meniscus increases from its bulk value, C_B, up to a maximum instantaneous value, C_M. Because C_M is greater than C_B there will be diffusion of HCl from the meniscus region down to the bulk electrolyte. As we shall see in chapter 3, the entire AIEP cell may be viewed as a concentration cell with transference between the exposed electrode which is at HCl concentration C_M and the immersed electrode which is at HCl concentration C_B. At the boundary of contact of the "two half-cells" a diffusion potential will be set up. Of course, we could just as easily use KCl or NaCl as the bulk electrolyte thus providing only one common ion with the vapor. For the latter electrolytes, the situation would be essentially the same as that described above except that the treatment would be mathematically complicat-

ed. Therefore, in view of the foregoing, we should examine the concepts of liquid-junction potentials and the emf of concentration cell with transference.

When two different electrolyte solutions are brought into contact, an electrical potential arises across the contact.interface. The potential difference can be termed "diffusion potential" because the ions not initially present in both solutions, or present at unequal concentrations, diffuse from regions of higher to lower concentrations under a force proportional to the gradient of concentration (or more appropriately a gradient of activity) of the ion. Since ions have different speeds (ionic mobilities), under a given force, a slight separation of charge results because the faster ions outrun the slower ones. This charge difference is the cause of the liquid-junction potential (E_j). Once the liquid-junction potential has been established, it acts in such a way that the faster ions are retarded while the slower ions are accelerated until some steady state is achieved which corresponds to a constant separation of charge. There are three types of liquid junctions [69(p42)] and they are illustrated in figure 2.1.

(1) Type I Liquid-junction

In the first type (fig. 2.1) two solutions containing the same electrolyte, but at different concentrations are brought into contact. Consider the salt MX at concentrations 0.1M and 0.01M with the mobility of $M^+ > X^-$, e.g. HCl, NaCl. In this case, both M^+ and X^- diffuse from left to

right but since the mobility of M^+ is greater than that of X^-, M^+ outruns X^- and the right side of the junction (contact interface) acquires a positive charge (+) and E_j is positive.

A cell which employs a liquid-junction of this type is a concentration cell with transference such as:

$Ag/AgX, MX\ (C_1)\ /\ MX\ (C_2)\ ,\ AgX/Ag$ eq. 2.1

or $Cu/CuCl_2\ (C_1)\ /\ CuCl_2\ (C_2)\ /\ Cu$ eq. 2.2

In ε concentration cell, the net process is not a chemical reaction but rather a physical transfer of some substance from one phase to another. In general, the emf of a concentration cell with transference can be expressed as:

$$E_t = -(vtRT\ /\ nF)\ \ln\ C_1/C_2 \qquad \text{eq 2.3}$$

if we let v represent the total number of ions produced by the dissociation of one molecule of the salt, t is the transference number of the ion not involved in the electrode reaction and n,F,R and T have their usual significance. If there had been no liquid junction, them the emf of the cell (such as 2.1 or 2.2 above) would be the sum of the two electrode potentials, i.e.:

$$E = -(RT/n\,F)\ \ln\ C_1/\ C_2 \qquad \text{eq 2.4}$$

Since the emf of a concentration cell with transference is the sum of the liquid junction potential (E_j) and the electrode potentials (eq. 2.4), it follows that:

$$E_j = (1\text{-}vt)\ (RT/nF)\ln\ C_1/C_2 \qquad \text{eq 2.5}$$

Both the sign and magnitude of E_j are independent of which ion of the salt is involved in the electrode reaction[69 (p45) 70(p223)]. Although concentrations were used in the fore-

going, activities of the species are the proper quantities to use. When the activity coefficients are available in the literature corrections can be made. Because of the uniquely large transference numbers of H^+ and OH^-, liquid-junction potentials for either strongly acid or basic solutions are relatively large.

An interesting feature of the type 1 junction is that the liquid-junction potentials are independent of the manner in which the junction is experimentally formed [69 (p46), 70(p224)].

(2) Type II Liquid-junction

In the second type of liquid-junction, solutions containing electrolytes that have an ion in common, at the same concentration, such as 0.1M KCl and 0.1M HCl, are brought into contact (fig. 2.1). In this system, virtually no diffusion of chloride takes place since the chloride ion concentration is the same on both sides of the junction. However, diffusion of H^+ faster than that of K^+ leaves the left side of the junction positively charged and E_j is negative. Consider the cell: Ag/AgCl, HCl (0.1M) / KCl, 0.1M, AgCl/Ag for which the measured emf is + 0.0268 v at 25°C[69 (p46)]. Since the chloride concentrations are the same in both half-cells, their activities are very nearly equal. Hence, the electrode potentials, which are only a function of the chloride ion activity, cancel and the measured emf is very nearly E_j. In cells of this type, with 1:1 salts, E_j is given by the Henderson-Nernst equation :[70(p233)]

$$E_j=(RT/\nu F)\ \ln\ (u_i^+ + u_i^-)/(u_k^+ + u_k^-) \quad \text{eq. 2.6}$$

and using the relationship : $\Lambda_i = \alpha_i F (\mu_i^+ + \mu_i^-)$

where the u_i's are the ionic mobilities and Λ_i are the equivalent conductances of solutions of i and k at equal concentrations, by the Lewis-Sargent equation:[69(p47)]

$$E_j = (RT/nF)\ \ln\ \Lambda_i/\Lambda_k \qquad \text{eq 2.6}$$

(3) Type III Liquid-Junction

The third type of junction is formed by the contact of two solutions completely different with respect to concentrations and types of ions, e.g. 0.1M HCl and 0.05M KNO_3 (fig. 2.1). The result is the interdiffusion of all ions. Since the ionic mobilities and concentrations are all different, the situation is very complicated and past mathematical treatments of this case have been largely unsuccessful.[69(p43)]

As we have just seen, the thermodynamic potentials arise from transport of a species across an interface. Unlike the thermodynamic potentials, the electrokinetic potentials arise from the transport of a charged species along an interface. The magnitude of the electrokinetic potentials depend upon the presence and nature of the ionic double layer.

B. The Electrokinetic Potentials

A number of electrical phenomenon have in common the feature that relative motion between charged surface and the bulk solution gives rise to either a potential or a current. The transport of a species along an interface under various

conditions forms the basis for the electrokinetic phenomenon among which are electrophoresis, electroosmosis, sedimentation potential and streaming potential. In an electric field, a charged surface will experience a force and conversely, the motion of a charged surface will induce an electric field. In either case, a plane of slip, located between the electrical double layer and the bulk solution, is involved. 36(p189), 71(p79) The results of the experimental measurements have been interpreted in terms of an electrokinetic potential, or zeta potential, at this shear surface. The zeta potential can be thought of as the potential difference between a point some distance from the surface and a point on the plane of shear, both points within the same given phase. The zeta potential is therefore related to the work required to transport unit charge from one point to another in the same phase.

It has been shown by Elton [41], that the drainage of thin electrolyte films is opposed by viscous and electroviscous forces. The electroviscous force was found by Elton[41] to be a retarding force proportional to the finite zeta potential at the solid/liquid interface, i.e. at the double layer. This retarding force arises because the shearing of a double layer at an interface in an ionic solution sets up a potential difference (stream potential) in the plane of shear. This potential difference will tend to resist the flow of liquid owing to the electrical retarding forces acting on the liquid. However, Elton demonstrated that the effect (and the potential) is quite small for electrolyte

concentrations 1N or greater. In experiments such as those presented in the present work, the electroviscous effect and the electrokinetic potential are negligible in view of the high electrolyte concentration, i.e. 1M, HCl.

II. Processes Occurring at Electrode/Solution Interface

Up to now, we have been discussing electrical potentials because the injection of HCl vapor into an absorption induced electrode potential cell comprised of an exposed Ag/AgCl blade, aqueous HCl and an immersed Ag/AgCl counter electrode generates a transient emf. However, as we shall see in chapter 3, if an external emf is applied to the electrodes of the same cell, the injection of vapor into the cell will produce a transient current. Therefore, it is of value to briefly discuss electrical currents which may arise from (1) the formation of a double layer (non-Faradaic current) and (2) an electron transfer reaction (Faradiac current).

A. Non-Faradiac Current [72(p2127)]

In the absence of an electroactive species, it has been found experimentally that a finite current passes when the potential of an electrode of constant area is changed. This current is termed "non-Faradiac" since it is not the result of an electron transfer process. The effect may be explained on the basis of the formation of the electrical double-layer at the electrode surface.

B. Faradiac Current [68(p93), 72(p2122)]

In the presence of an electroactive species, the rate of electrochemical reaction, and hence the current, is controlled in part by (a) the rate of an electron transfer reaction and (b) the rate of transport of a reactive species into a "pre-electrode layer".[72] Considering the case in which the former is the slowest process, the solution is essentially homogeneous and the surface concentration of the electroactive species is equal to its bulk concentration. The rate of electron transfer depends on the nature of electroactive species and its concentration and on the nature and potential of the electrode. For an electron transfer from one form to another, i.e. from the reduced to oxidized form of a redox couple, and energy barrier $\Delta G^{\#}$, the free energy of activation, must be surmounted. This varrier is the free energy necessary to convert a mole of reactant to the activated state of the reaction.

The classification of electrochemically "reversible" and "irreversible" reactions is based on the rate of electrode reaction, e.g. electron transfer, through the free energies of activation. An electrode process is classified "reversible" if the activation overpotential is immeasureably small ($\eta \approx 0$), and "irreversible" if the activation overpotential is measureable ($|\eta| > 0$). That is, for large values of η, the back reaction can be neglected and the reaction is said to be irreversible.

C. Mass Transfer of Reactant to the Electrode/Solution Interface

Consider the case in which the rate of electron transfer is much greater than the rate of the mass transfer process. The current, under these conditions, is controlled by the latter process. Mass transport may be accomplished by (1) diffusion, (2) convection, and (3) migration. Only the first two modes of mass transport will be discussed since they are of interest in the present work.

(1) Diffusion

Diffusion has its origin in a gradient of chemical potential (or approximately in a concentration gradient). Thus if the concentration of a given species in the bulk of the solution is greater than its concentration at the electrode surface, e.g. as a result of an electrode reaction, the species will tend to diffuse form the bulk of the solution toward the electrode surface. The direction of diffusion is therefore, from regions of larger to smaller concentrations. However, the rate of diffusion is proportional to the magnitude of the concentration differences.

In particular, with regard to the present work, the process involved in the cell: Ag/AgCl/ 1M HCl/AgCl/Ag is the absorption of HCl vapor from the gas phase into the electrolyte meniscus formed on the exposed electrode of the cell with subsequent diffusion of the absorbed HCl to the electrode surface. Therefore, the HCl concentration at the

electrode surface increases with time from its bulk value to some instantaneous maximum due to the injected HCl vapor. After a given time, the diffusion of HCl from the meniscus to the bulk electrolyte depletes the electrode surface of the excess HCL (i.e., diffusion down the meniscus overshadows diffusion to the electrode surface; the latter having initially predominated). It has been suggested that the technique be called "concentration pulse" voltammetry since we are actually sweeping the electrode surface with a concentration excitation in the form of a concentration / change, viz.$C(O,t) = K\exp(Jt)$ during the initial absorption phase and $C(O,t) = L\exp(-Mt)$ during the depletion phase where $C(O,t)$ is the concentration at the electrode surface at time t, K,J,L and M are constants for a given injection of vapor. One might view this process as a composite excitation there:

$$C90,t) = \left[K\exp(Jt)\right]_{t=0}^{t=t_p} + \left[L\exp(-Mt)\right]_{t=t_p}^{t=t}$$

initially the concentration at the electrode surface increases exponentially with time up to $t = t_p$ at which time another excitation replaces the original one.

(2) Convection

Convection transport of a species is accomplished whenever the solution containing the species is stirring into the path of the electrode. This stirring obviously increases the rate of transport of the species to the electrode. Because quantitative treatment of this mode of mass transport is exceedingly difficult, experimenters have frequently

resorted to the use of empirical expressions in the interpretation of techniques such as coulometric titrations.[72(p2145)] An important concept in the treatment of convection is that proposed by Nernst.[72(p2146)] His model assumed that (a) a stagnant layer of definite thickness, δ, exists at any solid/liquid interface, (b) the solution in immediate contact with the stagnant film was kept homogeneous by stirring and (c) the steady state currents which are obtained result from a linear concentration gradient within the stagnant layer (fig. 2.2). In the case where the applied potential is not sufficient to reduce the concentration of the diffusing species to zero at the electrode surface, the current, i, is given by:

$$i = nFAD \left[(C_b - C_s)/\delta \right] \qquad \text{eq. 2.32}$$

If the applied potential does not cause appreciable reduction of the species then $(C_b - C_s)$ is zero. At sufficiently high potentials $(C_b - C_s) \approx C_b$ and the current is said to be the limiting current, I_l, and is given by:

$$I_L = \left[nFAC_b/\delta \right] \qquad \text{eq. 2.33}$$

Advanced works in hydrodynamics demonstrated that while stagnant films do exist they are not necessarily of definite thickness.[67] Actually, the solution immediately adjacent to the electrode surface is most likely unstirred. However, proceeding away from the electrode surface, the degree of stirring increases continuously. The diffusion profile is probably better represented by the dashed line in figure 2.2.

Figure 2.1

TYPE I

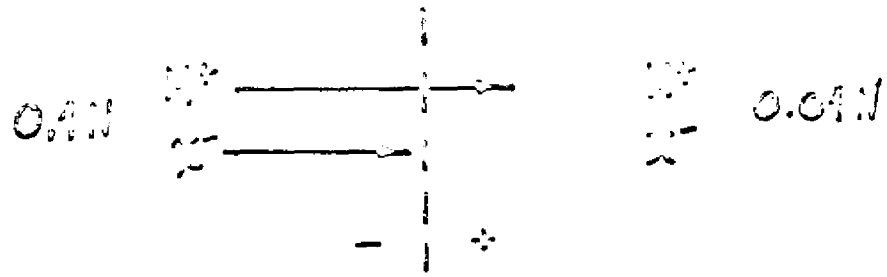

TYPE II

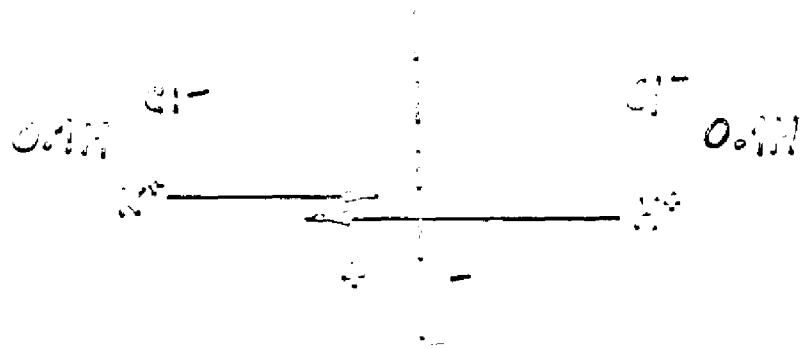

TYPE III

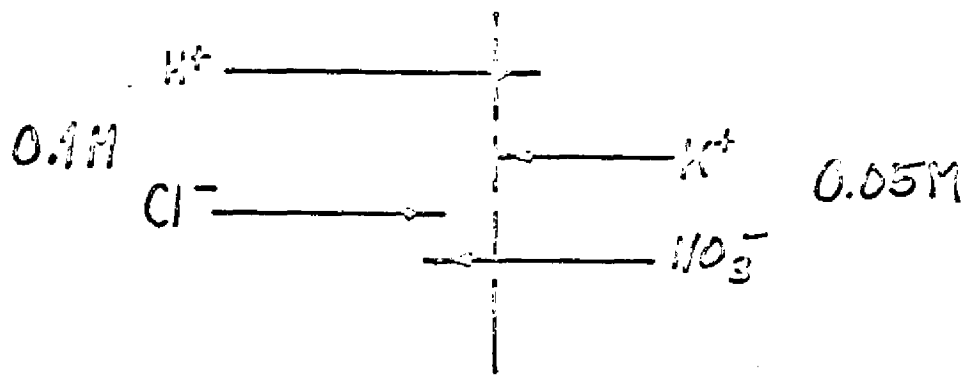

Figure 2.2

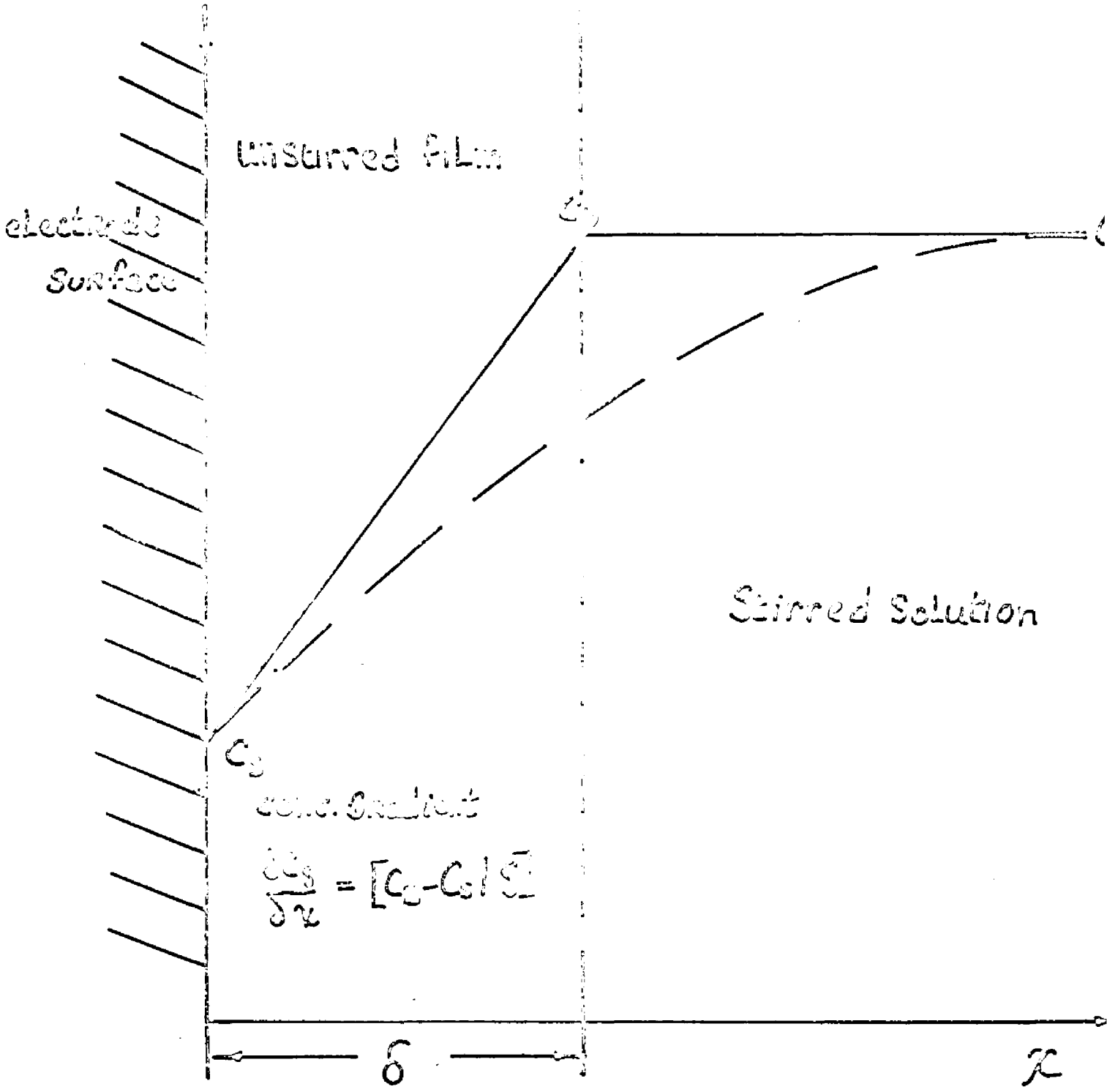
Unstirred Film
electrode surface
C_s
C_b
Stirred Solution
conc. Gradient
$\frac{dC_s}{dx} = [C_b - C_s]\frac{1}{\delta}$
δ
x

CHAPTER 3

Study I: Ionizable Vapor Injected into a Cell Having Electrodes Reversible to One Component of the Vapor

Part A: Mechanism of the AIEP Cells I. Nature of the Potential

Part B: Mechanism of the AIEP Cells II. Nature of the Current

Study I, Part A:

I. Experimental Procedure

The electrolytes used in these investigations were aqueous solutions of potassium chloride and hydrochloric acid. The exposed electrodes were either (1) a Ag/AgCl blade (2.25cm x 1.0 cm x 0.05cm) or (2) a semi-silvered, sandblasted, glass blade and the immersed counter electrode was a Ag/AgCl wire (0.06 cm in diameter). Sandblasted slides were covered with silver by sucrose reduction of a silver ammonia complex. The lower half of the blade was again sandblasted to remove the silver on that section. Sandblasting insures the wettability of the electrode. The vapor was hydrogen chloride. Dry nitrogen continuously flowed through the cell at a flow rate of 60 ml/min.. The nitrogen was passed through a series of filters (anhydrous calcium chloride, potassium hydroxide and charcoal) before entering the cell. The basic cell design in all experiments is shown in figure 3.1. The glass container (internal diameter, 3.6 cm) of the cell has a total volume of 60 ml. The volume of electrolyte used in all experiments was 15 ml.

A hydrochloric acid solution (12M) in a closed Erlenmeyer flask w as allowed to reach equilibrium with its own vapor. A given volume of the HCl vapor was then withdrawn from the flask with syringes and subsequently injected into the carrier gas stream. All chemicals were reagent grade and distilled water was used in the preparation of all solutions. The various electrolytes were uniformly stirred by a magnetic stirrer. These experiments were performed at

room temperature (26_ 1°C).

A. Measurement of Cell Potential

Given volumes of HCl vapor were injected into a regulated stream of nitrogen entering the cell, Ag/AgCl (exposed blade)/ HCl or KCl, aqueous/ AgCl/Ag (immersed wire). Two different experiments were performed: (1) for a fixed bulk concentration of KCl or HCl, the change in cell potential was recorded as a function of the volume of HCl vapor injected and (2) the change in cell potential was recorded when the bulk electrolyte concentration was varied while the volume of HCl vapor injected was kept constant. An electrometer (D.C. Multimeter, model MV77B, Millivac Instruments) was used to measure the maximum potential changes which were recorded (Sargent model SR recorder) as a function of time. In order to justify the use of the recorder (balancing speed: 1 second for full scale travel), it was necessary to determine the duration of the potential rise in a measurement of emf vs. time. An oscilloscope (Hewlett-Packard, model 130C with Dumont camera attachment) was used in place of the recorder. The time of the potential rise was found to be of the order of 3 to 6 seconds depending upon the volume of vapor injected. Therefore, for convenience, the recorder was used in all our experiments. After injection of HCl vapor into the cell, the cell emf increases to a maximum value (fig. 3.2). With time, the cell emf decays to its initial value. After repeated injections of HCl vapor, the cell emf does not return to its initial value but

levels off at some higher emf due to the change in bulk electrolyte concentration. The difference between the maximum instantaneous emf and the initial emf was selected as the parameter to be reported.

B. Emf of HCl Concentration Cells with Transference

The emf of HCl concentration cells with transference were measured, e.g. Ag/AgCl/ 1M HCl// HCl, xM/AgCl/Ag where 1M $\leq$ xM $\leq$ 12M; where the junction is made with a 1M HCl bridge.

A priori it was postulated that the absorption of HCl vapor at the level of the meniscus formed on the exposed electrode would create a momentary concentration cell with transference between the exposed blade and the immersed wire electrodes of the absorption induced electrode potential cell. In order to estimate the maximum momentary concentration of HCl on the exposed electrode of the AIEP cell, the emf's obtained with the cell were compared to the emf's of a classical concentration cell with transference. According to our hypothesis, for the same emf's the difference in concentrations must be comparable for the two systems. The analogy between the "classical" concentration cell with transference and the AIEP cell can be seen from the following. After injection of HCl vapor into the cell, the exposed electrode is at a concentration C_M ($C_M > C_B$ is the bulk electrolyte concentration). The exposed electrode and meniscus region would then correspond to the x_M compartment of the classical cell while the bulk electrolyte (1M

HCl) and the immersed electrode correspond to the 1M HCl compartment of the classical cell. The junction in the AIEP cell is the direct contact between C_M and C_B.

C. Influence of the Dimensions of the Exposed Blade Electrode on the Cell Emf

2 cc of HCl vapor were injected into the AIEP cell described in II-A. The dimensions of the exposed blade electrode were changed in order to determine their effects on the emf obtained with a given injection. Experimentally, the emf is practically independent of the width of the blade. It is dependent upon the relative position of the bottom of the blade with respect to the planar portion of the solution/air interface (fig. 3.3).

D. Influence of the Position of the Bottom Edge of the Exposed Electrode at Different Levels in the Meniscus

Practically, the bottom of the Ag/AgCl blade cannot be above the planar portion of the solution/air interface otherwise the blade will not support a meniscus. Instead, a sandblasted, semi-silvered, glass blade electrode was used. With this electrode it is possible to position the silvered part of the blade at any level in the meniscus; the bottom part of the electrode (sandblasted glass) supports the meniscus. Electrode positions were measured with a Gaertner precision cathetometer to ± 0.05 mm.

II. Results

A. Influence of the Volume of HCl Vapor Injected on the Cell Emf

In the first series of experiments the bulk electrolyte concentration was fixed at 1M so that data were obtained for the changes in emf as a function of the volume of HCl vapor injected. The experimental results are shown in figure 3.5. The upper abscissa of figure 3.5 represents the volume (cc) of HCl vapor injected on a log. scale. A curve was traced through the experimental points.

B. Emf's of Concentration Cells with Transference

The emf's of the concentration cells with transference were plotted on the ordinate of figure 3.5 in the following manner. A horizontal line, intersecting the experimental curve, was drawn for each measured emf. The intersections of these horizontal lines with the previously traced curve determined the position of the values of xM on the middle abscissa of figure 3.5.

C. Variation of Cell Emf as a Function of the Bulk Electrolyte Concentration for a Given Injected Volume of HCl Vapor

A fixed volume of HCl vapor was injected into the carrier gas stream entering a Ag/AgCl (exposed blade)/HCl, aqueous/AgCl/Ag (immersed wire) cell. The maximum changes in emf for various concentrations of the electrolyte were measured. The results are shown in figure 3.6 where the measured emf's have been plotted as a function of the Log. of the bulk concentration of electrolyte. In the potential measurement experiments, no visible physical changes of the silver-silver chloride electrodes were observed.

D. Influence of the Position of the Bottom Edge of the Exposed Blade Electrode vs. the Plane of the Liquid/Air Interface

Figure 3.4 is a representative experiment of the emf response vs. the relative position of the bottom of the silvered segment of the semi-silvered electrode with respect to the maximum upper meniscus boundary. The surface tension of the electrolyte was measured before and after each experiment. From the results, the maximum height of the meniscus was calculated and taken as the origin on figure 3.4. An arrow indicates the vertical distance between the top of the meniscus and the horizontal plane of the electrolyte.

III. Discussion

A. Apparent HCl Concentration in the Meniscus

When HCl vapor penetrates into a Ag/AgCl (exposed blade)/HCl, aqueous/AgCl/Ag (immersed wire) cell, it can be assumed that the concentration of chloride ion around the exposed electrode increases suddenly. The difference in chloride ion activity between the exposed and immersed electrodes suggests, as we have already mentioned, a concentration cell with transference. The maximum apparent concentration of HCl in the meniscus was estimated experimentally. The experimental approach has been to assume that identical emf's obtained with an AIEP cell and a classical concentration cell with transference must correspond to comparable concentration differences. Therefore, the variable concentration of the classical cell with transference is plotted

in the lower abscissa of figure 3.5 to fit the experimental curve of emf vs. volume injected (log. cc.) obtained with the AIEP cell. The middle abscissa represents, then, the apparent HCl concentration in the meniscus. Figure 3.5 therefore has two abscissae which represent from top to bottom: (1) the volume of HCl vapor injected into the cell and (2) the HCl concentrations (xM) of the concentration cells with transference.

B. Respective Contributions of the Sheath of Wetting and the Meniscus of the Exposed Electrode to the Cell Emf.

When a wettable blade is vertically withdrawn from a liquid surface, it forms a meniscus. Beyond a certain height, h, the maximum height of the meniscus, any further extension of the blade will only increase the sheath of wetting which covers the blade above the top of the meniscus. If the blade is situated in an atmosphere saturated with water vapor, the sheath of wetting will cover the entire blade. Eventually, the sheath of wetting will slowly thin out due to drainage. On the other hand, if the blade is situated in a continuously replenished atmosphere, as in our experiments, the sheath of wetting will evaporate down to a position relatively close to the upper boundary of the meniscus. The thickness of the sheath of wetting is determined by the electrolyte and the surface of the electrode [39-41]. It represents the minimum possible liquid thickness on the electrode.

Let us consider two cases in which: (1) the meniscus and the sheath of wetting are taken into account and (2) the existence of the meniscus is disregarded and replaced by a film of uniform thickness, $\mathcal{E}$, which forms a right angle boundary with the bulk electrolyte at the liquid/gas interface.

Let us assume for the first case that n moles of HCl vapor enter the cell and are absorbed into a volume A $x \mathcal{E}$ where A is the total liquid/gas interface; 10.8 sq. cm. in our case and $\mathcal{E}$ is a thickness. The area of the meniscus and adjacent film can be estimated geometrically to be 10% of the total liquid/gas area of 0.1A. As an example, when 1cc of HCl vapor was injected into the carrier gas stream entering a Ag/AgCl (exposed blade)/1M HCl/ AgCl/Ag (immersed wire) cell, the emf changed by 20.2 mV. From figure 3.5 (middle abscissa) the maximum apparent HCl concentration in the surface volume A x $\mathcal{E}$ should be 1.4×10^{-3} moles/cc. The increase in the number of moles of HCl after injection was 36.4×10^{-7}moles. This increase was determined by injecting the stated volume of vapor into an equivalent system in which the HCl electrolyte is replaced by distilled water. By measuring the pH of the distilled water before and after the injection of vapor, the increase in the number of moles of HCl was calculated. Of these moles, 3.64×10^{-7} were in a volume 0.1A x $\mathcal{E}$ cc's with an apparent concentration of 1.4×10^{-3} moles/cc. Therefore:

$$\epsilon = (3.64 \times 10^{-7} / 1.08 \times 1.4 \times 10^{-3}) \simeq 2.4 \mu$$

For the second case, let us assume that (1) a film of uniform thickness, $\mathcal{E}$, exists in place of a meniscus and (2) that only 10% of the total moles of HCl entering the cell are absorbed into the volume: 2 x L x H x $\mathcal{E}$ (where L is the length of the blade along the liquid/gas interface, H is the height of the blade and $\mathcal{E}$ is the thickness of the sheath of wetting on the blade). For the experiment cited in case (1), the blade was 2.25 cm long by 0.6 cm high, therefore for case (2):

$$\mathcal{E} = (3.64 \times 10^{-7} / 2 \times 0.6 \times 2.25 \times 1.4 \times 10^{-3}) \approx 1\mu$$

Mathematically the shape of the meniscus on a vertical planar surface is represented by:

$$X = X^{o} - (2h^2 - y^2)^{\frac{1}{2}} + (h/\sqrt{2}) \ln \left[\frac{(h\sqrt{2} + \sqrt{2h^2 - y^2})}{y} \right]$$

eq. 1.6

where h is given by eq. 1.5, the Laplace equation of capillarity, y is the vertical position in the meniscus, X is the horizontal distance from the vertical surface and X^{o} is a constant of integration which is given by : $0.377 (\gamma/\rho g)^{\frac{1}{2}}$. By substituting for X the values of $\mathcal{E}$ (calculated above), 1μ and 2.4μ, the corresponding values of y are $\approx$ h, i.e. right at the top of the meniscus (upper 0.2mm). Therefore, the main contribution to the emf comes from the very top of the meniscus and from the sheath of wetting which extends vertically from the boundary of the meniscus. The fact that for a given injection of HCl vapor the emf's obtained is the same regardless of the blade height above the meniscus line (fig. 3.3 indicates that a blade 0.6cm high and one 2 cm high give similar emf's when their bottoms are in the plane

of the liquid/gas interface) demonstrates that the sheath of wetting on silver cannot extend vertically much more than 1 or 2 mm.

In addition, by using a semi-silvered, sandblasted, glass electrode we were able to probe from the bottom to the top of the electrolyte meniscus and beyond. When the bottom edge of the silvered segment is placed at the top of the meniscus (the lower portion of the electrode is glass and is supporting the meniscus), the emf drops abruptly. If the silvered edge is raised beyond the top of the meniscus, the emf drops off to zero indicating that contact with the electrolyte has been broken-measurement of current and electrical resistance further indicate that there is no longer any electrical contact. This fact (fig. 3.4) further supports the above conclusion.

According to the previous argument, it was expected that a maximum emf would be obtained when the bottom of the blade was at the maximum height of the meniscus and even slightly above (in the sheath of wetting). At least thirty experiments similar to the one shown in figure 3.4 were performed. The maximum emf measured was generally obtained when the bottom of the exposed electrode had not yet reached the top of the meniscus.

This apparent contradiction between the experimental results and our prediction can be explained by assuming that the height of the meniscus can change instantaneously upon the arrival of vapor (transient lowering of the surface tension and consequent decrease in the maximum height of the

meniscus during the process of adsorption). In addition, within 0.2mm, 1mm below the maximum height, the sheath of wetting is essentially constant. We will examine these factors more closely in part B of this study.

Essentially our conclusion is similar to the conclusion of Will[2], who studies the electrochemical oxidation of hydrogen on partially immersed platinum electrodes. He concluded that the electrode surface above the intrinsic meniscus is covered with a thin electrolyte film of a thickness comparable to or smaller than the surface roughness. The electrochemical process occurs almost exclusively at the upper edge of the meniscus and adjacent film close to it.

In a numerical example given by Will[2], the narrow band (active region) is 0.35mm of the meniscus and 0.38mm of the adjacent film with a film thickness of 1.0 μ for the case of SN H_2SO_4 electrolyte and an applied potential of 400 mV. The active region is responsible for 98% of the total response.

C. Emf Variation as a Function of Bulk Electrolyte Concentration for a Fixed Injected Volume of HCl Vapor

In the case of HCl vapor, the exposed electrode is the anode. When HCl vapors are injected into the cell, the blade electrode senses a whole range of HCl concentrations from the meniscus-sheath of wetting zone down to the bottom of the blade (which is positioned in the bulk of the meniscus). In conclusion, the use of the Nernst equation allows only the calculation of the apparent instantaneous HCl

concentration in the meniscus for a given volume of injected vapor. The solid lines on figure 3.6 have been calculated using equation 3.3 and the X values obtained from figure 3.5. It can be seen that the agreement with the experimental results is quite good. This agreement indicates that by using the Nernst equation we are in fact calculating an apparent concentration of HCl which corresponds to a uniform concentration along the exposed electrode. However, in reality there is a gradient of concentration from the top to the bottom of the meniscus.

IV. Conclusion

In the case of an ionizable vapor (HCl) and an absorption induced electrode potential cell with reversilbe electrodes, it is concluded that the emf response can be described as that of a concentration cell with transference. Moreover, the sensitivity of the cell (Δ mV) depends primarily on the presence of a meniscus on the exposed electrode. Although a concentration gradient is set up on the exposed electrode when HCl vapor is injected into the cell, the emf between the exposed and immersed electrodes can be thought of as a concentration cell with transference.

This study also shows the unusual fact that the response of this type of electrochemical cell is solely due to the active zone formed by the upper part of the meniscus and the lower part of the adjacent film.

Study I, Part B

I. Experimental

The electrolytes used in this investigation were aqueous solutions of hydrochloric acid. All chemicals were reagent grade and distilled water was used in the preparation of the electrodes, the preparation of the test vapor (hydrogen chloride), instrumentation and the pre-treatment of the nitrogen carrier gas have been described elsewhere and in Part A of this chapter. [63,76,77] These experiments were performed at room temperature (26±1°C).

A. Influence of the Volume of Vapor Injected and the Applied Potential on the Cell Current

Given volumes of HCl vapor were injected into a regulated stream of filtered nitrogen entering a Ag/AgCl (exposed blade) anode/1M HCl/ AgCl/Ag (immersed wire) cathode cell. A fixed potential was applied to the electrodes of the cell. Using either an electrometer-recorder system or an oscilloscope-camera system (see part A, I), the variation of the cell current was then measured as a function of time as HCl vapor was injected into the stream.

The cell current increases to a maximum within 3 to 5 seconds after injection of HCl vapor. With time, the cell current decays to its original value. After repeated injections of HCl vapor, the cell current does not return to its initial value but levels off at some higher value due to the change in the bulk electrolyte concentration. The experi-

ments were repeated at several values of the applied potential and for several bulk electrolyte concentrations. The difference between the initial current and the maximum in the transient current, Δ i, was selected as the parameter to be reported.

B. Influence of the Dimensions and Position of the Exposed Blade Electrode on the Current

2cc's of HCl vapor were injected into the AIEP cell described in II-A. The dimensions of the exposed blade electrode were changed in order to determine their effects on the cell current obtained with a given injection of vapor. A Gaertner precision cathetometer was used to measure the vertical electrode position relative to the horizontal plane of the electrolyte to $\pm$0.05 mm. Experimentally the current is dependent upon the relative position of the bottom of the blade with respect to the plane of the electrolyte and upon the length of the blade along the electrolyte/air interface (see figure 3.7). It is pratically independent of that portion of the blade above the upper boundary of the meniscus.

Practically, the bottom of the Ag/AgCl blade cannot be above the plane of the solution otherwise the blade will not support the meniscus. Therefore in place of a Ag/AgCl blade, a semi-silvered, sandblasted, glass blade electrode was used. With this electrode, it is possible to position the silvered part of the blade at any level in the meniscus; the bottom portion of the electrode (sandblasted glass)

supports the meniscus.

C. Electrical Resistance Measurements

Electrical resistance measurements were obtained as a function of electrode position in the electrolyte using a conductivity bridge (Industrial Instruments Inc., model RC-18J operated at 1000 and 3000 cps. The exposed electrode was raised and lowered by means of a screw device. A Gaertner precision cathetometer was used to measure electrode positions to ±0.05mm.

In all the experiments described in II-A-D, the surface tension of the electrolyte was measured and found to be the same before and after each experiment.

II. Results

A. Effect of Applied D.C. Potential on the Cell Current

With the bottom of the Ag/AgCl (solid) blade at the electrolyte/air interface, i.e., in the bulk of the meniscus, the current due to the bulk electrolyte of a Ag/AgCl (blade) anode/ 1M HCl/ AgCl/Ag (immersed wire) cathode cell increases from a few μamps to about 1500 μamps as the exposed blade was made more anodic (applied potential was increased from 0 to 1200 mV . (See figure 3.8 curve i). The current change (Δi) produced by the injection of a fixed volume of HCl vapor (0.5cc) into the cell increases to a maximum of approximately 600 μamps at applied potentials between 900-1000 mV. (see figure 3.8, curve Δi).

B. Influence of the Volume of Vapor Injected into the Cell

When HCl vapor is injected into the carrier gas stream entering the AIEP cell described in III-A at an applied potential of 800 mV, a change in current (Δ i) is recorded. The maximum change in current (Δimax) as a function of the volume of HCl vapor injected into the cell is shown in figure 3.9. A plateau is reached as increasing volumes of HCl vapor are injected into the cell.

When HCl molecules enter the cell, some of the molecules are adsorbed at the liquid/gas interface and some are swept out of the cell by the carrier gas stream. The adsorbed molecules can either (1) desorb into the gas phase, (2) become absorbed and diffuse into the bulk or (3) react at the partially exposed electrode. For this system (at a flow rate of 60cc of nitrogen per minute), the curve of Δ i vs. volume injected showed a constant value of Δi beyond 9 cc's (and emf vs. volume injected). Therefore, for a given flow rate, the meniscus/gas interface can accommodate only a certain number of HCl molecules; not to imply saturation of the meniscus.

At the beginning of an experiment, the exposed electrode is covered by a thin layer of silver chloride. By performing repeated experiments a thin dark band appears at the upper horizontal edge of the meniscus while the bottom of the blade shows no change. At the upper level of the meniscus the reaction $Ag_{(s)} + Cl^-_{(l)} \xrightarrow{-e^-} AgCl(s)$ is occuring. After a period of time, the thin dark band extended

to that area of the blade anode in contact with the bulk of the meniscus, i.e. at the solid/liquid interface.

C. Influence of the Position of the Bottom of the Exposed Blade Electrode vs. the Plane of the Liquid/Air Interface

Figure 3.10 is a representative experiment of the response vs. the position of the bottom edge of the silvered portion of the semi-silvered electrode with regard to the top of the meniscus. Using eq. 1.5, the maximum height of the meniscus was calculated from the experimental surface tension and taken as the origin on figure 3.10. An arrow indicates the vertical distance between the top of the meniscus and the horizontal plane of the electrolyte,

D. Electrical Resistance of Meniscus and Film

The results obtained from the resistance measurements are reported in figure 3.11 for 1M HCl. The abscissa of figure 3.11 represents the position of the bottom edge of the metallic conductor with respect to the calculated upper meniscus boundary.

III. Discussion

A. Interpretation of Current vs. Time Curves

Analysis of the current vs. time curves indicates that there are two segments to the curves, each of which has a different exponential variation with time. The rising part of the curve varies as exp (Kt) while the decaying part varies as exp (-Jt) where J and K are constants. This can be interpreted as follows.

When HCl vapor is injected into the cell, some of the vapor is absorbed at the liquid/gas interface. The absorbed vapor then diffuses through the meniscus to the electrode surface (x direction). Using Fick's second law, it can be shown (appendix A) that the concentration flux of HCl at the electrode surface is given by:

$$(\partial C/\partial x)_{x=0} = k C_M \exp[\theta^2 D(t-t_p)]$$

The current is then given by $i = nFA\ (\ dC/dx)$ at $x=0$ which explains why the rising part of the current vs. time curve varies as exp (Kt). At a given time t_p, the absorption of vapor and diffusion of HCl to the electrode surface is overshadowed by diffusion down through the meniscus to the bulk electrolyte (y direction). The concentration flux of HCl at the electrode is now given by:

$$(\partial C/\partial y) = k'' C_M \exp[-\lambda^2 D(t_p-t)]$$

(see appendix A). Hence the decaying part of the curve should vary as exp (-Jt). Plots of log. i vs. time (appendix A) are linear thereby demonstrating the conclusion. At the peak, the current is almost independent of time (steady state). Essentially, the technique involves sweeping an electrode with an expontentially varying concentration of an electroactive species. The term "concentration pulse" amperometry has been suggested to describe it.

B. Respective Contributions of the Sheath of Wetting, the Meniscus and the Adjacent Film of the Exposed Electrode to the Cell Current

It was noted that the current change (Δi) resulting

from the injection of a given volume of HCl vapor into an AIEP cell when both electrodes were completely immersed in the cell electrolyte was negligible. However, Δ i increased as the anode (blade electrode) was vertically withdrawn from the bulk electrolyte. The maximum current change was obtained when a meniscus was fully formed on the exposed anode. Experimentally, the exposed electrode must be wettable by the electrolyte and form a meniscus in order to have a sensitive cell.

It can be shown from consideration of Fick's law (see appendix B) that the local current per unit electrode perimeter P(y) as a function of the vertical distance y along the exposed electrode is given by:

$$P(y) = \sqrt{K\,E(y)} \qquad \text{eq. B-12}$$

where E(y) is the local potential at a point y and K is a constant containing C_M, the maximum instantaneous concentration of HCl in the active zone of the meniscus and film, D_o, the diffusion coefficient of HCl at C_M , Q_o is the electrolyte resistivity at C_M and n,F with their usual significance. Although Dr. B. Sohmer of our mathematics department has made several attempts at obtaining a solution to eq. B-12, it remains unsolved because of the complexity of the integral $\int dy/X(y)$. However, for the special case of $y = 0$, ie. at the planar portion of the solution/air interface, the following solution is obtained for the total electrode current when the bottom edge of the silvered portion of the semi-silvered electrode is in the plane $y = 0$:

$$P(0) = \sqrt{K E_a} \qquad \text{eq. B-13}$$

A plot of $P(0)$ vs$(E_a)^{\frac{1}{2}}$ is reasonably linear thereby indicating that the initial assumptions are valid as a first approximation. (fig. 3.12)

Analytically, one would expect the potential $E(y)$ to decrease from E_a at the bottom of the electrode to some smaller potential E_S at the upper edge of the film (which extends vertically 1 or 2 mm above the upper boundary of the meniscus), since a gradient of concentration (dC/dy) of the electroactive species exists along the exposed electrode. However, the manner in which $E(y)$ decays from E_a at $y=0$ to E_S at $y=S$ cannot be determined since the function $\int dy/X(y)$ has not been solved.

The mechanism of the anodic oxidation of molecular hydrogen on partially immersed platinum electrodes has been investigated by Will [2]. In his theoretical treatment of the experimental results, he assumed that the rate of diffusion of hydrogen molecules (as in appendix B) for HCl) from a hydrogen vapor phase (which was blown through two gas wash bottles containing electrolyte of the same concentration as used in his cell) through the electrolyte meniscus and film determined the current. The parameter C_M is in Will's case the solubility of hydrogen in the electrolyte and D, Q are assumed constant for a given bulk electrolyte concentration, i.e. hydrogen doesn't alter the resistivity. In addition, Will approximated the mathematical expression describing the shape of a meniscus on a vertical planar surface with a parabola. Using Nernst's equation and Ficks diffusion law

he derived the following relationship between j(y), the current per unit circumference of a tubular electrode, and E(y) the potential at a given height, y, in the meniscus and adjacent film:

$$j(y) = (2nFDC/Q)^{\frac{1}{2}} \quad (E(y))^{\frac{1}{2}} \qquad \text{eq. 2a (ref. 2, eq.23)}$$

where Q is the electrolyte resistivity. This result implied that the same square root relationship applied at any point in the meniscus and film. For $y = 0$, i.e. the plane of the electrolyte, the potential E(y) equals the applied potential E_a and the total current j(y) becomes:

$$j(o) = (2nFDC/Q)^{\frac{1}{2}} \quad (E_a)^{\frac{1}{2}} \qquad \text{eq. 2b}$$

Will concluded that the contribution to the total current from the lower part of the meniscus from $y = 0$ to $y = 0.9h$ was of the order of 3%. The main contribution was attributed to the upper 10% of the meniscus and several tenths of a millimeter of the liquid film. What the relative contributions of the meniscus and film are depended on the applied potential, electrolyte concentration and film thickness. The potential along the vertical electrode surface was observed by Will to decrease very little over the larger length of the meniscus ($y = 0$ to $y = 0.9h$). The potential change occurred mainly at the upper part of the meniscus, i.e. $E(y) = E_a$ at $y = 0$ to $y = 0.9h$ and E(y) decreases to 0 from $y = 0.9h$ to the upper edge of the film.

At this point, we should contrast some of the differences and similarities between Will's work and mine.

In my system, dry nitrogen gas is continuously passed through the cell at a flow rate of 60 cc/min (at constant temperature). Under these conditions, the length of the electrolyte film, which extends vertically beyond the upper boundary of the meniscus, is relatively short- 1 or 2 mm. The reason that the film is so short (i.e. that it doesn't cover the entire electrode) is that evaporation of the electrolyte film into the dry gas phase reduces the film length to an equilibrium position relatively close to the top of the meniscus. However, in Will's work, hydrogen gas is passed through two wash bottles containing electrolyte of the same concentration as used in his experiment before entering the cell. The hydrogen is therefore saturated with respect to the electrolyte solution and film evaporation is minimized. Under these conditions, the electrolyte film will cover virtually the entire electrode above the meniscus.

Secondly, my test vapor, hydrogen chloride, is quite soluble in the cell electrolyte (1M HCl). After absorption at the meniscus/gas interface, the injected vapor diffuses to the electrode surface. The measured current is a function of the HCl flux $(dC/dx)_{x=0}$ at the electrode surface, and hence increases as a function of time. Since the concentration of HCl at the electrode surface increases with time, so does the diffusion coefficient and the electrolyte resistivity decreases. However, at some time t_p (the maximum in the transient), the vapor is (1) no longer being absorbed at the meniscus/gas interface and (2) now primarily diffuses down the meniscus to the bulk electrolyte: the

entire active zone of the meniscus being at a "uniform" instantaneous HCl concentration C_M. At this time (t_p), the ratio ($D_O C_M / Q_O$) is constant for a given injection of vapor. Therefore, the currentp per unit perimeter of electrode (i_{max}/perimeter) should vary linearly with E_A at constant injected volume of HCl

On the other hand, Will used sulfuric acid electrolytes containing dissolved hydrogen with his gas phase. Under his conditions, the measured current is a function of the equilibrium concentration of hydrogen in sulfuric acid (which is constant). Therefore D and Q for his system are also constant.

Finally, Will employed platinum tubing as his test electrode. With this electrode, one never eliminates the contribution of the bulk phase and lower meniscus to the total current as the Pt tube's upper edge is raised relative to the plane of the electrolyte. This is so because the Pt tube must be long enough to have part of the tube submerged at all times in order to support a meniscus. However, with my semi-silvered, sandblasted, glass electrode, I am able to position the bottom edge of the silvered portion at any level in the meniscus (the bottom segment of the electrode is sandblasted glass which will support the meniscus without contributing to the total current). Thus I am able to determine the contribution of the various parts of the meniscus and film to the total current.

One should note that the shape of a meniscus on a verti-

planar surface is given by:

$$X = X^{o} - \sqrt{2h^2 - y^2} + h/\sqrt{2} \ \ln \left[(h\sqrt{2} + \sqrt{2h^2 - y^2})/y \right] \quad \text{eq 1.6}$$

where all the terms have been previously defined. However, the choice of a parabola (by Will[2]) or any other function simpler than an epicycloid (eq. 1.6) as an approximation of the shape of a meniscus will yield the same result for the case cited above, i.e. $y = 0$, the planar portion of the solution/gas interface.

According to the foregoing discussion, it was expected that the maximum current change (Δi) would be obtained when the bottom edge of the silvered portion of the semi-silvered, sandblasted, glass blade was at the upper meniscus boundary or even slightly above into the sheath of wetting. Actually, the maximum Δi, as shown on figure 3.10 was generally obtained before the bottom edge of the silvered portion if the blade had reached the top of the meniscus. This apparent contradiction, which was also observed in the emf study of Part A, can be accounted for in two ways.

In the first, the maximum height of the meniscus can change instantaneously because of a transient lowering of the surface tension during the process of absorption of the test vapor. It is well known that the surface tension of liquids decrease with increasing temperature. [36(p53)] In a typical experiment where 2cc of HCl vapor ($2 \times 3.64 \times 10^{-6}$ moles of HCl) are injected into the cell, the injected HCl molecules will first be adsorbed on the cell's gas/liquid/ interface (area of interface, A; 10.8 sq.cm in our case). After

time t, the adsorbed molecules will have diffused away from the surface and can be considered to have been absorbed in a volume $Ax\mathcal{E}$; being the maximum distance travelled by the diffusing molecules normal to the gas/liquid interface. This absorption process is accompanied by a transient increase in temperature, $\Delta T(^{o}C)$. The heat of dissolution of HCl is 17.4 KCal/mole at 18°C. Calculated values of ΔT for $\mathcal{E} = 1\mu$ and 2.4μ (thicknesses of the sheath of wetting calculated in Part A of chapter 3) are 118 and 49°C respectively. Therefore, the transient lowering of the surface tension due to gas absorption leads to a corresponding transient lowering of the height of the meniscus. The above values of ΔT are really limiting cases since in actuality the absorption process requires finite time, Therefore, the temperature rise is actually only a fraction of the value given above yet it is significant.

From a computer analysis of the shape of a meniscus on a vertical planar surface (equation 1.6), p36, the following data were obtained for the thickness of the meniscus, X, at several heights, y, in the meniscus:

Table 3.1

Meniscus Thickness as a Function of Position

height, y, (mm)	relative height, y/h	Thickness, X (μ)
2.50	0.650	459.5 + $\mathcal{E}$
2.75	0.715	301.6 + $\mathcal{E}$
2.90	0.775	223.9 + $\mathcal{E}$
3.00	0.781	178.8 + $\mathcal{E}$
3.25	0.847	88.7 + $\mathcal{E}$
3.30	0.860	74.4 + $\mathcal{E}$
3.40	0.885	49.7 + $\mathcal{E}$

3.50 he3.60 3.75	tive height, y/h	Thickness, X (μ)
3.3.84 (top of meniscus)	0.910	15.1 + ϵ
3.60	0.936	9.9 + ϵ
3.75	0.975	2.3 + ϵ
3.84 (top of meniscus)	1.000	ϵ

From y = 3.25mm to y = h (top of the meniscus), the thickness X of the meniscus decreases rapidly. The volume of electrolyte surrounding the exposed electrode in the region y = 3.25 mm to y = h is small in comparison to the rest of the meniscus, i.e. from y = 0 to y = 3.25 mm. Therefore any variation of surface tension, γ , due to heat of absorption will be maximum in that region.

The last way is evident from the steady increase in current associated with the gradual vertical withdrawal of a blade electrode from an immersed position until a full meniscus is formed on the extended electrode surface. In the case of a semi-silvered glass electrode, further vertical extension of the electrode results in additional increase in Δi up to a maximum value when the bottom edge of the silvered segment is at approximately 0.75h. Between 0.75h and h (the top of the meniscus) Δi is essentially constant. When the bottom edge of the semi-silvered portion of the electrode is above the top of the meniscus, Δi decreases sharply (fig.3.10). This behavior is the result of two effects. First, a marked increase in electrolyte resistance is observed as the silvered portion of the electrode is brought through the upper 25% of the meniscus. Second, a discontinuity on the resistance vs. electrode position

curve (fig. 3.11) is noted. This discontinuity arises because at electrode position above the top of the meniscus the electrolyte is no longer on silver but on sandblasted glass. Therefore the sheath of wetting on silver cannot extend much more than 1mm above the calculated top of the meniscus although this is not necessarily true for the sheath of wetting on sandblasted glass surface. This result is not surprising in view of the following. When a wettable blade is vertically withdrawn from a liquid surface, it forms a meniscus. Beyond a certain height h, the maximum height of the meniscus, any further extension of the blade will only increase the sheath of wetting covering the blade above the top of the meniscus. If the blade is situated in an atmosphere saturated with respect to the electrolyte solution, e.g. as in the work of (a) Bennion and Tobias [31], (b) Lightfoot [6], (c) Muller [43] and (d) Maget and Roethlein[3,4] (where these authors a,b) estimated theoretically the stability of liquid films on partially exposed electrodes, (c) determined experimentally the length and thickness of liquid films on partially exposed electrodes and (d) studies the reduction of oxygen on platinum electrodes partially immersed in phosphoric acid respectively the sheath of wetting will cover virtually the entire electrode. On the other hand, if the blade is situated in an atmosphere continously being replenished by dry carrier gas, as in our experiments (Rosano et al[63]), the sheath of wetting will evaporate down to an equilibrium position relatively close to the upper boundary

of the meniscus.

IV. Conclusion

For the system: Ag/AgCl (exposed) anode/1M HCl/ AgCl/Ag (immersed) cathode, the main source of current for the electrochemical reaction: $Ag_{(s)} + Cl^-_{(i)} - e \longrightarrow AgCl_{(s)}$ on the partially exposed electrode is limited to a small active zone at the upper part of the electrolyte meniscus. This fact was established by using a semi-silvered, sandblasted, glass electrode as a probing electrode to determine simply and directly the respective contributions of the meniscus and film to the total cell response when HCl vapor was injected into the cell. With this electrode, we were able to probe from the bottom to the top of the meniscus and beyond by placing the bottom edge of the silvered segment of the electrode at various positions in the meniscus and adjacent film (the lower portion of the electrode is sandblasted glass and is supporting the meniscus). It was also noted that for our experimental system, the electrolyte film which extends vertically beyond the top of the meniscus is limited to about 1 mm in height.

In a recent publication, Will[2] showed that for the oxidation of hydrogen on platinum electrodes partially immersed in sulfuric acid, the measured current was proportional to the square root of the applied potential. This result stands in contrast to the usual proportionality to exp (NF Eapp/RT) found in bulk voltammetry. We decided to test the square root relationship with our system to see if the relationship

is a property of menisci electrodes. For our system, it was found that the current change obtained for a given injection of vapor was also proportional to the square root of the applied potential.

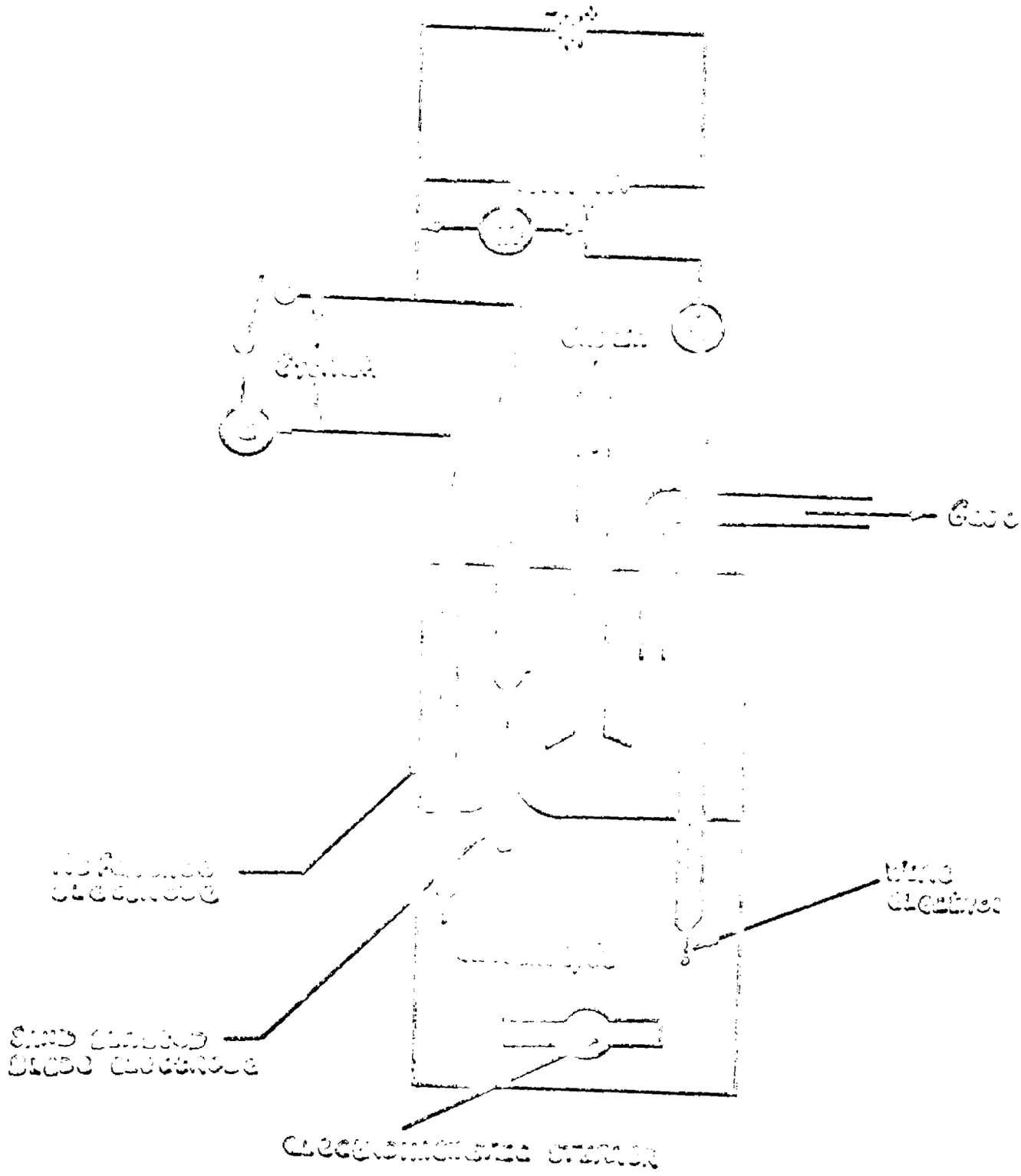

3.2

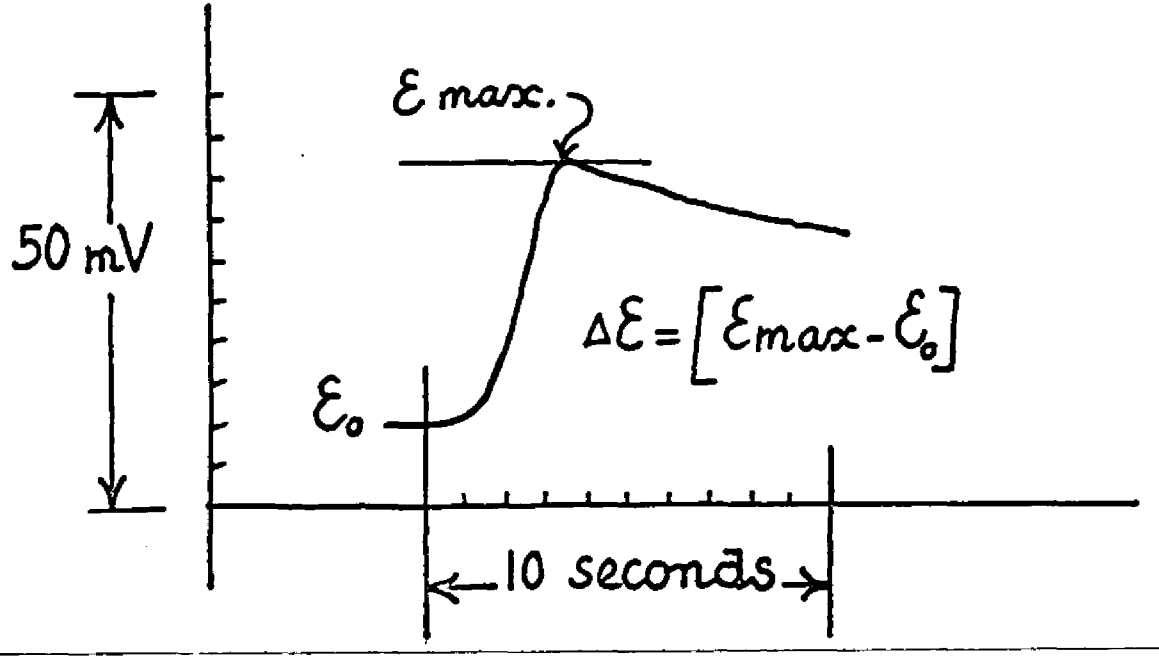

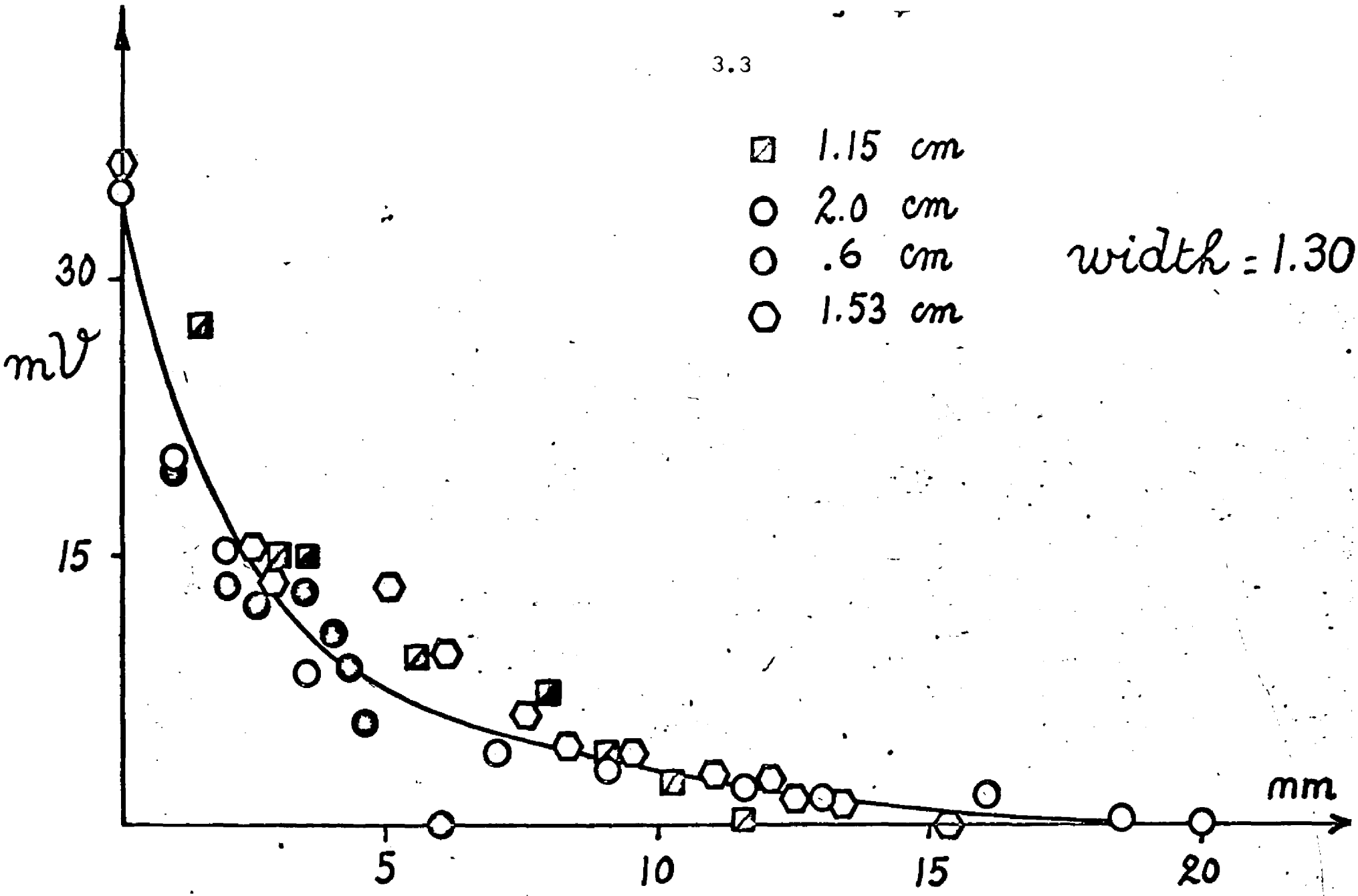

Relative Position of the Bottom of a Solid Blade with Respect to the Plane of the Electrolyte

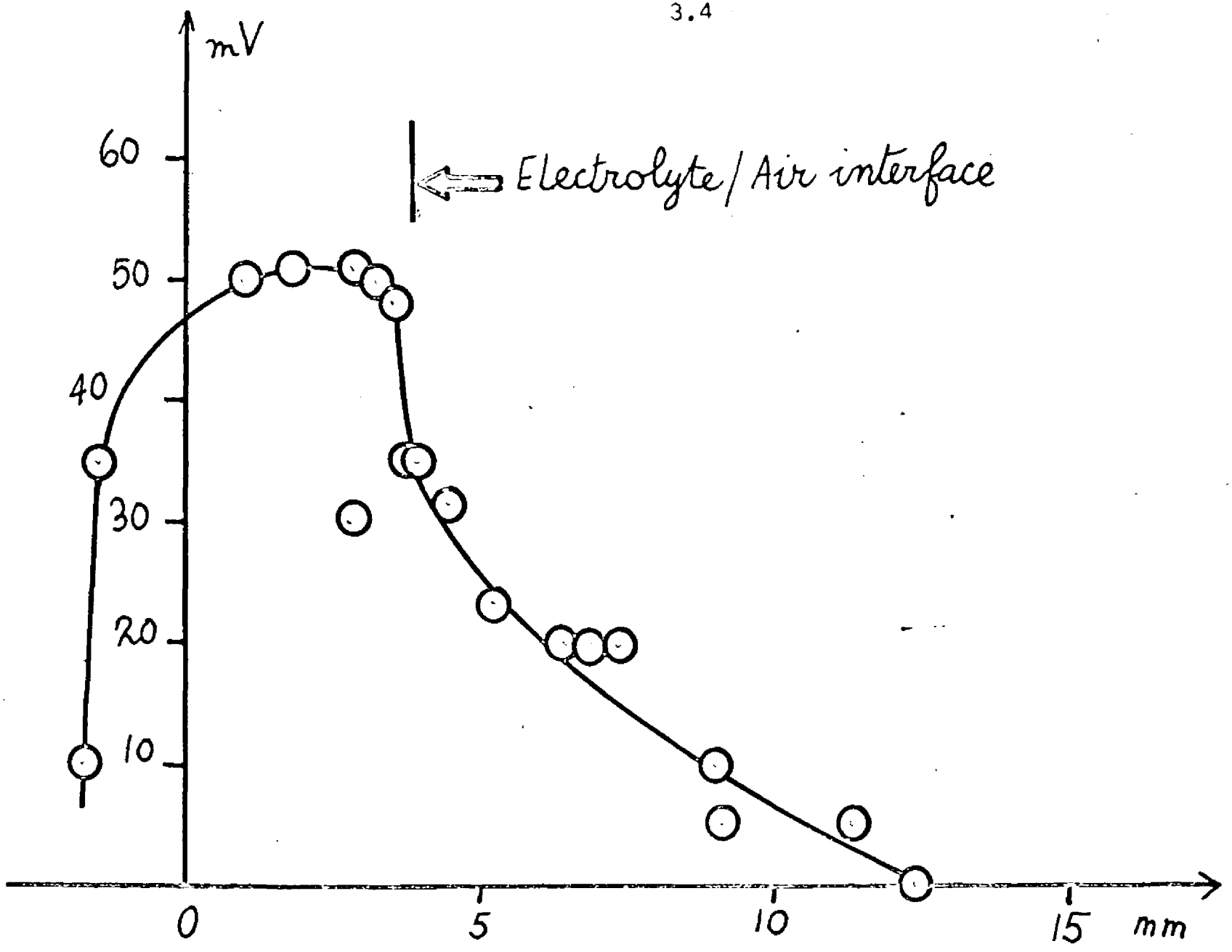

Relative Position of the Bottom of the Silvered Portion of the

Figure 3.5

Ag/AgCl blade / HCl, 1 M Cl / AgCl/Ag wire AIEP Cell: □ ○

Concentration cell with transference:

Ag/AgCl / 1M HCl// xM HCl / AgCl/Ag ○

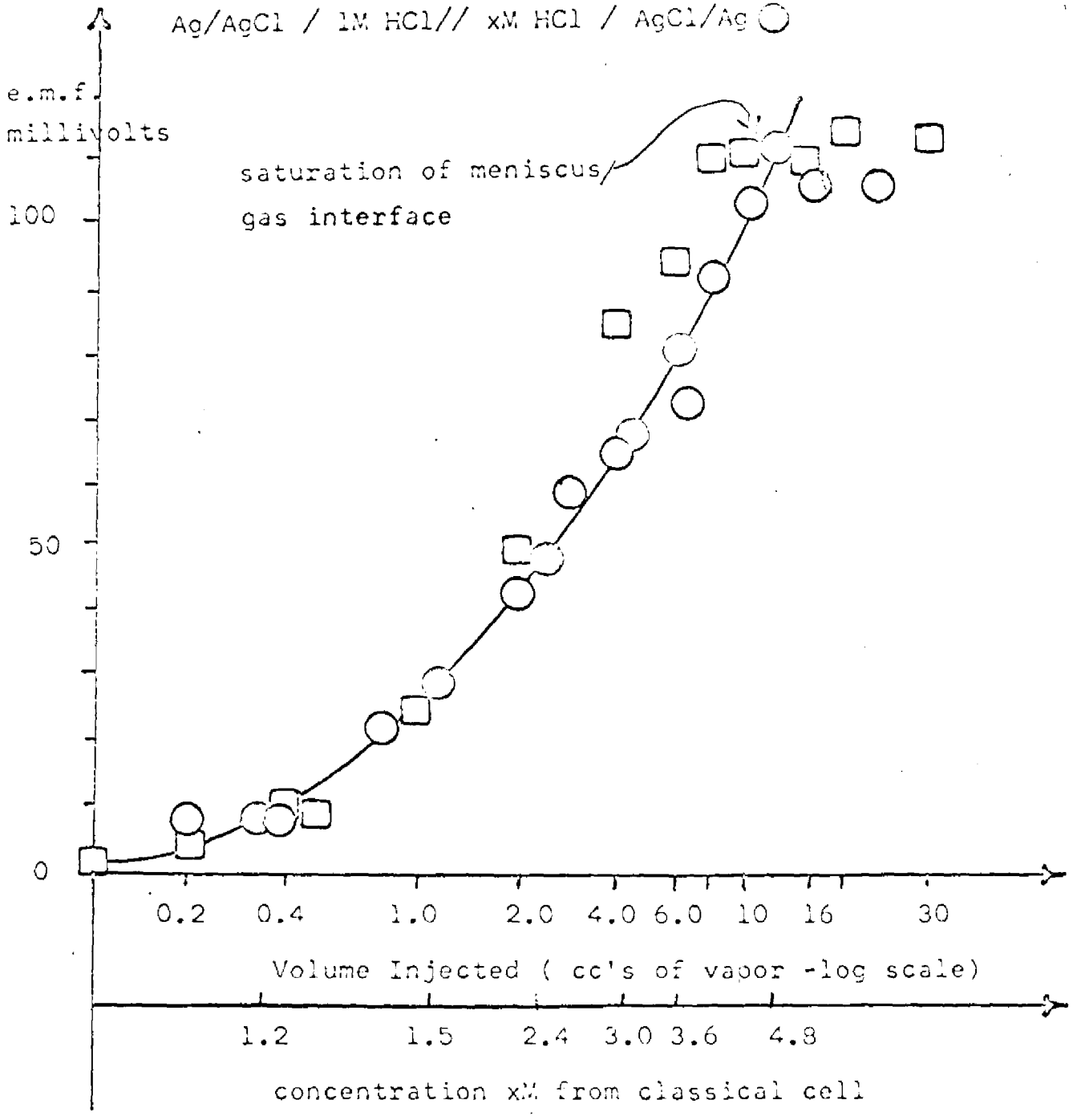

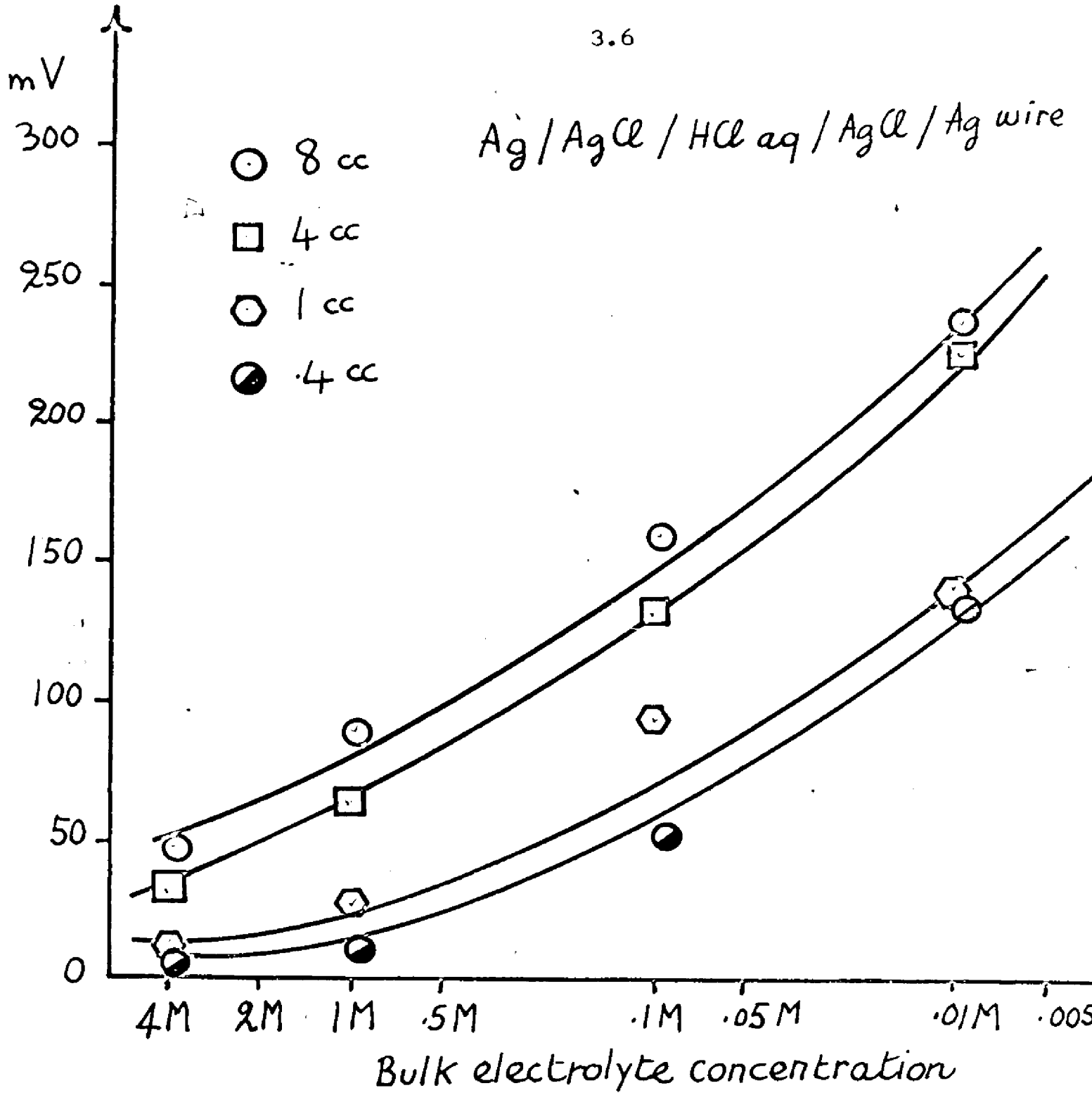
mV
300
250
200
150
100
50
0
8 cc
4 cc
1 cc
·4 cc
Ag / AgCl / HCl aq / AgCl / Ag wire
4M
2M
1M
·5M
·1M
·05M
·01M
·005
Bulk electrolyte concentration

Figure 3.7

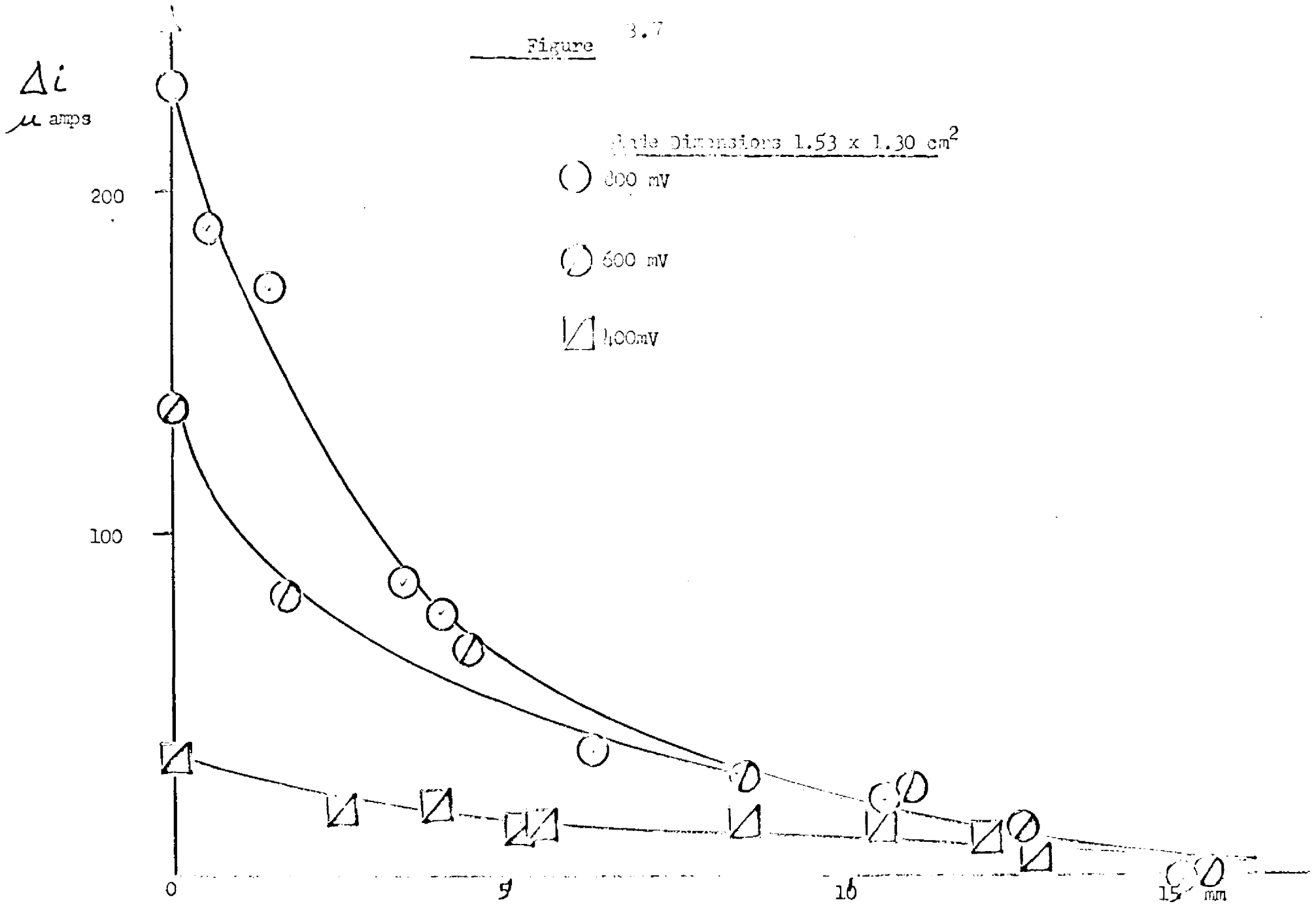

Position of the Bottom Edge of a Solid Blade Electrode with Respect to the Plane of the Electrolyte

Figure 3.8

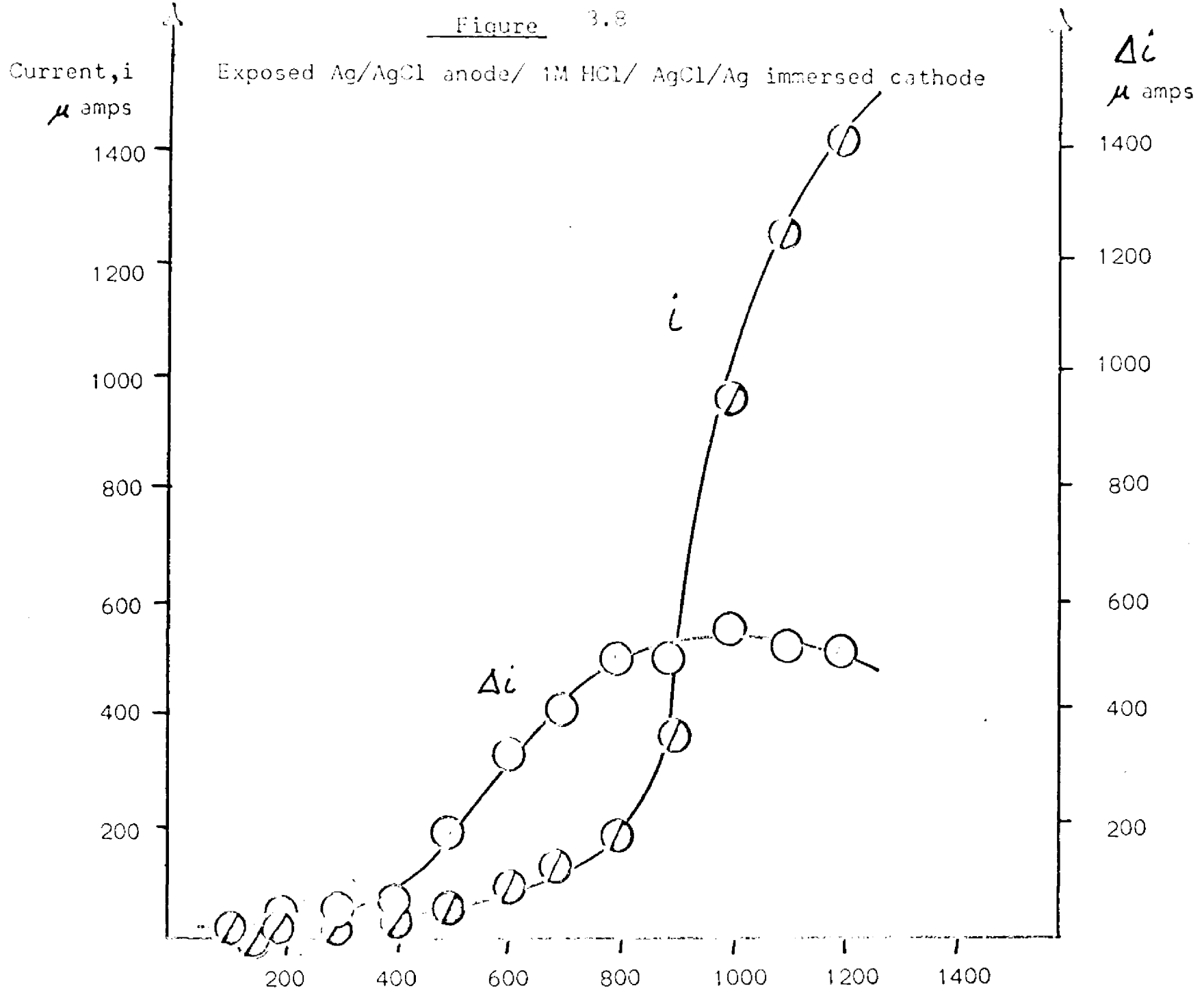
Exposed Ag/AgCl anode/ 1M HCl/ AgCl/Ag immersed cathode
Current, i
μ amps
Δi
μ amps
1400
1200
1000
800
600
400
200
i
Δi
200
400
600
800
1000
1200
1400
Applied Potential (millivolts)

Figure 3.9

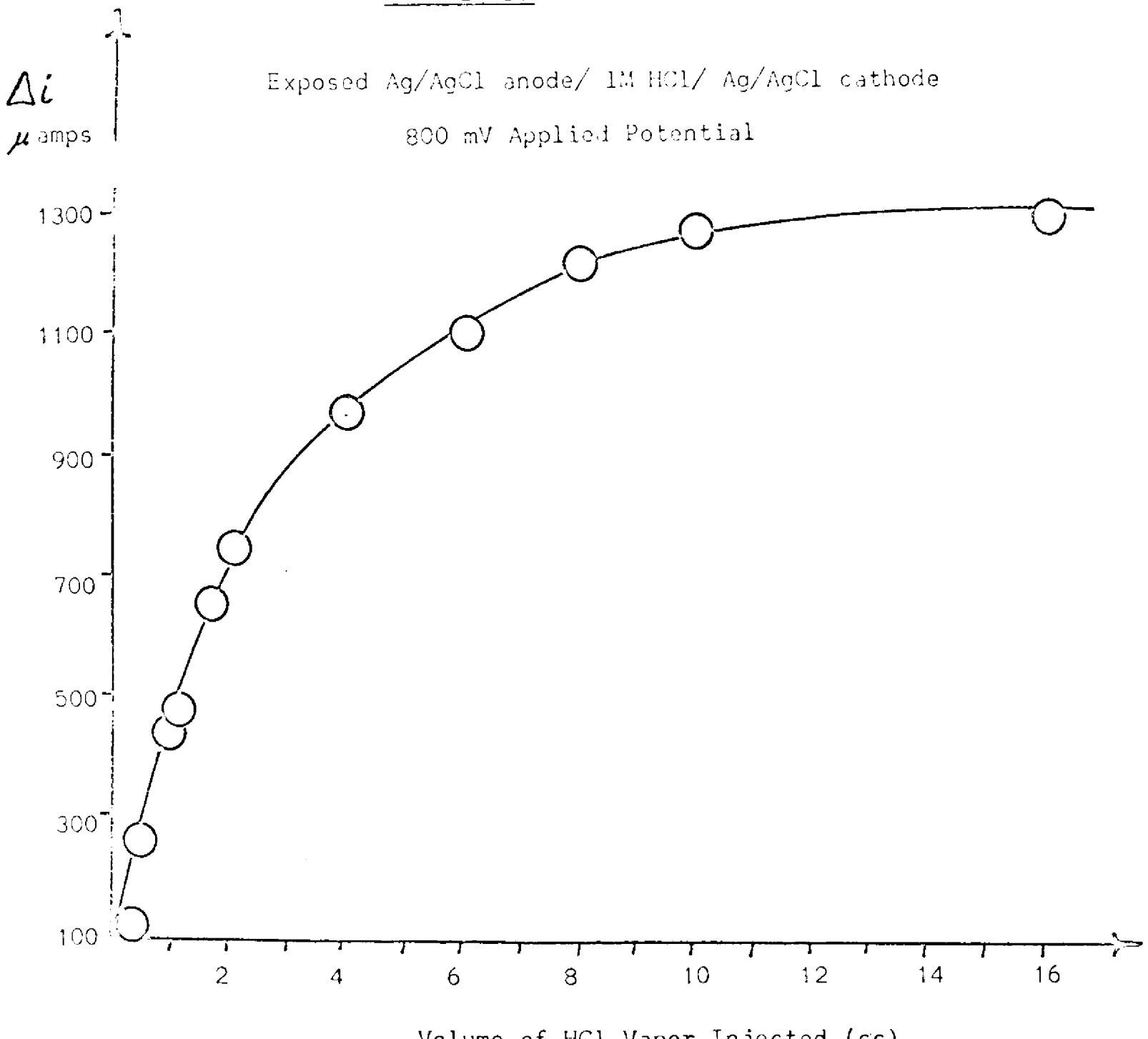
Δi
μ amps
Exposed Ag/AgCl anode/ 1M HCl/ Ag/AgCl cathode
800 mV Applied Potential
1300
1100
900
700
500
300
100
2
4
6
8
10
12
14
16
Volume of HCl Vapor Injected (cc)

Figure 3.10

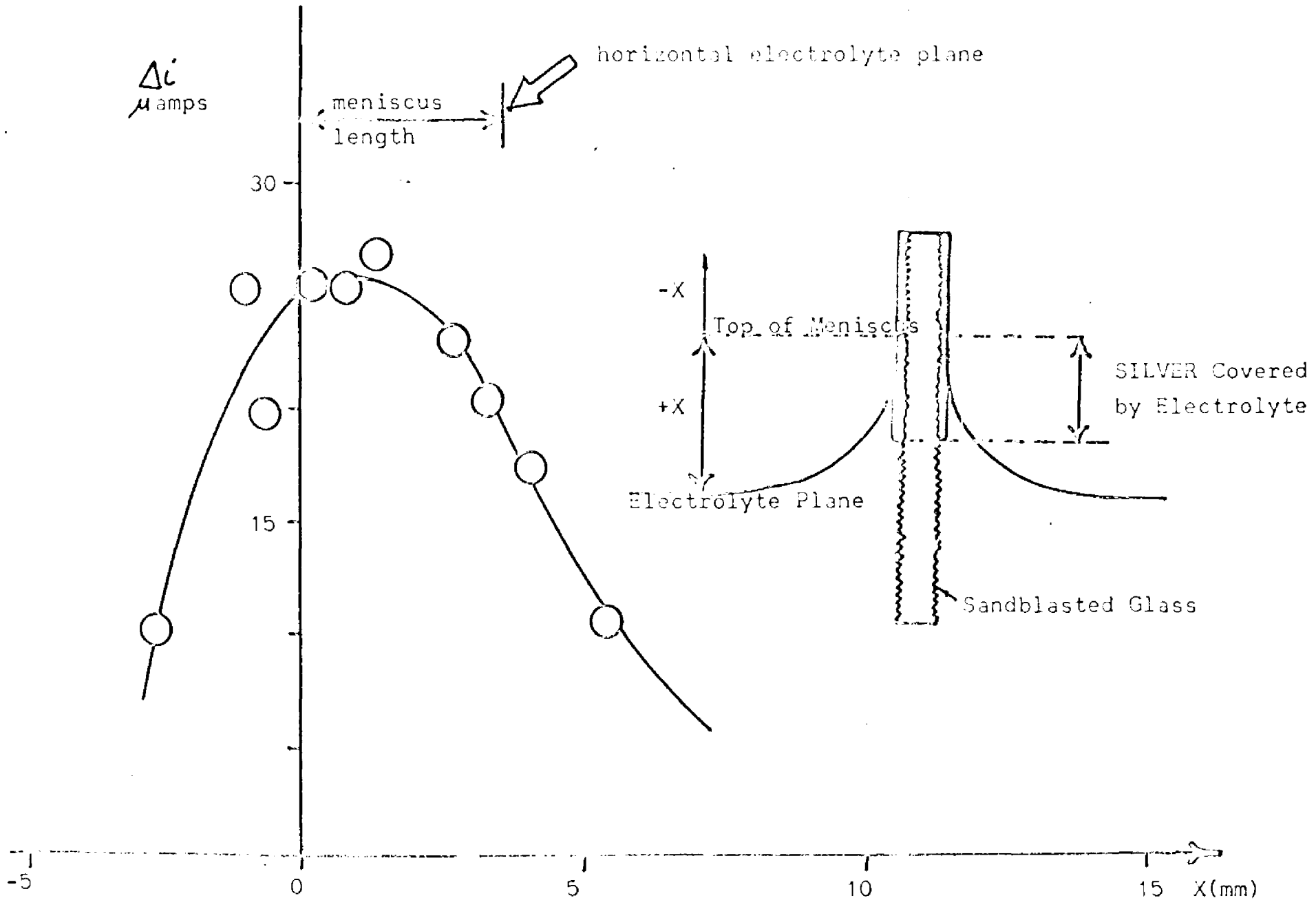

Blade Dimensions: 1.05 x 1.70 cm^2 (600 mV Applied Potential)

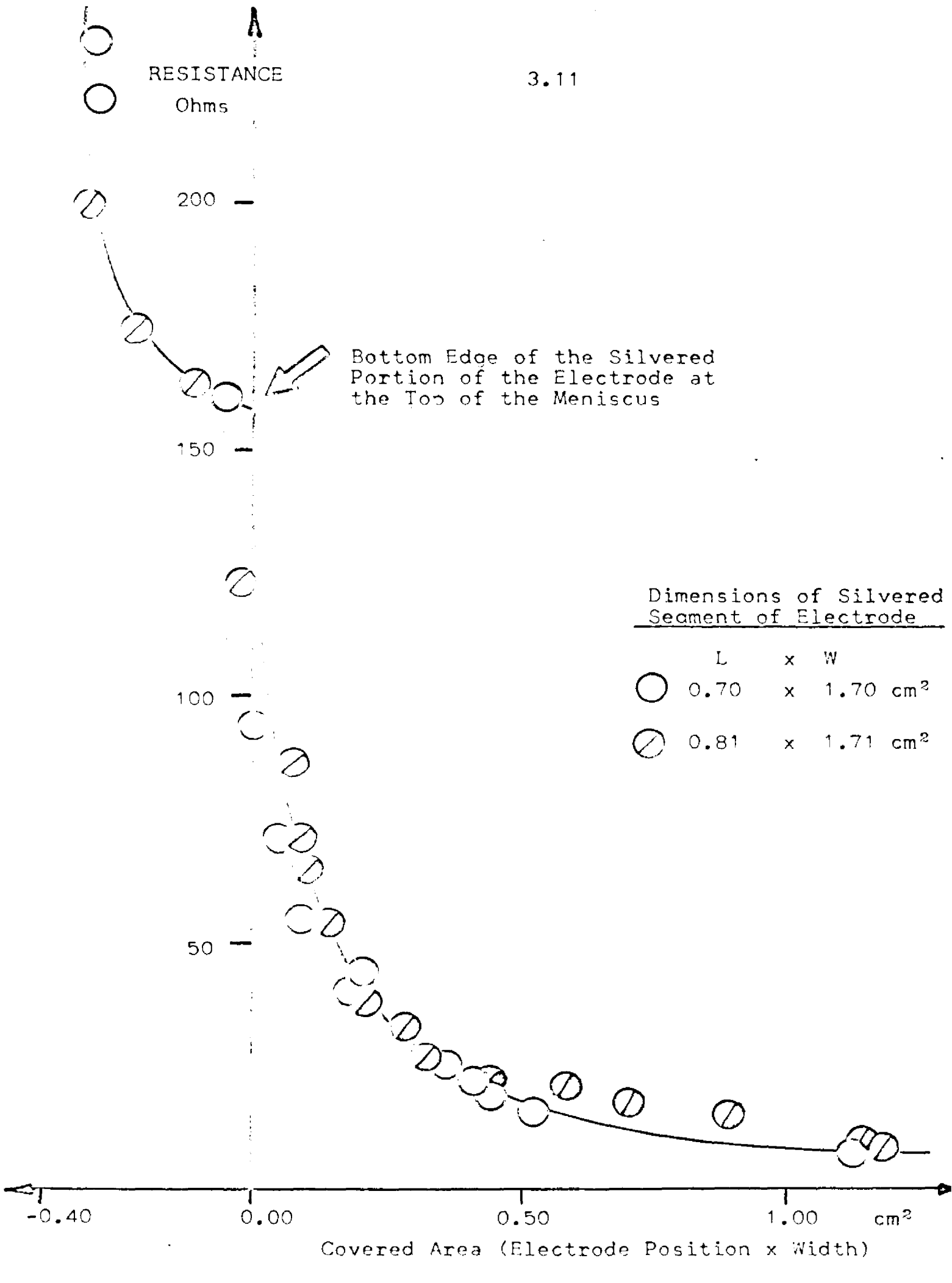
RESISTANCE
Ohms
200
150
100
50
Bottom Edge of the Silvered Portion of the Electrode at the Top of the Meniscus
Dimensions of Silvered Segment of Electrode
L x W
0.70 x 1.70 cm²
0.81 x 1.71 cm²
-0.40
0.00
0.50
1.00
cm²
Covered Area (Electrode Position x Width)

Figure 3.12

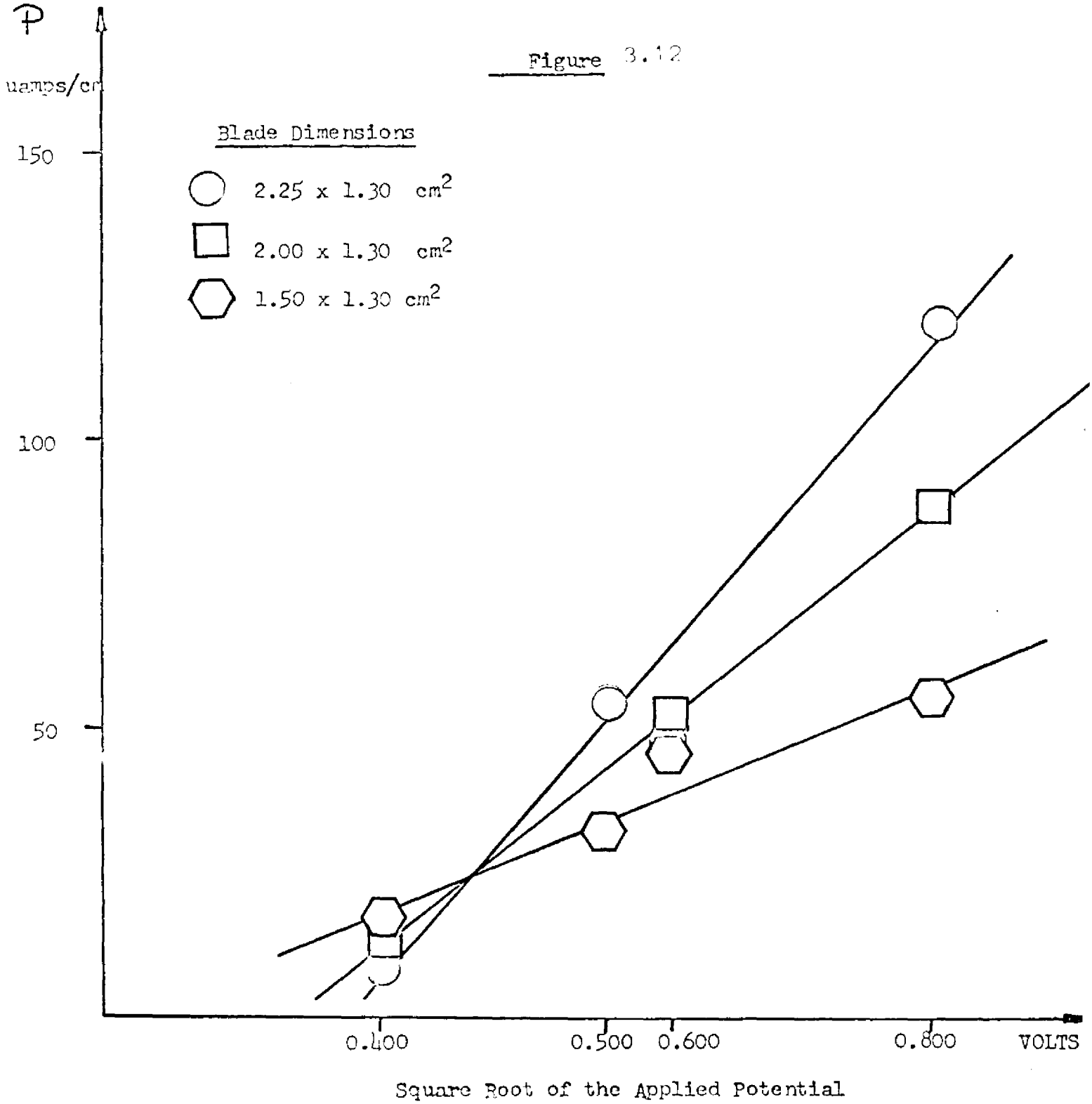
P
uamps/cm
150
100
50
Blade Dimensions
2.25 x 1.30 cm²
2.00 x 1.30 cm²
1.50 x 1.30 cm²
0.400
0.500
0.600
0.800
VOLTS
Square Root of the Applied Potential

CHAPTER 4

Study II: Irreversible Organic Oxidation on the Surface of Partially Exposed Platinum Electrodes in Acid Solution

I. Experimental

The AIEP cell whose basic design is shown in figure 3.1, has an internal diameter of 3.6 cm and a capacity of 60cc. The nitrochromic acid oxidizing mixture, which was employed as the cell electrolyte, was prepared by saturating 70.3% HNO_3 with 99.1% CrO_3. In our experiments, 15 cc of the electrolyte solution were used. The electrolyte was stirred at a constant rate by a magnetic stirrer. The test vapor was obtained by placing 2 cc of 1-butanol liquid in a closed Erlenmeyer flask. The liquid sample was allowed to reach equilibrium with its own vapor. Given volumes of the vapor were then slowly withdrawn from the flask with syringes and subsequently injected into the carrier gas stream. Purified Nitrogen (Evans Co., N.Y.), used as the carrier gas, continuously flowed through the cell at controlled rates. The experiments were performed at room temperature, 25±1°C.

A. Measurement of Transient Currents Produced by Absorbed Alcohol Vapors

A fixed potential was applied to the electrodes of an AIEP cell comprised of a partially exposed platinum anode (blade), a fresh nitrochromic electrolyte solution, and an immersed platinum wire cathode by means of a voltage divider. Using an electrometer (Millivac model 77B, DC Multimeter, Millivac Instruments) and a recorder (Sargent model SR), the transient current resulting from a given injection of alcohol vapor into the cell was measured at several applied potentials as a function of the volume of vapor injected. A

typical current vs. time response is shown in figure 4.1. The time of the current rise was long enough so that a faster response instrument was not required; the recorder has a full scale travel time of 1 second. The difference between the base current and the maximum instantaneous current was selected as the Δi to be reported.

The meniscus formed on the exposed electrode is visible to the naked eye. All the electrodes used in this study have been sandblasted to insure perfect wettability.

B. Determination of the Life-time of the Nitrochromic Electrolyte

We had learned from experience with the experiments in chapter 3 that after repeated injections of HCl vapor into the cell therein described the bulk concentration of the electrolyte changed. Consequently, the electrolyte solution in the cell had to be changed periodically. Since in the present experiments we wished to make as many injections of 1-butanol into the cell as possible before having to change the nitrochromic solution- it's an unpleasant material to handle- it was necessary to determine the "life-time" of the electrolyte solution. In order to evaluate the life-time of a given 15 cc sample of the electrolyte (the volume used in all experiments), 25 cc of alcohol vapor were repeatedly injected into the cell described in I-A over a period of four days. The results are shown on figure 4.2

II. Results

A. Background and Transient Currents

(1) Effect of the Volume of Vapor Injected

Air containing 1-butanol vapor was injected into the nitrogen stream (flow rate 40 cc/minute) entering a Pt anode (exposed blade)/ fresh nitrochromic solution/Pt cathode (immersed wire) cell at an applied potential of 800 mV. As soon as the vapor entered the cell an increase in current was obtained which reached a maximum and then decayed to its original value (fig. 4.1). Generally it takes several minutes before the current decreases to its original value.

In similar experiments, various volumes of air saturated with 1-butanol vapor were injected into the cell described above at carrier gas flow rates of 60,75,110,125,150 cc/ minute and an applied potential of 800mV. The Δ i's obtained as a function of the volume of alcohol vapor injected have been plotted on figure 4.3. Figure 4.4 presents some of the results which for convenience have been plotted as the change in current per cc of vapor (Δi /V) as a function of the volume of vapor injected.

(2) Effect of Applied Potential

The initial current of the AIEP cell described in II-A was less than 1 amp when the applied potential was below 375 mV. This background current (due to components in the electrolyte in the absence of alcohol) increased rapidly with increasing applied potential (figure 4.5). When the exposed electrode was made the anode, 1-butanol vapor produced maximum

currents between 675 and 975 mV (fig. 4.5). No appreciable current was produced when alcohol vapor was injected at applied potentials below 400 mV. Above 1300 mV the cell failed to respond to the incoming alcohol vapor. In addition, as the exposed electrode was made more and more cathodic, the currents obtained with a given injection of vapor fell off to zero. It was also observed that the cell current was dependent upon the length of the exposed blade electrode along the plane of the electrolyte. That is, the current was larger for a longer blade when comparing blades of equal heights. Also, the currents obtained with a solid blade electrode were smaller than those obtained using a gauze electrode of the same dimensions, e.g. same perimeter.

When the exposed electrode was completely submerged in the electrolyte, the current resulting from a given injection of vapor into the cell was negligible. However, Δ i, increased as the anode (blade electrode) was vertically withdrawn from the bulk electrolyte so as to expose it to the gas phase. Therefore, Δ i was also dependent upon the relative position of the bottom edge of the exposed electrode with respect to the planar portion of the solution/gas interface. This observation has also been made by Rosano and coworkers [8-10,63-4,76-78] (and was noted in chapter 3), who pointed out that an electrode partly covered by a stagnant electrolyte, partly emerging into a moving or stationary gas phase can be quite outstanding as a working electrode in an electrochemical cell. It is able to bring to reaction an

electroactive species (reducible or oxidizable) of the gas phase without prior dissolution of the component in the bulk of the electrolyte.

B. Stability of the Nitrochromic Electrolyte

25 cc of 1-butanol vapor were repeatedly injected into the cell described in I-A at an applied potential of 800 mV over a period of four days. The response of this cell appeared to decrease slowly as a function of the number of injections of 1-butanol vapor (fig. 4.2). Despite the fact that as much as 25cc of vapor was injected during each run, the cell's responsiveness remained very high after 42 runs; three days after the experiment had been started. The sudden decrease in responsiveness of the cell shown on figure 4.2 was due to the partial dewetting of the platinum blade since simply redipping the blade into the electrolyte, without disturbing the experimental set-up, and re-establishing the meniscus was enough to restore the high responsiveness of the cell.

III. Discussion

In considering the current produced by a given volume of alcohol vapor which has been injected into the cell under discussion, one must examine the various competing processes which at the very least are: (a) adsorption-desorption of the vapor across the electrolyte/gas interface, (b) chemical oxidation of the alcohol and (c) absorption and diffusion of the alcohol in the meniscus with subsequent electrochemical

oxidation at the exposed electrode.

(A) Adsorption-Desorption

When 1-butanol molecules enter the cell some of the molecules are adsorbed at the electrolyte/gas interface and some are swept out of the cell by the nitrogen stream. The adsorped molecules can either (a) desorb into the gas phase, (b) react chemically with the electrolyte or (c) absorb and diffuse into the meniscus and react electrochemically at the partially exposed electrode.

The amount of alcohol vapor which was not absorbed but was swept out of the cell by the nitrogen stream was estimated by passing the exiting gas stream into a second AIEP cell (secondary cell) which was maintained at the same operating conditions as the primary cell, i.e. the same applied potential, stirring rate, temperature, electrolyte volume, etc. The Δi of the primary and secondary cells were then combined to give the "corrected curve" shown in figure 4.6.

The oxidation of 1-butanol molecules in the meniscus formed on the exposed electrode probably involves the following sequences: adsorption at the gas/liquid interface-------→ (1) absorption into the electrolyte and diffusion through the meniscus to the surface of the electrode---------→(2A) chemical reaction of the alcohol with the electrolyte to form a depolarizer and end products or (2B) adsorption on the electrode surface----------→(3) chemical or electrochemical reaction of the alcohol to form an electroactive

species on the electrode surface---------→(4) electrochemical oxidation to form the end products. The rates of these steps can be represented as follows (the subscripts referring to the process mentioned above) expressed as currents:

	Path I(Chemical)	Path II (Electrochemical)
(1)	Rate $1 = n_1 FD (C_M - C_O)/\delta$	Rate $1 = n_1 FD (C_M - Co)/\delta$
(2)	Rate $2A = k_{2_A} (C_M)^x (\text{electrolyte})^y$	Rate $2_B = k_{2B}\, Co\, \theta_f^m$
(3)		Rate $3 = k_3 \theta_c$
(4)		Rate $4 = k_4 \theta_x \exp(\alpha nFE/RT)$

where D is the diffusion coefficient of the alcohol in the electrolyte; n_1 is the number of equivalents per molecule; C_M is the instantaneous concentration of the alcohol in the meniscus; C_o is the concentration of the alcohol adjacent to the electrode surface, δ is the thickness of the electrolyte later; through which diffusion takes place; θ_f is the fraction of the electrode surface free of adsorbed alcohol; θ_c is the fractional coverage of the adsorbed alcohol; θ_x is the fractional coverage of the species responsible for supplying most of the current at the potential E; m is the order of the absorption rate and x, y are the orders of the chemical reaction of the alcohol with the electrolyte. The k's are the rate constants in the appropriate units; α is the fraction of E aiding the forward reaction and n is the number of electrons in the electrochemical step.

The absolute overall rate of reaction for the net cell process is complex and is determined by paths I and II, the reaction rate constants and the mass transport properties.

The overall current is therefore proportional to either path I, II or a combination of I and II. At present we have not completely determined the contributions of I and II to the total cell response, hence only the results and a qualitative discussion will be given.

(B) Chemical Oxidation (path I)

Originally it was thought that if a given amount of 1-butanol were added to a fresh nitrochromic solution, a given amount of some depolarizer would be produced, e.g. reduced chromium ion. However, Professor Louis Meites of the Polytechnic Institute of Brooklyn suggested to us that the alcohol is electrochemically oxidized. He pointed out that the slow chemical oxidation of the alcohol by the nitrochromic solution to produce a depolarizer would not permit the current to increase much until some time after the alcohol had been injected. On the other hand, if the chemical reaction is rapid "there can be no alcohol left after a few instants and in that case the current should not decay exponentially" as we had observed. His opinion was that our data indicated that anodic oxidation of 1-butanol on platinum.

In order to determine the role played by the nitrochromic solution, we decided to perform the following experiment in bulk solution to see if there was a difference between bulk and surface behavior (ie. surface being in the meniscus). To a freshly prepared nitrochromic solution (bright orange), 10^{-5} - 10^{-2} moles of liquid 1-butanol were added directly into the bulk with a micrometer syringe. The

direction addition resulted in a color change to blue which is characteristic of Cr^{3} (peak absorbance at 575 mu; 10^{-3} moles gave an absorbance of 0.05 and 10^{-2} moles gave 0.8).

In contrast, despite the fact that relatively large amounts of 1-butanol vapor (25cc 10^{-5} moles) had been injected into the working cell during the previously mentioned experiments (including the experiments in which 25 cc's of vapor were repeatedly injected into the cell over a period of four days), the cell electrolyte remained orange (changing from bright orange to dark orange) and did not turn blue (absorbing very little light at 575 mu; absorbance $\approx$ 0.05). This indicated that only a small amount of Cr^{+3} was present in the working cell. In addition, traces of a brown gas, probably NO_2, were detected in the nitrogen stream exiting from the cell. These observations lead to the conclusion that NO_2 and Cr^{+3} are not produced to any appreciable extent by the interaction of the alcohol vapor with the electrolyte on the exposed electrode. (However, in bulk solution this does not hold). In fact, any chromium ion, which has been reduced by the interaction with the alcohol vapor, is not appreciably reoxidized in view of the irreversibility of the dichromate reduction in strongly acid media and therefore should have been detected at 575 mu if it were present. Apparently, the main role of the nitrochromic solution is that of a cathodic depolarizer. Since we did not try either nitric acid or CrO_3 alone or at various concentrations we cannot be certain.

(C) Electrochemical Oxidation (path II)

Because we do not have sufficient data to define precisely the contribution of either path I or II, we can only present evidence in the literature for the electrochemical oxidation of alcohols in strongly acid solutions.

Gilman and Breiter [79] have shown in their experiments with perchloric acid electrolyte and a linear chronamperometric technique that the adsorption of methanol and a subsequent discharge step are rate controlling in the anodic oxidation of methanol. They have also shown [80] that the equilibrium adsorption of methanol on platinum obeys a Temkin isotherm [68(p241)] to a first approximation. In addition, Breiter [81] has shown that in the anodic oxidation of formic acid in perchloric acid solution, the adsorption of formic acid at platinum electrodes suitably explains the nature of the currents which are observed experimentally.

Recently, Andrew[82] has treated published literature on limiting currents for the oxidation of methanol under several conditions. From his treatment, two major schemes arise for the oxidation in acidic solution. In the first scheme, the alcohol is adsorbed on the electrode and oxidized to an intermediate. The intermediate is then reacted in the rate controlling step to yield the end product. Any surface coverage is attributed to the intermediate. In the second, scheme, the intermediate is formed as in the first scheme but it now can react to give the end product or some other product. Andrew postulated[82] that the intermediate may be

chemically or electrochemically formed and may be removed from the electrode surface by desorption or electrochemical oxidation.

Evidence for adsorbed and chemisorbed species have been published. Giner postulated and then demonstrated [85,86] that the adsorption and partial oxidation of methanol on platinum in strongly acid solution yielded a chemisorbed intermediate $CH_3OH \quad Pt \quad -4e \longrightarrow Pt\text{-}CO + 4_H{}^+$ which was followed by the following rate determining step:

$$Pt\text{-}CO + H_2O \quad -2e \longrightarrow Pt + CO_2 + 2_H{}^+$$

Similar results have been obtained by Righmire et al [87] in their study of the oxidation of ethyl alcohol at platinum electrodes in 1_N sulfuric acid. They concluded that their data strongly suggested that the alcohol was chemisorbed on platinum to form a carbon-platinum surface bond. This intermediate then participated in a rate limiting electrochemical step to give the end products which in their case were acetaldehyde and acetic acid.

This is not surprising in view of the findings of Binder et al [83-84] who observed that in the electrochemical oxidation of methanol, ethanol and propanol in 5_N sulfuric acid the ease of oxidation of the respective aldehyde and carboxylic acids decreased with increasing chain length. In general, they observed that at 25°C the oxidation of these alcohols stopped at the carboxylic stage.

For most simple electrode processes the number of electrons per molecule of product is umambiguous. For more

complex reactions, it becomes necessary to determine the coulombic yield in order to account for the current and charge passed during the course of an experiment. This is particularly important in organic electrode reactions where a number of electrochemical pathways are often involved. In order to estimate the nature of the electromical reaction, the areas under the current vs. time curves (fig. 4.1) were measured using a compensating polar planimeter (K&E, model 62-0005, Kueffel and Esser Co., N.Y.). These areas represents the total number of coulombs, Q, passed in the overall electrode process. A plot of Q vs. V (volume injected) was made (fig. 4.7). The number of equivalents per mole of alcohol, n, is given by: $n = Q/MF$ where Q is the number of coulombs, F is the value of the Faraday and M is the number of moles of alcohol injected into the cell. M was calculated from vapor pressure data for 1-butanol at 26C (Chemical Engineers' Handbook, 3rd edition, McGraw-Hill Pulishers 1957) assuming that the gas volume in the closed Erlenmeyer flask to be 123 ml with the liquid 1-butanol sample occupying 2ml. In calculating the corrected values of n, primary and secondary cell Q values were combined and the calculated performed. Table 4.1 summarizes the results.

Table 4.1

Equivalents per mole of Alcohol as a Function of the Volume of Vapor Injected

Volume Injected, V (cc)	Equivalents per mole, n
1	4.0 ±0.2

Volume Injected, V (cc)	Equivalents per mole, n	
2	3.4	
3	3.5	
4	3.0	
5	2.8	
6	3.0	
10	2.8	(3.0)*
15	1.6	(2.1)*
20	1.7	(2.5)*
25	1.5	(2.3)*

* indicates corrected values.

It is difficult to say from the above that the cell response was due to the electrochemical oxidation of 1-butanol and not to butraldehyde or butyric acid (which may have been formed by the chemical oxidation of 1-butanol) or to the reduction products of the electrolyte. More data using different acids as the electrolytes is required and we plan to continue this work in the near future.

IV. Conclusion

Absorption of alcohol vapors into the electrolyte meniscus formed on the exposed electrode of an absorption induced electrode potential cell comprised of a partially exposed Pt anode, fresh nitrochromic solution and an immersed platinum cathode results in the oxidation of the alcohol to the corresponding aldehyde and carboxylic acid. A transient current is recorded which is proportional to the volume of vapor injected into the cell. Because of insufficient data, we have not been able to determine the nature of the oxidation, i.e. whether it is electrochemical, chemical or some combination of the two. However, we plan to continue this work in the near future.

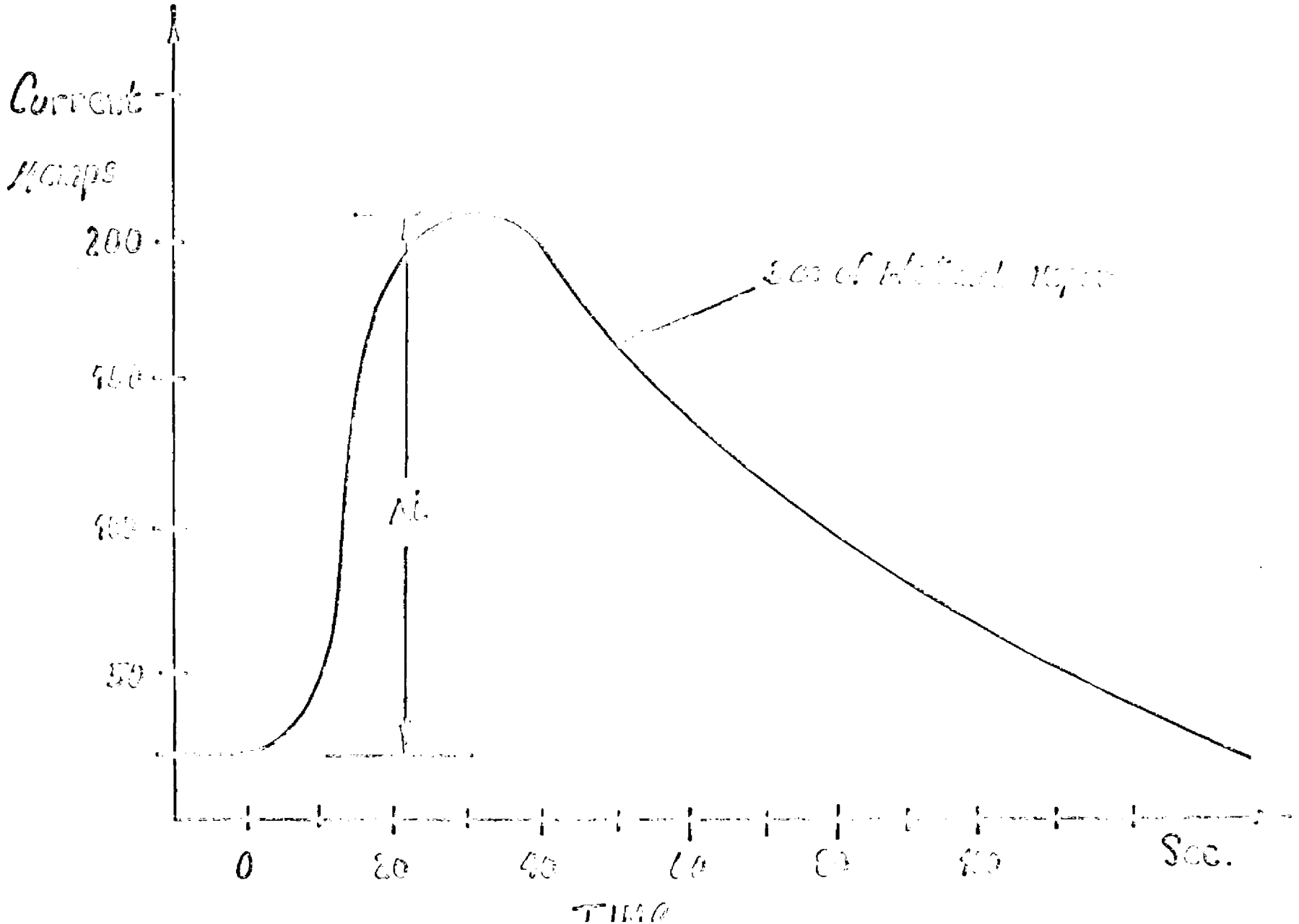
Current
Amps
200
150
100
50
M.
0
20
40
60
80
100
Sec.
TIME

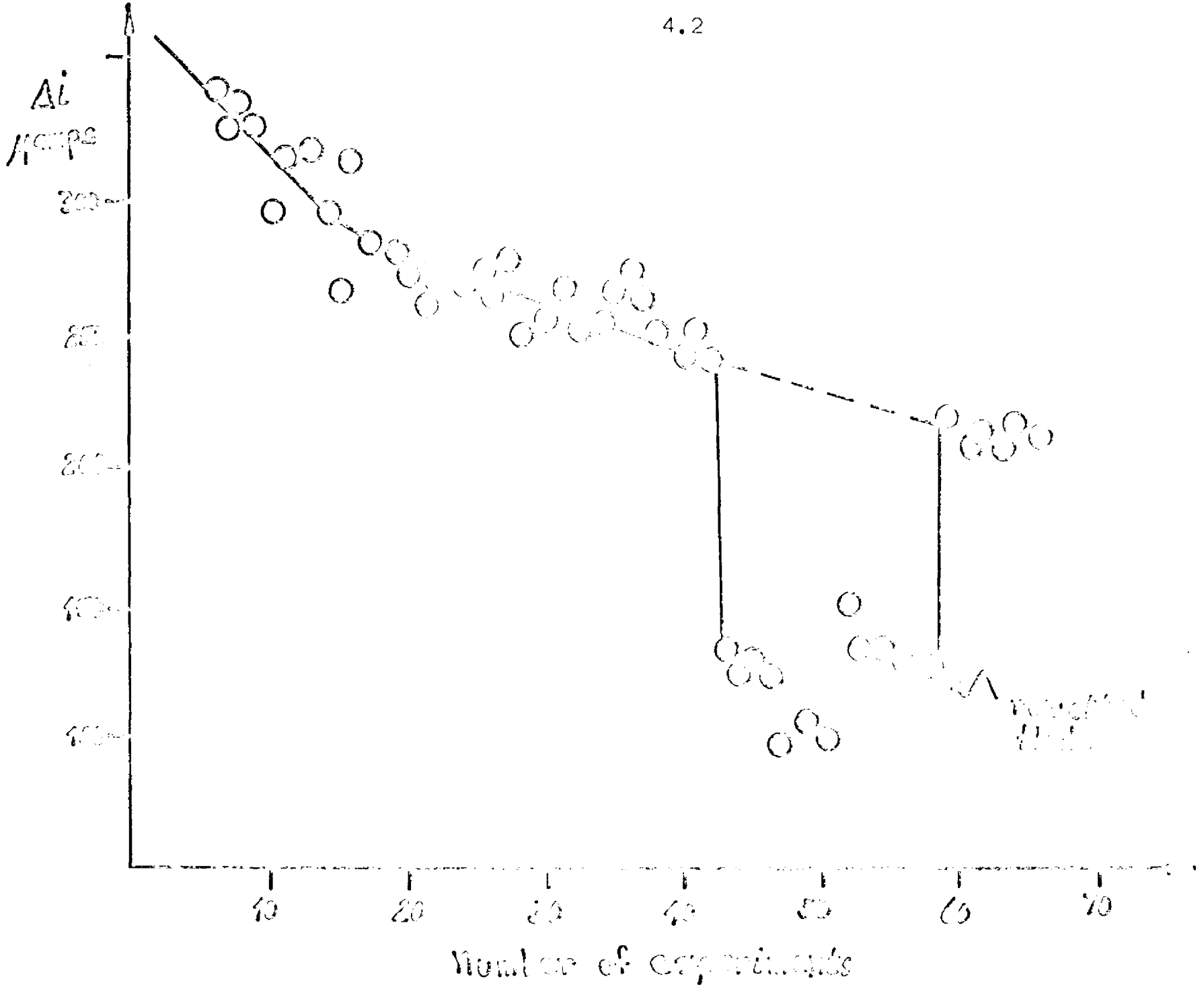
Ai
Number of experiments

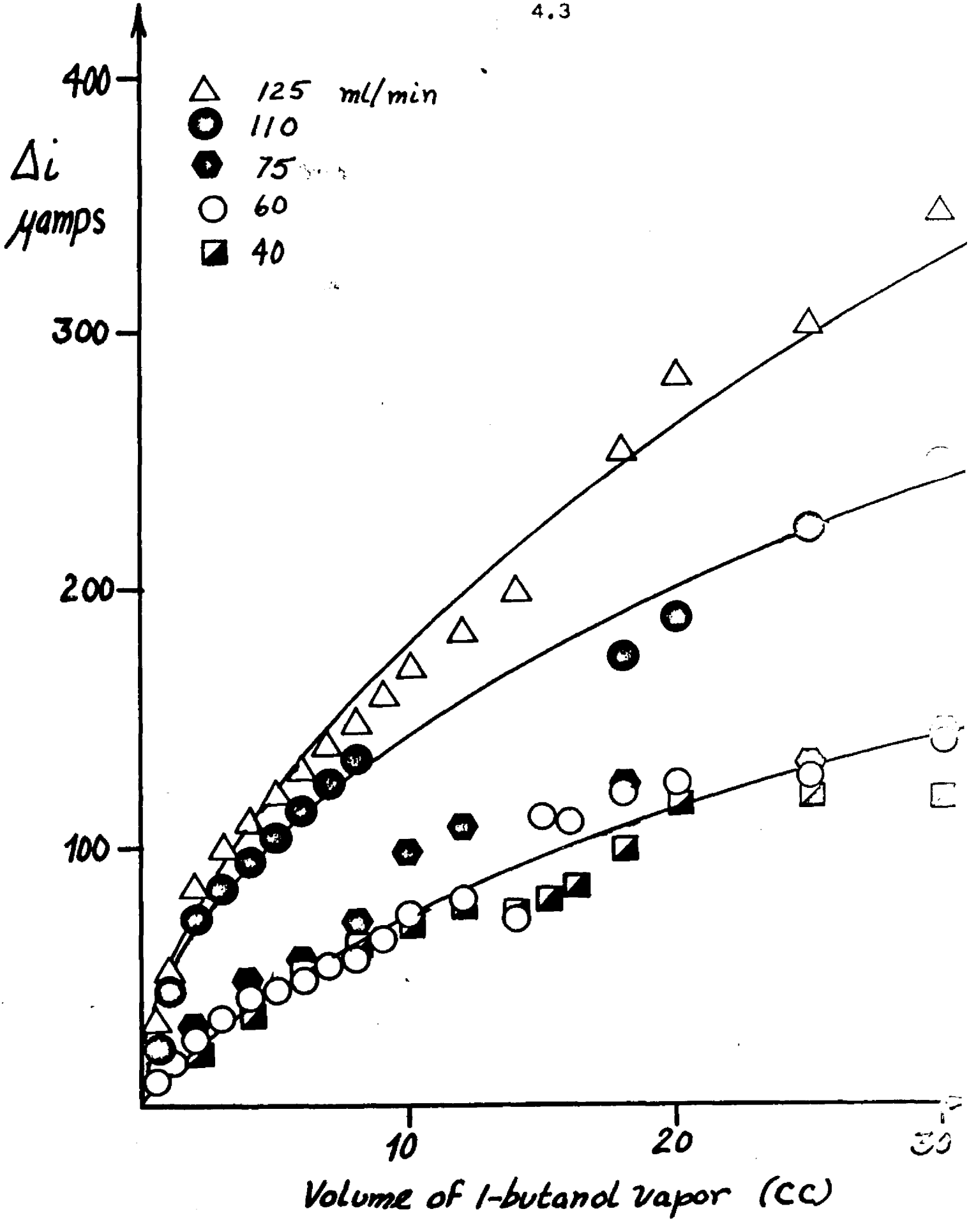
400
300
200
100
Δi
μamps
125 ml/min
110
75
60
40
10
20
30
Volume of 1-butanol vapor (cc)

4.4

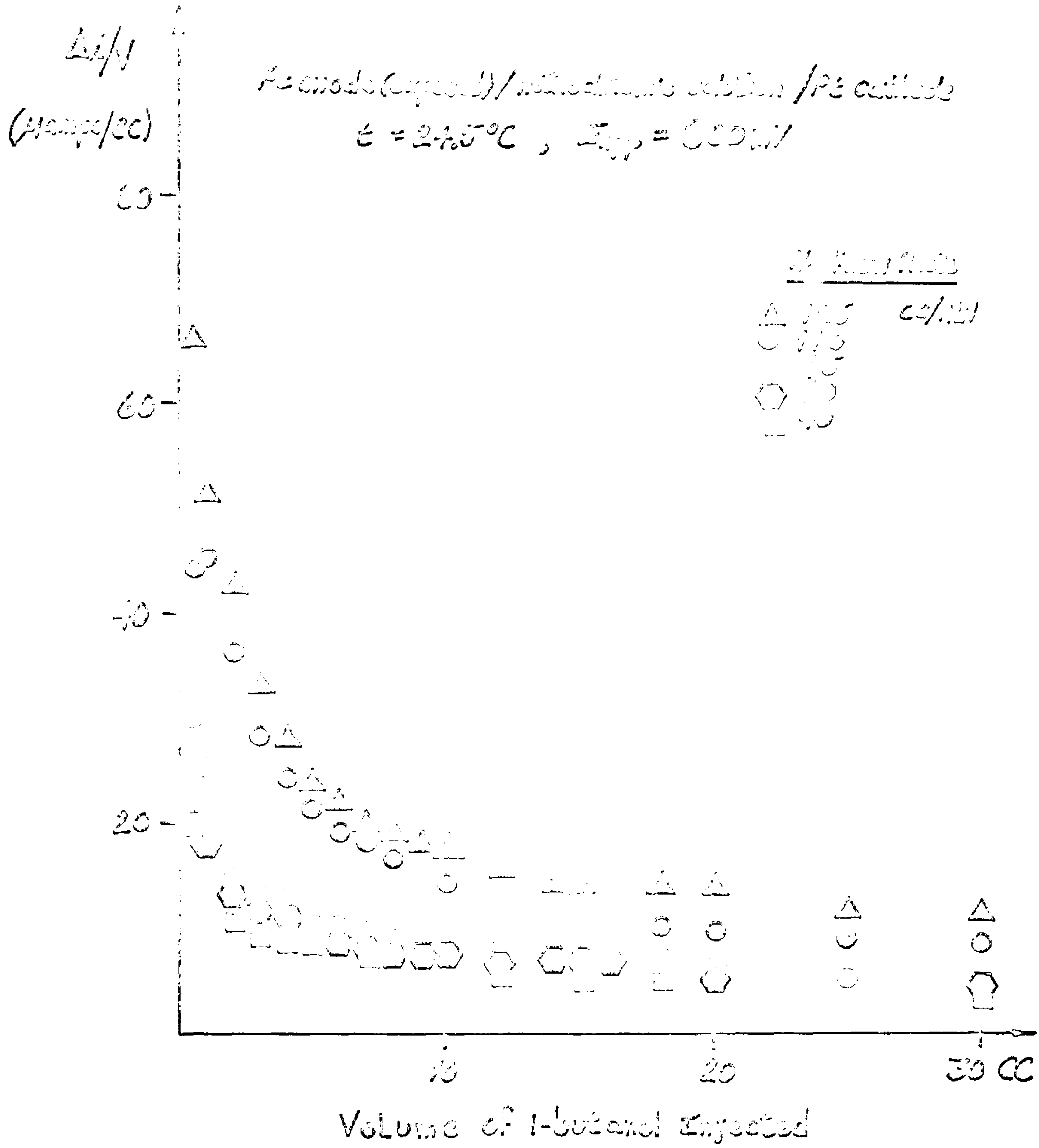

$\Delta i/V$
(μamps/cc)
60
40
20
10
20
30 cc
Volume of 1-butanol injected

Figure 4.5

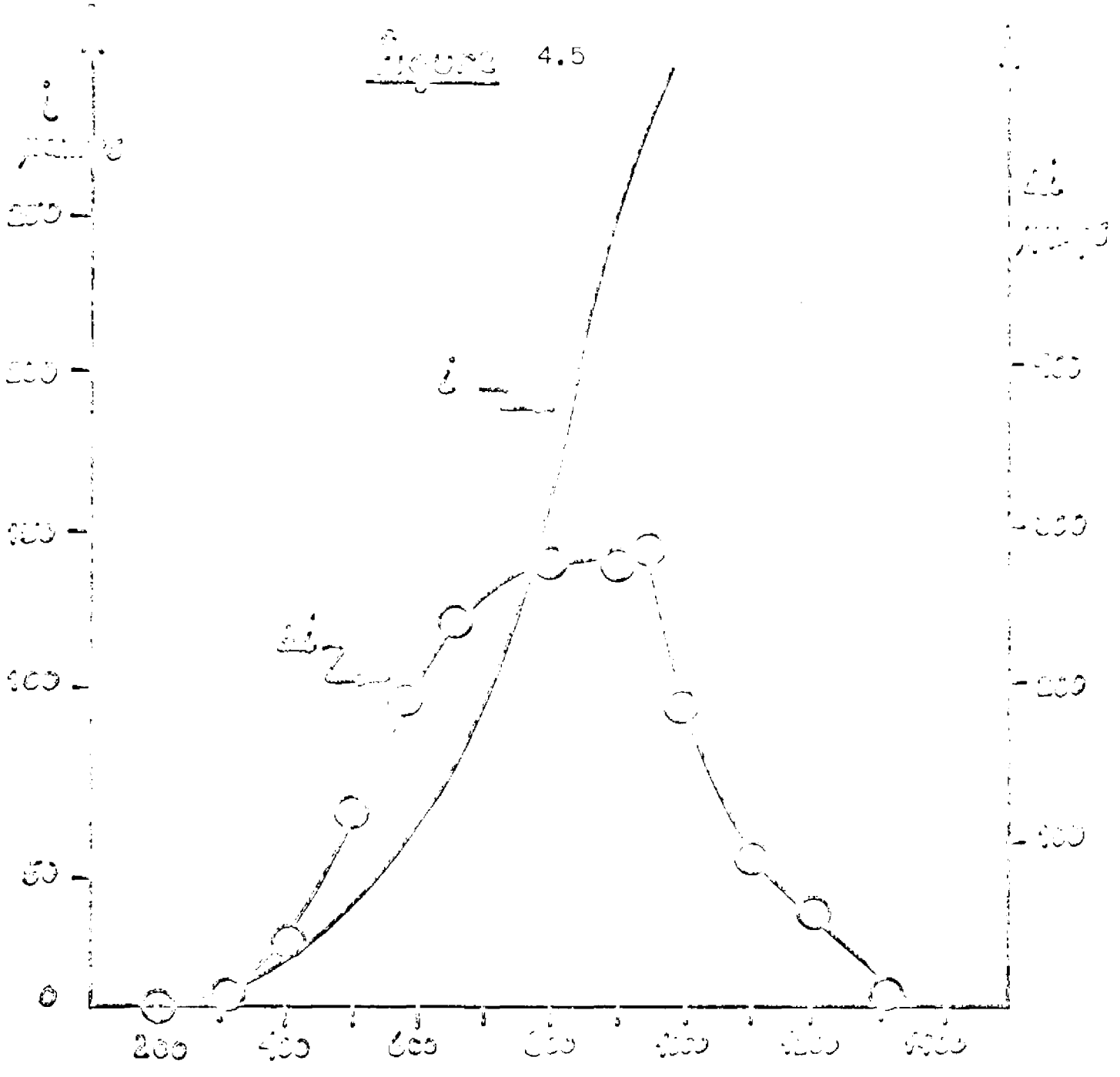

Figure 4.6

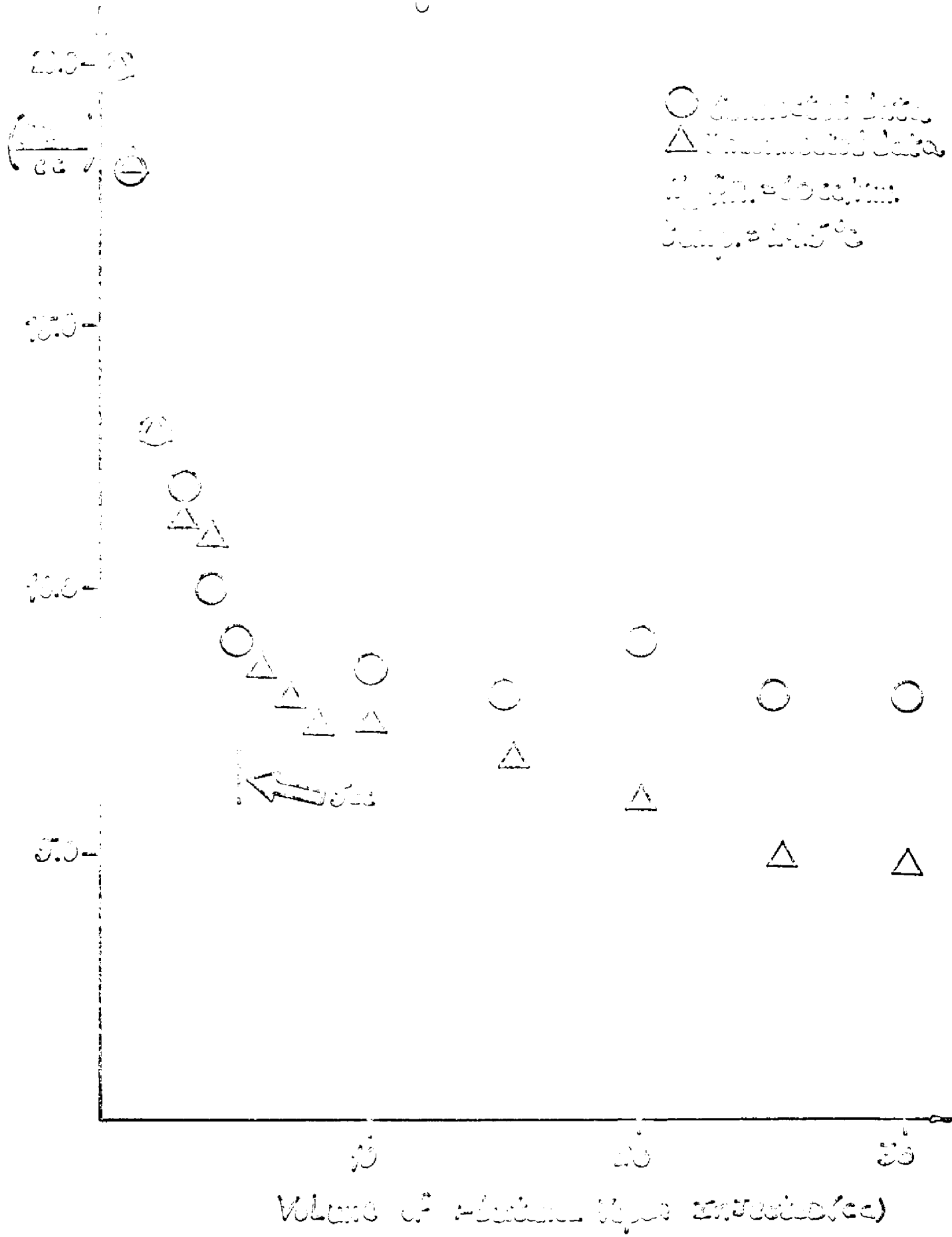

Figure 4.7

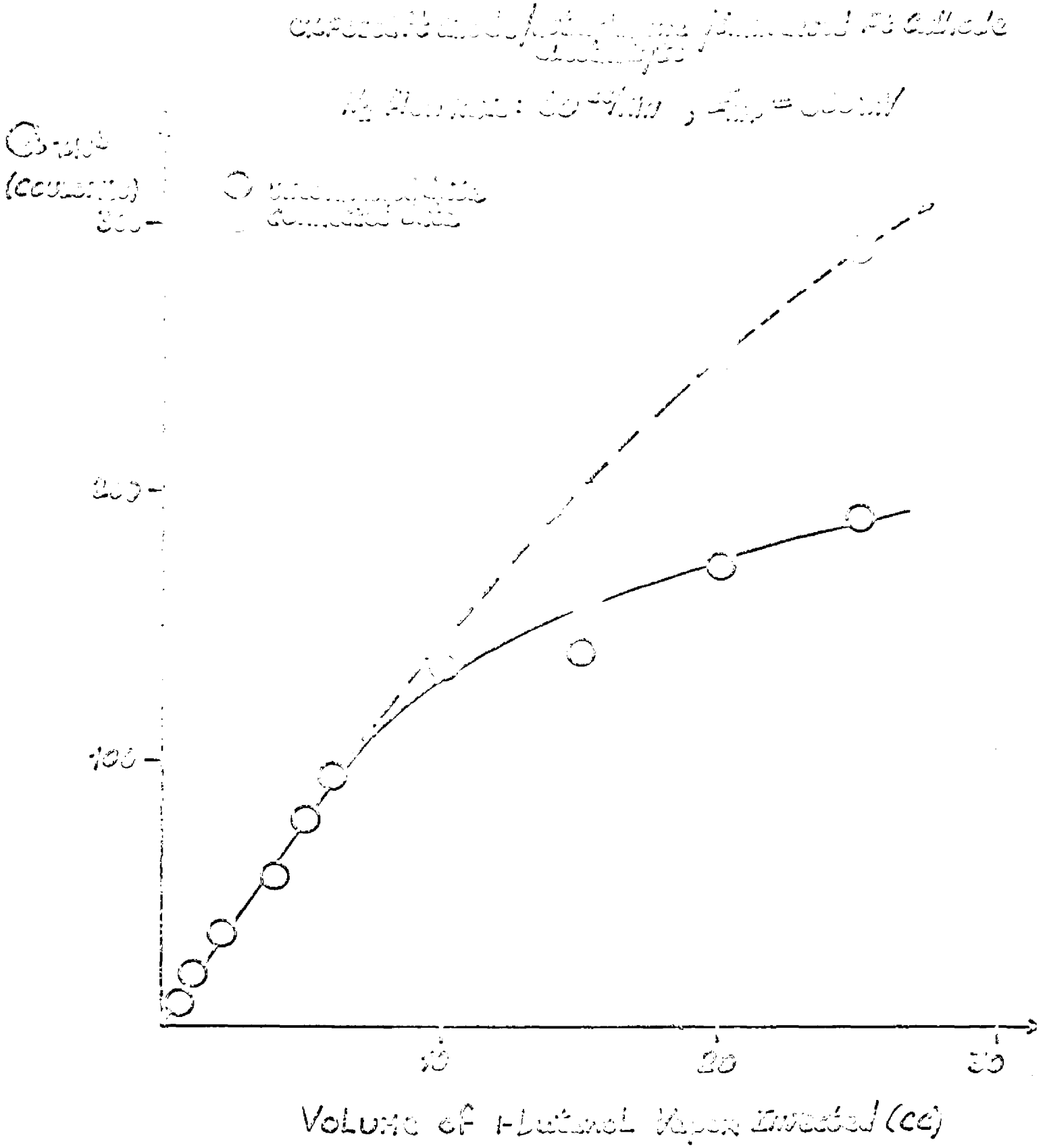
Theoretical
Experimental
200
100
10
20
30
Volume of 1-Butanol Vapor Injected (cc)

Chapter 5

Detection of Acidic Vapors at Partially Exposed Platinum Electrodes Via a Redox Couple

Lestienne[22] has suggested the use of an IO_3^-/I^- mixture for the detection volatile organic acids. He found that the interaction of the organic acids with the mixture in solution liberated iodine which can be determined, e.g. by titrating with a reductant. Therefore, we propose to use the IO_3^-/I^- mixture in a suitable absorption induced electrode potential (AIEP) cell in order to detect and determine acid vapors.

I. Experimental

The electrolyte used in this study was M/2 with respect to potassium iodide, m/10 with respect to potassium iodate and m/2 with respect to potassium nitrate (the supporting electrolyte). Enough solid sodium carbonate was added to the electrolyte to make it m/1000 with respect to Na_2CO_3 which made the solution basic. All chemicals were reagent grade and distilled water was used in the preparation of the electrolyte solution. All the experiments were performed at room temperature (25 ± 1^oC) using 15cc of the electrolyte. The electrolyte was stirred at a constant rate by a magnetic stirrer.

The exposed electrode was a rectangular piece of platinum foil 2.0cm long x 1.0cm wide and 0.002" thick which had been thermally connected to a platinum wire 0.012" in diameter. One end of the wire was sealed in a section of glass tubing where it made contact with mercury. The immersed electrode was prepared in the same manner using a piece of platinum wire 2cm long by 0.012" in diameter (Baker Platinum Division Englehard Industries, N.J.). The blade was sand-

blasted in order to make it perfectly wettable. The silver/silver iodide reference electrode was prepared by anodizing a silver wire (99.996% pure silver, 0.06cm in diameter) in a dilute solution of potassium iodide.

The basic cell design and circuitry is shown in figure 3.1. Filtered nitrogen, which serves as the carrier gas for the test vapor, was continuously passed through the cell at controlled flow rates. Before coming in contact with the vapor or entering the cell, the nitrogen stream was passed through a series of filters. [63]

A. Selection of a "Detecting" Potential: Voltammetric Study

Ideally, the sensing electrode should be at a potential which corresponds to the smallest residual current. In this manner, the effect of the acidic vapor will be enhanced, ie. the current produced by the I_2/I^- couple won't be masked by the residual current. In addition, the electrode potential should be sufficient for the desired reaction to occur. Therefore, the potential of the exposed electrode of the cell Pt (exposed blade)/ IO_3^-, I^- / Pt (immersed) was measured against a silver/silver iodide reference electrode as a function of the potential externally applied to the electrodes of the cell. Concurrent with that measurement, the cell current was also measured as a function of the applied potential. The results are presented in figures 5.1, 5.2.

B. Calibration of the Cell with Known Acid

The cell was calibrated at several convenient applied potentials by injecting given volumes of 0.255N solution of

hydrochloric acid directly into the cell and recording the current which was produced. The solution was delivered with a 1cc syringe which could be read to .01cc. The largest volume used was 0.50cc so that the electrolyte remained practically unchanged. The results are shown on figure 5.3.

C. Detection of Acidic Vapors

The test vapors were hydrogen chloride and acetic acid. They were prepared by placing hydrochloric acid ($\simeq$ 12N) and glacial acetic acid in separate, closed Erlenmeyer flasks. After allowing the solutions to reach equilibrium with their own vapors, a given volume of the vapor (hydrogen chloride or acetic acid) was then withdrawn slowly from the flask with syringes and subsequently injected into the nitrogen stream entering the cell. The cell current achieved a maximum value generally within 3-5 seconds after the injection of the acid vapor. No decay of the current was observed to occur within five minutes after it reached the maximum. Therefore, the next injection was made; after which a new steady current was obtained. For a given injection of vapor, the difference between the initial and the steady current was selected as the parameter I_1 to be reported. There was no difference in the response times of HCl and acetic acid vapors. The cell response was determined as a function of the volume of vapor injected into the cell, at several applied potentials. The results are shown on figures 5.4, 5.5.

II. Results and Discussion

The mixture iodate/iodide is quite sensitive to hydrogen ion. The chemical reaction:

$$IO_3^- + 5I^- + 6H^+ \longrightarrow 3I_2 + 3H_2O \qquad \text{eq. 5.1}$$

is a particularly fast one. However, reaction 5.1 does not take place in neutral or alkaline media. Therefore, it should be possible to utilize (5.1) for the detection of volatile acids. The approach which we have taken is to use the AIEP cell: Pt(exposed blade)/IO_3^-, I^-/Pt (immersed wire) at several applied potentials. The potassium nitrate serves as the supporting electrolyte so that the diffusion currents will not be masked by migration of the electroactive species. Reaction (5.1) was retarded in the cell by keeping the electrolyte basic with sodium carbonate. Essentially, the idea is to inject an acidic vapor into the nitrogen stream which flows continuously through the cell. Upon entering the cell the vapor is absorbed into the electrolyte meniscus at the exposed electrode where it reacts chemically with the electrolyte to produce iodine (via 5.1). The current which is produced is proportional to I_2 and hence to H since the two are related stoichimetrically.

In our system, the production of iodine by the interaction of the electrolyte with an acidic vapor in a solution in which hydrogen ions were initially absent provides the impetus for the electrical response of the cell to the acidic vapors.

A. Selection of "Detecting" Potentials and Cell Calibration

From figure 5.3, it can be seen that at a given applied potential the current flow is linearly related to the number of moles of hydrogen ion added to the electrolyte. In view of the electrode potential vs. applied potential curves (figure 5.1) which indicate that the exposed electrode is nonpolarized while the immersed electrode is polarized in the range $0 \leq E_a \leq 1000mV$, it appears that the system functions as in amperometry with one polarized electrode. The current measurement is of the limiting current, I_l, of iodine. As the concentration of iodine, C_{I_2}, in the electrolyte increases as a result of reaction 5.1, so does the diffusion current. Because I_l is proportional to C_{I_2}, the decrease in I_l due to the dilution of the electrolyte with the added volume of the calibrating solution. However, the correction is quite small (maximum 4%) since the added volume was kept at less than 0.5cc and can therefore be neglected.

B. Detection of Acidic Vapors

From figures 5.4-5.5, we can see that the measured current also increases linearly with the volume of vapor injected into the AIEP cell. Therefore, the system is quite satisfactory for the detection of acidic vapors.

Schulze [88] has used the depolarization of a platinum electrode by the I_2/I^- couple to detect ozone amperometrically. In his system, the iodine is liberated by the oxidation of iodide ion by ozone. Schulze[88] standardized his system by means of coulometrically generated iodine. The

ammeter in his circuit was then calibrated to read the concentration of ozone directly.

Hersch and Sambucetti[23] coulometrically monitored carbon monoxide in air and other gases by passing the carbon monoxide through a column of iodine pentoxide (I_2O_5); any carbon monoxide forms a proportional amount of iodine vapor. The iodine vapor is then made to impinge on the platinum screen cathode of a fuel cell with activated carbon as the anode. The resulting current is related by Faraday's law to the rate of supply of carbon monoxide. All the iodine entering the cell is reduced at the cathode. In contrast to our method and to that of Schulze [88], where iodine is formed in the cell electrolyte, in the carbon monoxide monitor of Hersch and Sambucetti[23], the iodine forms outside the cell and is led as directly as possible to the platinum cathode.

III. Conclusion

We have seen that the system IO_3^-/I^- (pH > 7) can be used in the AIEP cell: Pt(exposed blade)/ (IO_3^-, I^-) KNO_3 supporting electrolyte/ Pt(immersed wire) to detect acidic vapors. The acidic vapor enters the cell in a nitrogen stream and is absorbed in the liquid menisucs formed on the exposed electrode of the cell. The absorbed vapor reacts chemically with the electrolyte to produce iodine:

$$IO_3^- + 5I^- + 6H^+ \longrightarrow 3I_2 + 3H_2O$$

A current is recorded which is proportional to the amount of iodine which formed, and is therefore also proportional to the amount of acidic vapor since the two are related

stoichiometrically. The method is an indirect one which utilizes the acid nature of the vapor in a chemical reaction to produce and electroactive species. At a given applied potential, the current increases linearly with the volume of vapor injected into the cell. The system was calibrated by injecting given volumes of 0.255N HCl into the cell and measuring the resulting current; which also increased linearly with the added moles of HCl. The above system was found to be quite satisfactory for the detection of hydrogen chloride, acetic acid and acid vapors in general for the range studied, i.e. 10^{-6}-10^{-4} moles which produce 3 and 250 μamps respectively.

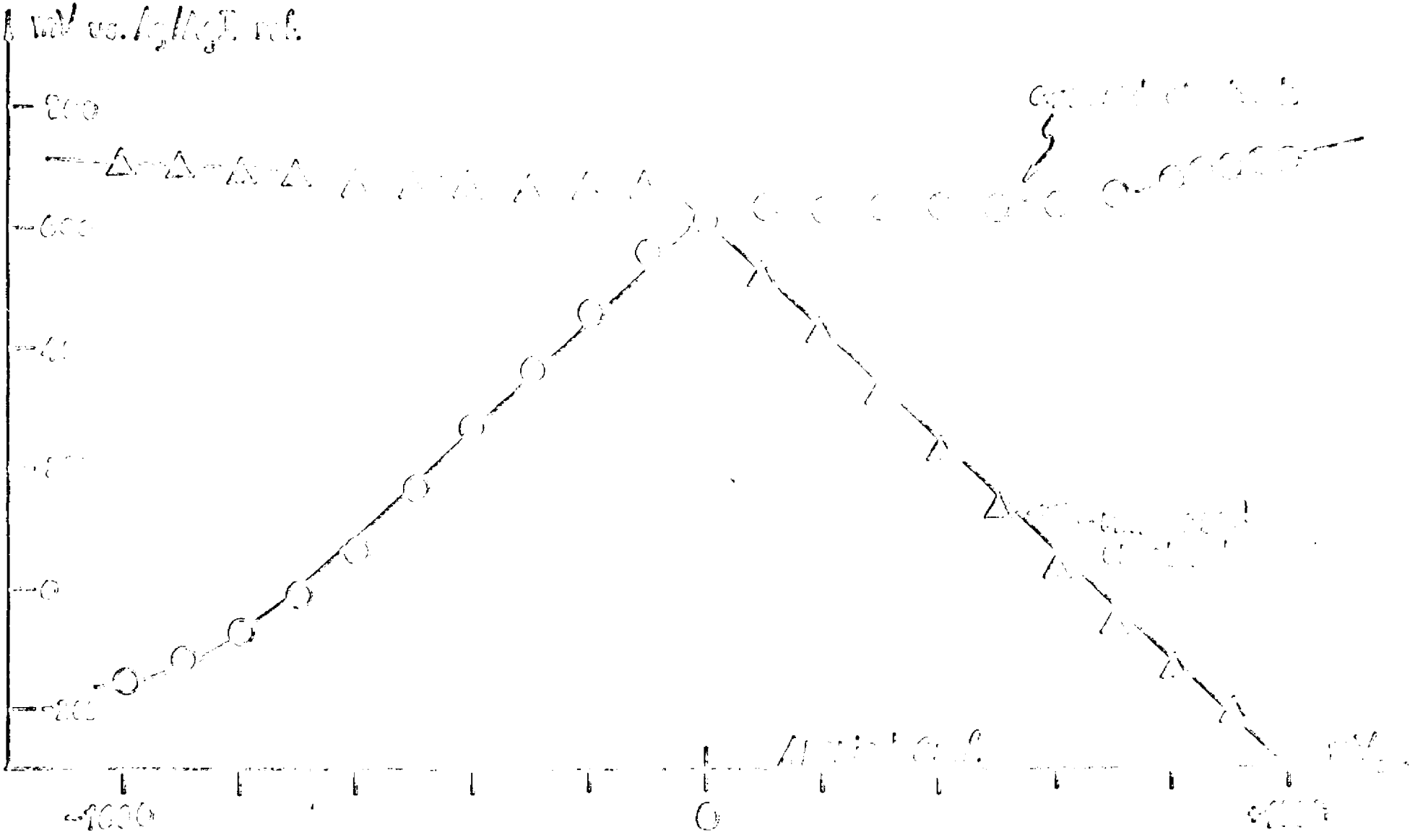

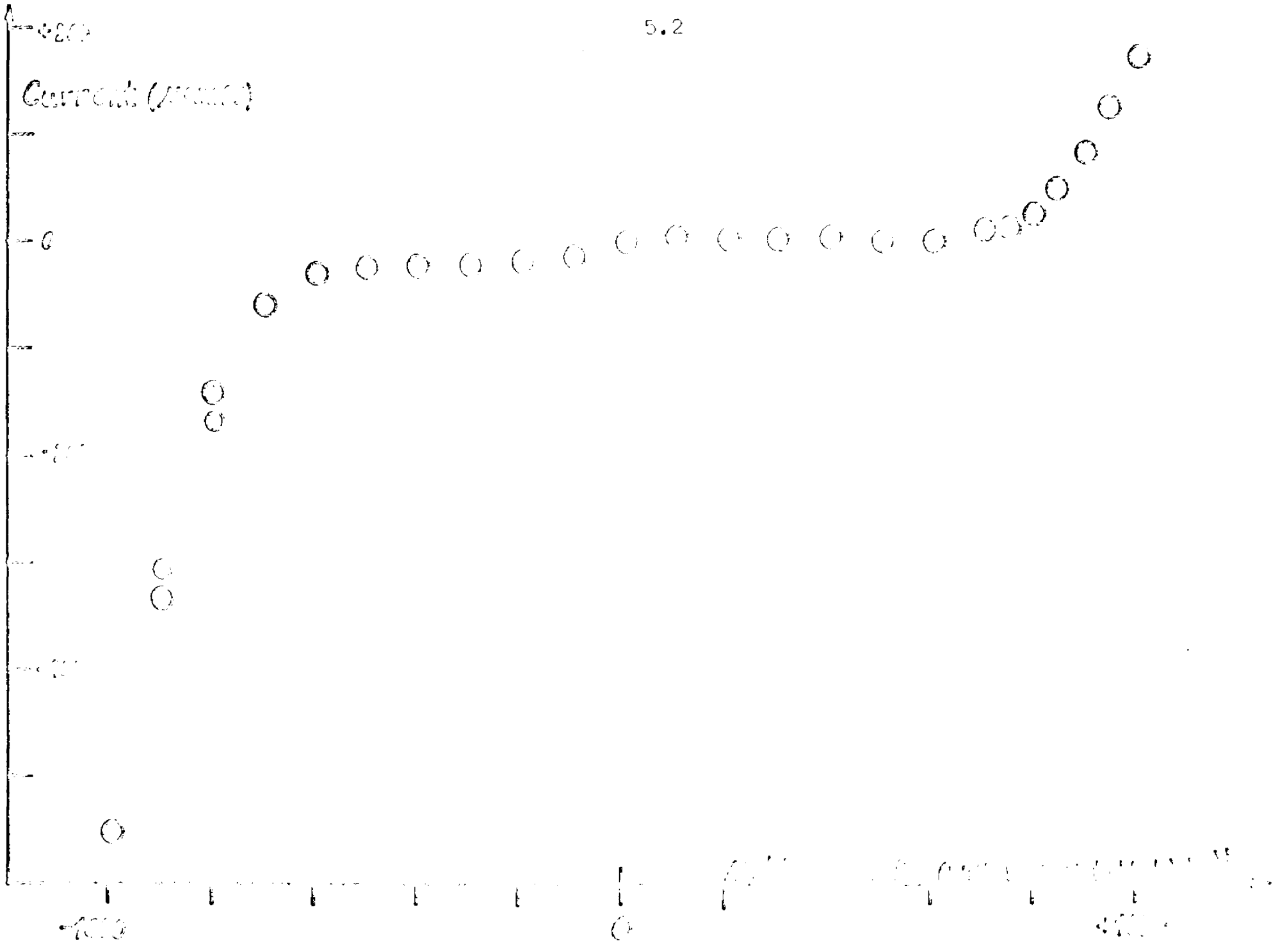
Current (μA)
0

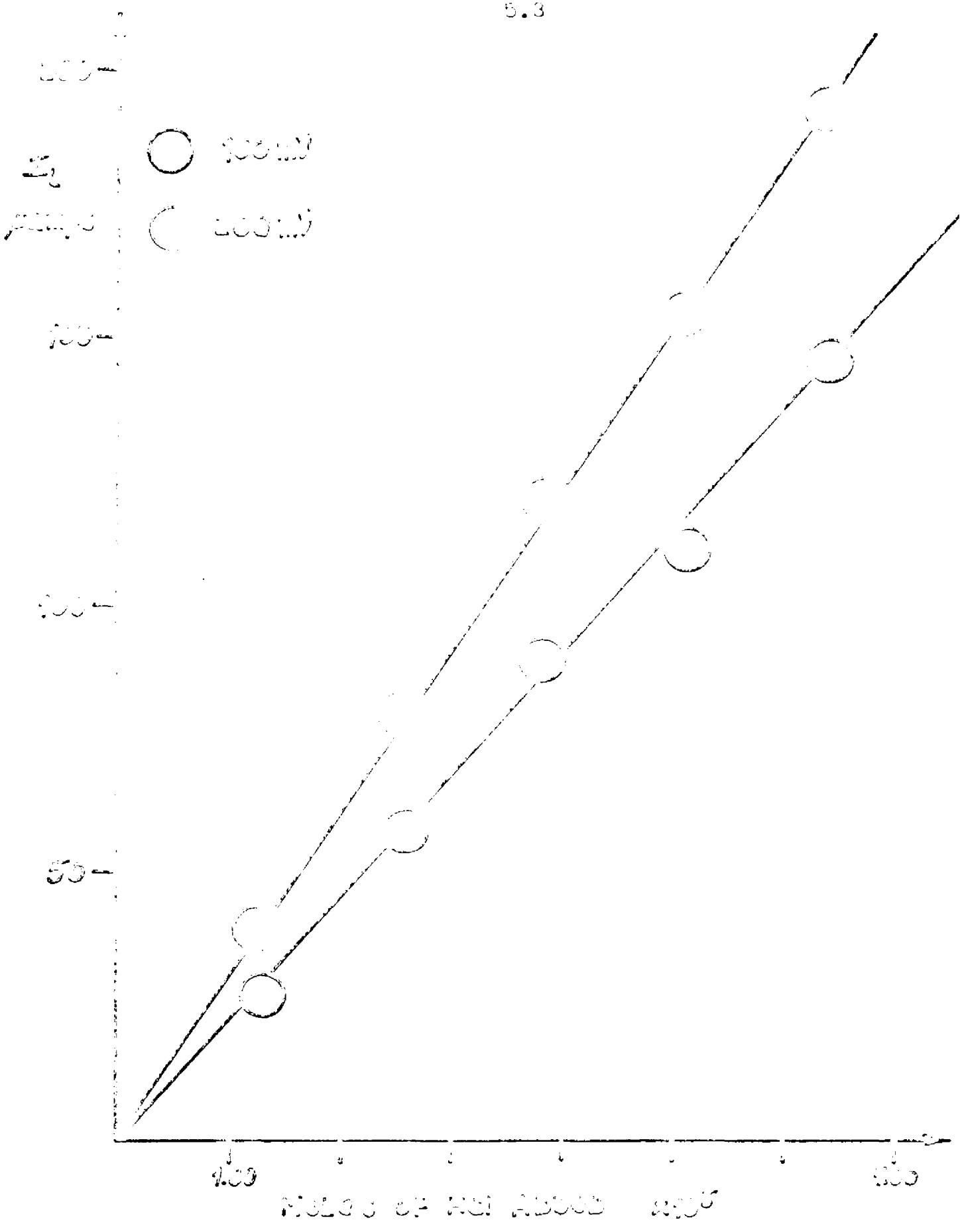

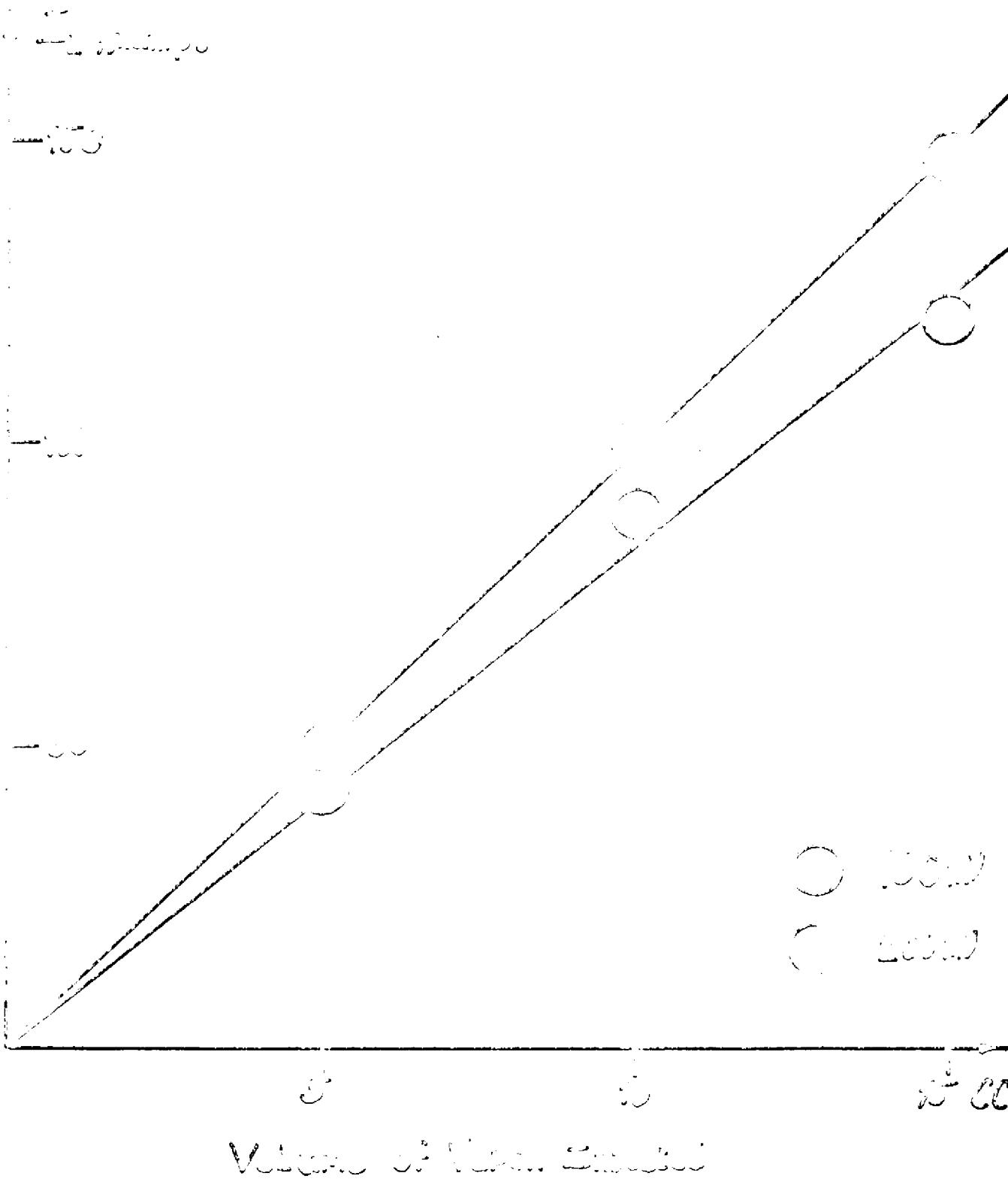

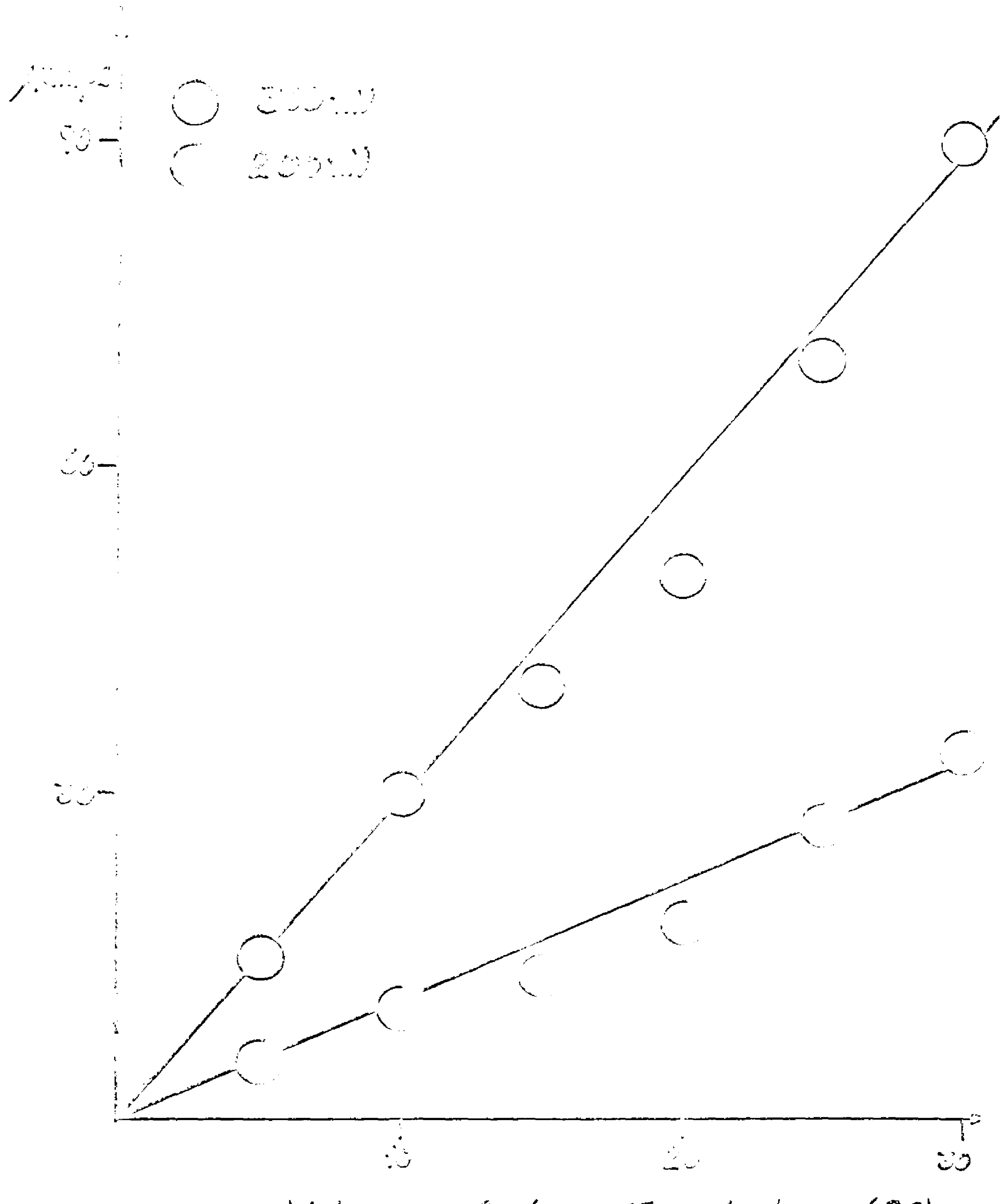
90
60
30
10
20
30
Volume of Vapor Injected (CC)

Appendix A

I. Treatment of the Current Rise

Assumption 1: The current rise results from HCl diffusion in the X direction to the exposed electrode. The diffusion process in the y direction is negligible up to the maximum in the current transient.

The generalized expression of Fick's second law is given by:

$$(\partial C/\partial t) = \frac{\partial}{\partial x}\left[D(c)\,\partial C/\partial x\right] \qquad \text{eq. A-1}$$

In reality, the diffusion coefficient is a function of the HCl concentration, i.e. $D(C) = D^{o} + KC$ eq. A-2

where D^{o} is the diffusion coefficient for the bulk HCl.

Upon substisuting eq. A-2 into eq. A-2 one obtains:

$$(\partial C/\partial t) = \frac{\partial}{\partial x}\left\{\left[(D_{b}\,\partial C/\partial x)\right] + \left[(KC)\,\partial C/\partial x\right]\right\} = \left[D^{o}\frac{\partial^{2}C}{\partial x^{2}} + \frac{\partial}{\partial x}\left(KC\frac{\partial C}{\partial x}\right)\right] \text{eq. A-3}$$

Term II of eq. A-3 represents the variation of diffusion with a varying diffusion coefficient.

Assumption 2: As a first approximation, we will assume that term II is negligible, i.e. $D(C) = D^{o}$

II. Treatment of the Current Decay

Assumption 3: The decay of the current is a result of HCl diffusion from the meniscus to the bulk of the electrolyte (y direction); this process predominating after the maximum in the transient has been reached.

A summary of the results of the mathematical treatment of I and II follows; subsequent to which the actual treatment is given.

Summary of Results

The Current rise is described by:

$$\text{Log.}i = K + Ds^2\pi^2(t-t_p) \Big\} \begin{matrix} t = t_p \\ t = 0 \end{matrix} \qquad \text{eq. A-I}$$

The current decay is given by:

$$\text{Log.}i = Q - q^2 D\pi^2 (t-t_p) \Big\} \begin{matrix} t = t \\ t = t_p \end{matrix} \qquad \text{eq. A-II}$$

$$K = \log.\left[nFAs\,\pi \tan(sL\pi)C_M\right] = Q = \log.\left[nFAq\pi \tan(q^R\pi)C_M\right]$$

where: i is the instantaneous current given by $nFA\left(\partial C/\partial x\right)_{x=0}$

$X = 0$;

D is the diffusion coefficient of HCL;

n,F,A have their usual significance;

C_M is the maximum instantaneous concentration of HCl in the active zone of the meniscus and is a function of the volume. of HCl vapor injected;

t_p is the time at which the maximum in the transient is obtained and q,s are constants such that $s \neq q$ with q,s 0,1,2,3, etc.

Plots of the experimental data in the form of log. i vs. time (shown on the following pages) indicate that equations A-I and A-II are good first approximations to the physical process.

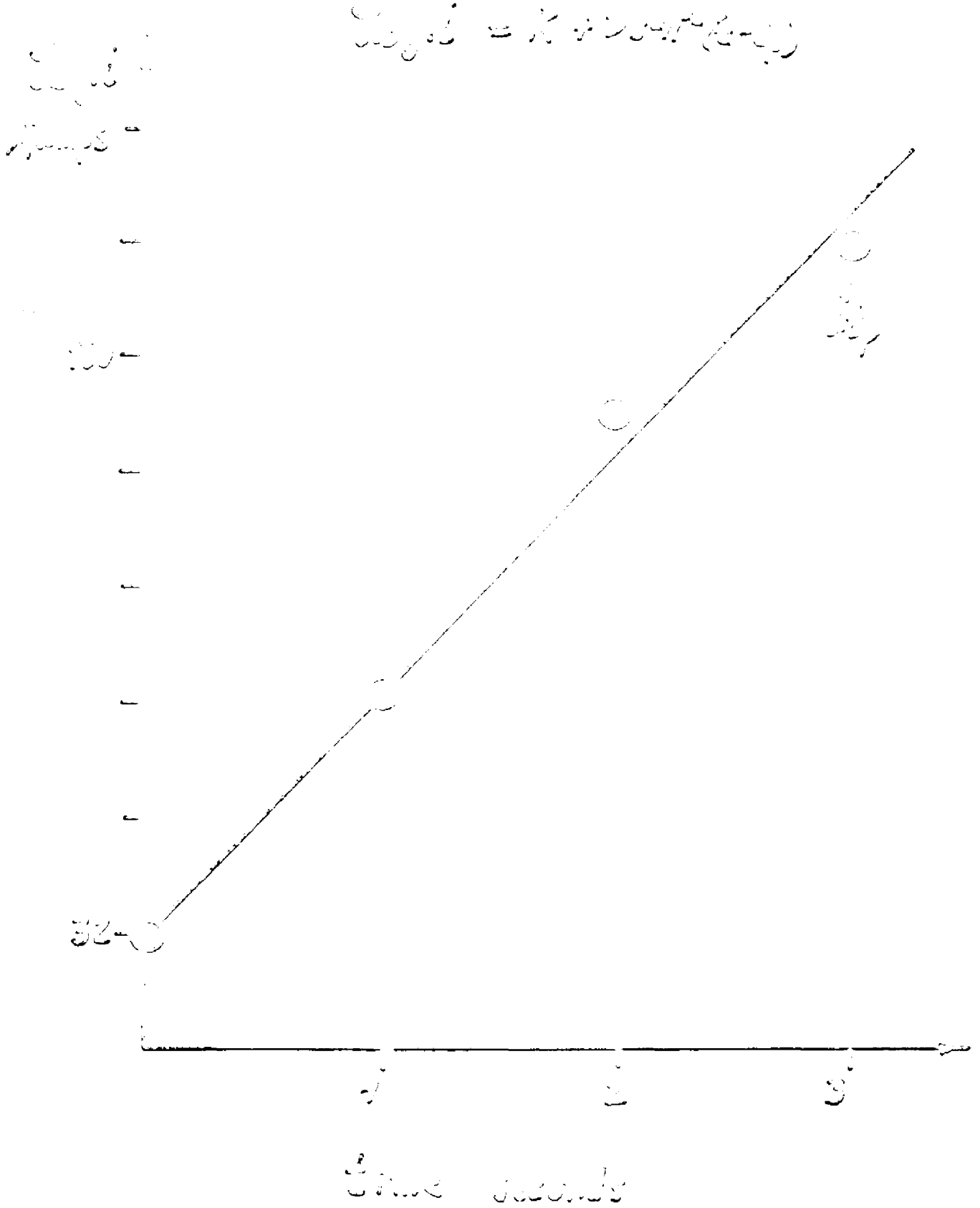

Mathematical Treatment

I. Current Rise

$$\left(\frac{\partial C}{\partial t}\right) = D\frac{\partial^2 C}{\partial x^2} \quad , \text{ Let } C = f(x,t) = f(t)\,g(x)$$

then: $\left(\frac{\partial C}{\partial t}\right) = g(x)f'(t)$ and $D\frac{\partial^2 C}{\partial^2 x} = D f(t) g''(x)$

therefore, $g(x)f'(t) = D f(t) g''(x)$

or $\frac{f'(t)}{f(t)} = D\frac{g''(x)}{g(x)} = +\alpha^2$

$f'(t) = f(t)\alpha^2$	$g''(x)/g(x) = \alpha^2/D$
$df/dt = +\alpha^2 f$	$g''(x) + \frac{\alpha^2}{D} g(x) = 0$
$\frac{df}{f} = +\alpha^2 dt$	Let $\beta^2 = \alpha^2/D$
$\ln f = +\alpha^2 t + \ln N_0$	$g''(x) + \beta^2 g(x) = 0$
$f(t) = N_0 e^{+\alpha^2 t}$	$g(x) = N_1 \cos \beta x + N_2 \sin \beta x$
where N_0 is a constant	where N_1, N_2 are constants

$\therefore\ C(x,t) = N_0 e^{+\beta^2 D t}(N_1 \cos \beta x + N_2 \sin \beta x)$ eq A-4

Boundary Condition I: $E_{Applied} = E^0 + \frac{RT}{nF} \ln a^S_{Cl^-}$,

i.e., the activity of Cl^- at the electrode surface must adjust, because of E_{app}, to satisfy the Nernst equation

$$\ln a^s_{Cl^-} = nF/RT\,(E_{App} - E^0)$$

Let $a^s_{Cl^-} = \gamma^s_{Cl^-} C^s_{Cl^-}$ therefore,

at $t=0$, $x=0$ (the electrode surface)

$$C^s_{Cl^-} = \left(\frac{1}{\gamma^s_{Cl^-}}\right) exp\left[nF/RT\,(E_{app} - E^0)\right] = \phi \quad \text{eq. A-5}$$

applying the above condition to eq. A-4, one obtains:

$$C_{(0,0)} = N_0 N_1 = \phi$$

Boundary Condition II: at the peak of the transient, $C(0, t_p) = C_M$

$$C(x, t_p) = C_M \quad \text{for } 0 \le x \le L$$

$$C(0, t_p) = C_M = N_0 e^{+\beta^2 D t_p}$$

$$C(x, t_p) = C_M = N_0 e^{+\beta^2 D t_p}(N_1 \cos \beta x + N_2 \sin \beta x)$$

therefore, $N_1 \cos \beta x + N_2 \sin \beta x = 1$

$$\cos \beta x + \left(\frac{N_2}{N_1}\right) \sin \beta x = 1/N_1 \quad \text{eq. A-6}$$

at $x=0$, $1 + 0 = 1/N_1 \;\therefore\; N_1 = 1$

to find N_2 we make use of $\left(\partial C/\partial x\right)_{\substack{x=0 \\ t=t_p}} = 0$

where h is the source of HCl (the meniscus/gas

interface):

$$\left(\frac{\partial C}{\partial x}\right) = N_0 e^{+\beta^2 D t} \left(-N_1 \beta \sin \beta x + N_2 \cos \beta x\right) \quad \text{eq. A-7}$$

or at $x = L, t = t_p$

$$\left(\frac{\partial C}{\partial x}\right)_{x=L} = 0 = N_0 e^{+\beta^2 D t_p} \left(-N_1 \beta \sin \beta L + N_2 \beta \cos \beta L\right)$$

$$\therefore \; 0 = -N_1 \beta \sin \beta L + N_2 \beta \cos \beta L$$

and $N_2 = N_1 \tan \beta L$ eq. A-8

substituting eq. A-8 into A-6, one obtains:

$$\cos \beta x + \tan \beta L \sin \beta x = 1$$

$$\cos \beta x + \left(\frac{\sin \beta L}{\cos \beta L}\right) \sin \beta x = 1$$

$$\cos \beta x \cos \beta L + \sin \beta L \sin \beta x = \cos \beta L$$

$$\cos (\beta L - \beta x) = \cos \beta L$$

$$\cos \beta (L - x) = \cos \beta L$$

obviously, β must be $s\pi$, where $s = 0, 1, 2, \ldots$ etc.

$i = nFA\left(\frac{\partial C}{\partial x}\right)_{x=0}$ where $\left(\partial C/\partial x\right)$ is given by eq. A-7

$$\therefore \; \left(\partial C/\partial x\right)_{x=0} = \beta N_0 N_2 e^{+\beta^2 D t} = \beta N_0 \tan \beta L \, e^{+\beta^2 D t}$$

and $i = nFA \beta N_0 \tan \beta L \, e^{+\beta^2 D t}$

but $N_0 = C_M e^{-\beta^2 D t_p}$ therefore,

$i = nFA\beta C_M e^{-\beta^2 D t_p} e^{+\beta^2 D t} \tan(\beta L)$ or

$i = nFA\beta C_M e^{+\beta^2 D(t-t_p)} \tan\beta L$; since $\beta = S\pi$

$i = nFAS\pi \tan(S\pi L) C_M e^{+S^2\pi^2 D(t-t_p)}$ eq. A-9

which can be rewritten as:

$\log.i = \text{Log.}[nFAS\pi \tan(S\pi L) C_M] + S^2\pi^2 D(t-t_p)$ eq. A10

or $\log.i = K + S^2\pi^2 D(t-t_p)$ eq. A-11

the limits of eq. A-9,10,11 are $0 \leq t \leq t_p$

(A) at $t=0$, i is proportional to the bulk electrolyte concentration, C_B

(B) at $t=t_p$, i is proportional to C_M, the maximum meniscus Cl^- concentration (which is a function of the volume of vapor injected into the CELL.

II. Current Decay

$(\partial C/\partial t) = D(\partial^2 C/\partial y^2)$; $C = f(y,t)$, let $C = f(t)\,g(y)$

$\therefore D(\partial^2 C/\partial y) = g''(y)\,Df(t)$ and $(\partial C/\partial t) = g(y)\,f'(t)$

$g(y)\,f'(t) = Df(t)\,g''(y)$

or $f'(t)/f(t) = D\,g''(y)/g(y) = -\theta^2$ eq A-12

$$f'(t) = -f(t)\theta^2$$

$$\frac{df}{dt} = -\theta^2 f$$

$$\frac{df}{f} = -\theta^2 dt$$

$$\ln f = -\theta^2 + \ln Z_0$$

$$f(t) = Z_0 e^{-\theta^2 t}$$

$$g''(y)/g(y) = -\theta^2/D$$

$$g''(y) + \theta^2/D\,(g(y)) = 0$$

Let $\lambda^2 = \theta^2/D$

$$g''(y) + \lambda^2 g(y) = 0$$

$$g(y) = Z_1 \cos \lambda y + Z_2 \sin \lambda y$$

$$C(y,t) = Z_0 e^{-\theta^2 t}(Z_1 \cos \lambda y + Z_2 \sin \lambda y) \qquad \text{eq. A-13}$$

Boundary Condition I: at $y=0$, $t=t_p$ $C(y,t) = C_M$

$$\therefore \quad C_M = Z_0 Z_1 e^{-\lambda^2 D t_p}$$

Boundary Condition II: at $t=t$, $y=R$ (where R is a point in the bulk solution such that $R \gg 0$) at which $\left(\frac{\partial C}{\partial y}\right)_{y=R} = 0$

differentiating eq. A-13, one obtains eq A-14

$$(\partial C/\partial y) = Z_0 e^{-\lambda^2 D t}(-\lambda Z_1 \sin \lambda y + \lambda Z_2 \cos \lambda y)$$

$$\therefore \left(\partial C/\partial y\right)_{y=R} = 0 = Z_0 e^{-\lambda^2 D t}(-\lambda Z_1 \sin \lambda R + \lambda Z_2 \cos \lambda R)$$

Which leads to: $\lambda Z_1 \sin \lambda R = \lambda Z_2 \cos \lambda R$

OR $\qquad Z_2 = Z_1 \tan \lambda R$

Boundary Condition III: at $t \gg t_p$, $0 \leq y \leq R$

$C(y,t) = C_B$

(1) $y = 0$, $C(0,t) = C_B = Z_0 e^{-\lambda^2 D t}$

(2) $y = y$, $C(y,t) = C_B = Z_0 e^{-\lambda^2 D t}(Z_1 \cos \lambda y + Z_2 \sin \lambda y)$

by comparison $Z_1 \cos \lambda y + Z_2 \sin \lambda y = 1$

$\cos \lambda y + \left(\frac{Z_2}{Z_1}\right) \sin \lambda y = \frac{1}{Z_1}$ but $\left(\frac{Z_2}{Z_1}\right) = \tan \lambda R$

$\cos \lambda y + \tan \lambda R \sin \lambda y = 1/Z_1$

$\cos \lambda y \cos \lambda R + \sin \lambda R \sin \lambda y = \frac{\cos \lambda R}{Z_1}$

$\cos \lambda (R-y) = \cos \lambda R / Z_1$

by inspection $Z_1 = 1$, $\lambda = q\pi$ where $q = 0, 1, 2, 3 \ldots$ etc.

the instantaneous current is given by:

$i = nFA \left(\partial C / \partial y\right)_{y=0}$ where $\left(\partial C / \partial y\right)$ is given by eq. A-14

$\therefore\ i = nFA\, Z_0 \lambda Z_2\, e^{-\lambda^2 D t}$

$i = nFA\, Z_0 \lambda Z_1 \tan \lambda R\, e^{-\lambda^2 D t}$

$i = nFA\, \lambda \tan \lambda R\, C_M e^{+\lambda^2 D t_p} e^{-\lambda^2 D t}$

$i = nFA\, \lambda \tan \lambda R\, C_M e^{+\lambda^2 D (t_p - t)}$

$i = nFA q\pi \tan(q\pi R)\, C_M e^{+q^2 \pi^2 D (t_p - t)}$ eq. A-15

$\log. i = \log.[nFA q\pi \tan(q\pi R) C_M] + q^2 \pi^2 D (t_p - t)$ eq. A-16

Appendix B

Each infinitesmal height element of the electrode contributes the current: $dI_t = -2L \; i \; dy$ eq. B-1 to the total electrode current I_t, where i is the local current density which is a function of the local electrode potential E(y), y is the vertical position in the meniscus and film and L is the length of the electrode along the plane of the solution. Introducing the current per unit length of the electrode: $P = I_t / 2L$ eq. B-2

eq. B-1 can be rewritten as: $dP/dy = -i$ eq. B-3

Since each height element dy of the meniscus and film adds the increment dR to the total resistance R there is an ohmic drop in the potential along the electrode surface of:

$dE = -I_t dR = -\frac{Q(C) I_t}{2LX(y)} dy . Q'(t)$, we will make the simplifying assumption that these quantities are constant. This is not unreasonable since the reported parameter is the maximum in the current transient. At the maximum, the instantaneous HCl concentration in the active zone of the exposed electrode/electrolyte interface (which is responsible of 90% of the current response) can be regarded as uniform and D and Q as constant, i.e. the ratio $(D_o C_M / Q_o)$ at the maximum in the transient (time = t_p) is a constant for a given injection of vapor.

Upon substituting eq. B-4 into eq. B-2 one obtains:

$P = [-X(y)/Q_o][dE/dy]$ eq. B-5

Differentiating eq. B-5 and substituting the result into eq. B-3, the second order differential equation:

$Q_o \left[X(y) \ (d^2E/dy^2) + (dX(y)/dy) \ (dE/dy) \right] = i = f(E,y)$ eq.B-6

Depending on the complexity of the function X(y) and f(E,y), an analytical solution to the differential equation may or may not be possible .

Mathematically, the shape of the meniscus plus the sheath of wetting on a vertical planar surface is represented by: $X(y) = \epsilon + X_o - \sqrt{2h^2 - y^2} + h/\sqrt{2} \ \ln \left[(h\sqrt{2} + \sqrt{2h^2 - y^2})/y \right]$

eq. B-7

where X_o is a constant of integration, X(y) is the horizontal distance from the vertical surface, h is the maximum height of the meniscus, y is the vertical distance in the meniscus and ϵ is the thickness of the sheath of wetting.

It is postulated that the current change resulting from the injection of HCl vapor into the cell can be described using the Nernst diffusion layer equation and Fick's law (appendix B). That is , by assuming that at the maximum in the transient current (at time = t_p):

$(dC/dx) \approx k''C_M/X(y)$ where k'' is a constant. As a first approximation, this is reasonable since the current is controlled by the rate of diffusion of the reactant through the electrolyte in the meniscus and adjacent film.

Therefore: $i_B = \left[K_B / X(y)\right] \left[1-\exp(-nFE_a/RT)\right]$ eq. B-8a

$i_M = \left[KM/ X(y)\right] \left[1-\exp(-nFE_a/RT)\right]$ eq.B-8b

where $K_B = nFDC_B$ and $K_M = nFDC_M$, i_B and i_M are the currents due to the bulk electrolyte and injected vapor respectively. The change in current Δi is given by:

$\Delta i = (i_M - i_B) = (K_M - K_B) \ (1-\exp(-nFE_a/RT))/X(y)$ eq.B-8c

where n,F,D have their usual significance, E_a is the applied potential in volts, C_B and C_M are the bulk electrolyte and instantaneous concentrations of HCl respectively. Substitution of eq. B-7 into eq. B-8c leads to a complicated nonlinear differential equation which is not analytically solvable. However, since the present work was performed at applied potentials greater than o.2v, an approximate solution is possible. This is because the exponential term in eq.B-8c is much smaller than unity and may be neglected. Therefore, equation B-8c becomes:

$\Delta i = [K_M - K_B/X(y)]$ eq. C-8c" and $dP/dy = -[K_M - K_B/X(y)]$ eq. C-9a. For $y \leq h$ this equation describes dP/dy in the meniscus. For $h \leq y \leq S$ (where S is the length of the film) eq. B-9a reduces to: $dP/dy = -[K_M - K_B/\epsilon]$ eq.B-9b which describes the current in the film above the upper meniscus boundary. If one assumes that $X(y) = \epsilon$ for all $y > h$, then eq. B-9a can be applied to the meniscus and film. The first integration leads to the current, P, per unit length as a function of y:

$$P = \int_0^P dP = (K_M - K_B) \int_0^Y dy/X(y) \qquad \text{eq. B-10}$$

The second integration leads to the E(y):

$$E(y) = -Q_0 \int_0^Y (K_M - K_B) \left\{ \int_0^Y dy/X(y) \right\} dy/X(y) \qquad \text{eq. B-11}$$

But;

$$P = \int_0^Y (K_M - K_B)\, dy/X(y) \quad \text{and} \quad dy/X(y) = dP/(K_M - K_B)$$

hence: $E(y) = -Q_0 (K_M - K_B)^{-1} \int P\,dP = Q_0 P^2/2(K_M - K_B)$ eq.B-11"

P is then given by:

$$P(y) = [2(K_M - K_B)/Q_0]^{1/2} [E(y)]^{1/2} \qquad \text{eq. B-12}$$

Eq. B-12 cannot be solved since the integral of B-10 has not been obtained. However, for the special case of $y = 0$, eq. B-12 reduces to:

$$P(0) = \left[2 (k_M - k_B)/Q_o\right]^{1/2} \left[E_a\right]^{1/2}$$

References

1) Hersch, P., "Galvanic Analysis", Advances in Analytical Chemistry and Instrumentation, 3, pp183-249, Johen Wiley and Sons, Inc. (1964)

2) Will, F.G., J. Electrochem. Soc., 110, pp145-160 (1963)

3) Maget, H.J.R. and R. Roethlein, ibid, 112, p1034 (1965)

4) Roethlein, R. and H.J.R. Maget, ibid, 113, p581 (1966)

5) Borucka, A. and J.N. Agar, Electrochimica Acta, 11, p603 (1966)

6) Lightfoot, E.N., J. Electrochem. Soc., 113, p614 (1966)

7) Rosano, H.L. and H.H. Friedman, "Objective Approaches to Odor Measurement", Advances in Chemistry Series 56 (Flavor Chemistry), pp53-63, ACS Publication, Washington, D.C. (1966)

8) Rosano, H.L., 4th Intern'l Cong. on Surface Activity, B/II p10-17, Brussels (September 1964)

9) Rosano, H.L., Chem. Eng. News, 39, Nos. 15, 52 (1961)

10) Rosano, H.L. and S.Q. Scheps, Ann. N.Y. Acad. Sci., 112, p590 (1964)

11) Hersch, P. and R. Deuringer, Anal. Chem., 35, p897 (1963)

12) Pierrain, J., Chim. Anal. (Paris), 41, p477 (1959)

13) Rostenbach, R.E. and R.G. Kling, Air Pollution Control Assoc. J., 12, p459 (1962)

14) Keidel, F.A., Ind. Eng. Chem., 52, p490 (1960)

15) Berton, A., Chim. Anal. (Paris), 41, p351 (1959)

16) Berton, A., Compt. Rend., 250, p126 (1960)

17) Berton, A., Chim. Anal. (Paris), 45, p585 (1963)

18) Guillot, M., and A. Berton, Compt. Rend., 250, p1857 (1960)

19) Berton, A., Rev. Franc. Corps. Gras, 4, p187 (1962)

20) Berton, A., Compt. Rend. (Acad. Sci. Paris), 262, p904 (1966)

21) Macleod, P. and A. Cavoy, J. Physiol. 52, p158 (1960)

22) Lestiene, A., Chim. Anal. (Paris), 44, p377 (1962)

23) Hersch, P. and C.J. Sambucetti, paper entitled, "Galvanic-Coulometric Monitoring of Carbon Monoxide", presented at the 14th Pittsburgh Conference onfAnalytical Chemistry and Applied Spectroscopy, Pittsburgh, Pa.(March 1963)

24) Hersch, P., Nature, 180, p1407 (1957)

25) Weber, H.C., H.P. Meissner and D.A. Sama, J. Electrochem. Soc., 109, p884 (1962)

26) Hersch, P., ibid, 110, p1284 (1963)

27) Bianchi, G., ibid, 112, p233 (1965)

28) Posey, F.A. and Misra, S.S., ibid, 113, p608 (1966)

29) Vergnolle, J., ibid, 111, p799 (1964)

30) Hartner, A.J., M.A. Vertes. V.E. Medina and H.G. Oswin, paper entitled "Effect of Oxygen Partial Pressures on Fuel Cell Cathodes" presented to the Division of Fuel Chemistry of the American Chemical Society in New York City (Sept. 8-13, 1963)

31) Bennion, D.N. and C.W. Tobias, J. Electrochem. Soc., 113, p589 (1966)

32) Moncrieff, R.W., J. App. Physiol., -16, p742 (1961)

33) Moncrieff, R.W., Amer. Perfumer and Cosmetics, 81, p29 (1966)

34) Dravnieks, A. and H.S. Weber, Ann. N.Y. Acad. Sci., 116, p429 (1964), Proceedings of the Conference on Surface Effects in Detection, Washington, D.C. (June 29-July 1, 1964)

35) Jirgensons, B. and M.E. Straumanis, "A Short Textbook of Colloid Chemistry" 2nd edition, the MacMillan Co., New York (1962)

36) Adamson, A.W., "Physical Chemistry of Surfaces", Interscience Publishers, New York (1960)

37) Sears, F.W. and M.W. Zemansky, "College Physics", Part I, 3rd edition, Addison-Wesley Publishing Co., Inc., New York (1960)

38) Danielli, J.F., K.G.A. Pankhurst and A.C. Riddiford, "Surface Phenomena in Chemistry and Biology",

Pergamon Press (1958)

39) Derjaguin, B. and M. Kussakov, ACTA Physiocochimica (URSS), vol. X, p25, (1939)

40) Derjaguin, B. and M. Kussakov, ACTA Physiocochimica (URSS), vol. X, no. 2, p1 (1939)

41) Elton, G.A.H., Royal Society of London, Proceedings #1037, pp259-287 (1948)

42) Derjaguin, B., N.N. Zakhavaeva, S.V. Andreer, A.A. Milovidov and A.M. Khomumov, "Research in Surface Forces", p110, Consultants Bureau, New York (1963)

43) Muller, R.H., J. Electrochem. Soc., 113, p943 (1966)

44) Bascom, W.D., R.L. Cottington, and C.R. Singleterry, "Contact Angle Wettability and Adhesion" Advances in Chemistry, series 43, p355, ACS Publication, Washington, D.C. (1964)

45) Lightfoot, E.N. and V. Ludviksson, J. Electrom. Soc., 113, p1325 (1966)

46) Gomer, R. and C.S. Smith, "Structure and Properties of Solid Surfaces", the University of Chicago Press (1953)

47) Sarkar, N. and A.M. Gaudin, J. Phys. Chem., vol 70, p2512 (1966)

48) Hoernschemeyer, D., ibid, 70, p2628 (1966)

49(Pease, D.C., ibid, 49, p107 (1945)

50) Johnson, R.E. Jr. and R.H. Dettre, ibid, 68, p1744 (1964)

51) Dettre, R.H. and R.E. Johnson Jr., "Contact Angle Wettability and Adhesion", Advances in Chemistry, series 43. art. 7, p112 and art. 8, p136, ACS publication, Washington, D.C. (1964)

52) Adam, N.K. and G. Jessops, J. Chem. Soc.,127, p863 (1925)

53) Ray, B.R. and F.E. Bartell, J. Colloid Sci., 8, p214 (1953)

54) Bartell, F.E. and J.E. Shepard, J. Phys. Chem. 57, p211 (1953)

55) Shuttleworth, R. and G.L.J. Bailey, Discussions Faraday Soc., 3, p16 (1948)

56) Hickling, A. and D. Taylor, ibid, 1, p277 (1947)

57) Wagner, C., J. Electrochem. Soc., 97, p71 (1950)

58) Turpin, M.R. and M.K. Testerman, ibid, 109, p168 (1962)

59) Bowden, S.P. and D. Tabor, "Friction and Lubrication of Solids", vol. 2, Cambridge University Press, London (1964)

60) Ross, S. and I.J. Wiltshire, J. Phys. Chem. 70, p2107 (1966)

61) Cassies, A.D.D., Discussions Faraday Soc., 3, p11 (1948)

62) Matalon, R., Thesis, University of Lyons, France (1948)

63) Rosano, H.L., C.J. Cante and E. Morgans, J. Electrochem. Soc. vol. 114, p319 (1967)

64) Cante, C.J. and H.L. Rosano, "Mechanism of the AIEP cells II Nature of the Current", submitted to J. Electrochem. Soc., January 1967

65) Cante, C.J. and H.L. Rosano, "Anodic Oxidation of 1-Butanol Vapor on the Surface of Partially Exposed Platinum Electrodes", submitted to Electrochimica Acta, April 1967

66) Bouasse, H.P.L., Cappilarité Phenomenes Superficiels, Librairie Delagrave, Paris (1924)

67) Levich, V.G., "Physicochemical Hydrodynamics" Prentice-Hall Inc., Englewood Cliffs, N.J. (1962)

68) Conway, B.E., "Theory and Principles of Electrode Processes", the Ronald Press Co., New York (1965)

69) Ligane, J.J., "Electroanalytical Chemistry", Inter-Science Publishers, Inc., New York (1953)

70) MacInnes, D.A., "The Principles of Electrochemistry", Dover Publications, Inc., New York (1961)

71) Sennett, P. and J.P. Olivier, "Chemistry and Physics of Interfaces", pp73-92, ACS Publications, Washington, D.C. (1965)

72) Reilley, C.N. and R.W. Murray, "Electroanalytical Principle" reprinted in full from "Treatise

on Analytical Chemistry", Interscience, N.Y. (1963)

73) Glasstone, S., "Introduction to Electrochemistry", Van Nostrand Co., Inc. (1942)

74) Kortum, G.F. and J.O'Mc.Bockris, "Textbook of Electrochmistry", vol.2, Elsevier, New York (1951)

75) Kortum, G.F., "Treatise on Electrochemistry", 2nd edition, Elsevier Publishing Co., New York (1965)

76) Rosano, H.L. and C.J. Cante, paper No.23 presented to the Division of Analytical Chemistry at the First Middle Atlantic Regional Meeting of the American Chemical Society, Philadelphia, Pa. (February 3-4, 1966)

77) Rosano, H.L., C.J. Cante and E. Morgan, paper No. 151V presented to the Division of Physical Chemistry at the 152nd National Meeting of the American Chemical Society, New York, N.Y. (September 11-16, 1966)

78) Cante, C.J. and H.L. Rosano, paper No. 170 presented to the Division of Physical Chemistry at the 153rd National Meeting of the American Chemical Society, Miami Beach, Fla. (April 9-14, 1967)

79) Gilman, S. and M.W. Breiter, J. Electrochem. Soc., 109, p1099, (1962)

80) Breiter, M.W. and S. Gilman, ibid, 109, p623 (1962)

81) Breiter, M.W., Electrochimica Acta, 10, pp503-508 (1965)

82) Andrew, M.R., ibid, 11, p1425 (1966)

83) Binder, H., A. Kohling, H. Krupp, K. Richter and G. Sanstede, "Fuel Cell Systems", Advances in Chemistry, series 47, ACS Publication, Washington, D.C. (1965) art. 20, pp269-282

84) Binder, H., A. Kohling and G. Sandstede, ibid, art. 21, pp283, 291 (1965)

85) Giner, J., Electrochimica Acta, 8, p857 (1963)

86) Giner,J., ibid, 9, p63 (1964)

87) Rightmire, R.A., R.L. Rowland, D.L. Boos and D.L. Beals, J. Electrochem. Soc., 111, p242 (1964)

88) Schulze, F., Anal. Chem., vol 38, p749 (1965)

Autobiographical Sketch

Name: Charles J. Cante

Born: 31 October 1941 (Brooklyn, New York)

Education: M.A. (Chemistry), The City College of The City University of New York (16 June 1965)

B.S. (Chemistry), The City College of CUNY (12 June 1963)

Brooklyn Technical High School (June 1959)

Military: Commissioned 2nd Lt (USAR), 11 June 1963, Ser. No. O 501 6211

Promoted to 1st Lt (USAR), 10 June 1966

Present Branch: INFANTRY

Current Status: Delay in call to active duty for educational purposes. (Begin active duty, Fiscal Year 1967-68)

Professional: Lecturer, Chemistry Department, The City College of The City University of New York, January 1964 to date

Honors: Recipient of the E.I. Du Pont de Nemours Postgraduate Teaching Award for the Academic Year 1966-67

Professional Societies: American Chemical Society, member

Association for the Advancement of Science, member